MEASUREMENT OF THE DYNAMIC TIRE FORCES OF A LARGE TRUCK

SEPT. 1965
NO. 21

by

G.W. KIBBEE

Joint Highway Research Project

PURDUE UNIVERSITY
LAFAYETTE INDIANA

MEASUREMENT OF THE DYNAMIC TIRE FORCES

OF A LARGE TRUCK

To: G. A. Leonards, Director
Joint Highway Research Project

September 24, 1965

From: H. L. Michael, Associate Director
Joint Highway Research Project

File No: 6-20-6
Project No: C-36-52F

Attached is a Final Report "Measurement of the Dynamic Tire Forces of a Large Truck." This report together with the accompanying Final Report by J. L. Sanborn constitutes the Final Report on the Stresses and Deflection HPR research project.

The attached report has been authored by Mr. Gary W. Kibbee who also used it for his Ph.D. dissertation. The research reported was conducted under the guidance of Professor B. E. Quinn of the School of Mechanical Engineering.

The report is submitted for acceptance by the Board and for referral to the Highway Commission and the Bureau of Public Roads for their review, comments and acceptance.

Respectfully submitted,

Harold L. Michael

Harold L. Michael, Secretary

HLM:bc

Attachment

Copy:

F. L. Ashbaucher
J. R. Cooper
J. W. Delleur
W. L. Dolch
W. H. Goetz
W. L. Grecco
F. F. Havey
F. S. Hill
J. F. McLaughlin
F. B. Mendenhall
R. D. Miles
J. C. Oppenlander
W. P. Privette
M. B. Scott
J. V. Smythe
F. W. Stubbs
K. B. Woods
E. J. Yoder

Final Report

MEASUREMENT OF THE DYNAMIC TIRE FORCES OF A LARGE TRUCK

by

Gary W. Kibbee
Research Assistant

Joint Highway Research Project

File No: 6-20-6

Project No: C-36-52F

Prepared as Part of an Investigation

Conducted by

Joint Highway Research Project
Engineering Experiment Station
Purdue University

in cooperation with

Indiana State Highway Commission

and the

Bureau of Public Roads
U S Department of Commerce

Not Released for Publication

Subject to Change

Not Reviewed by

Indiana State Highway Commission
or the
Bureau of Public Roads

Purdue University
Lafayette, Indiana
September 24, 1965

Digitized by the Internet Archive
in 2011 with funding from
LYRASIS members and Sloan Foundation; Indiana Department of Transportation

http://www.archive.org/details/measurementofdyn00kibb

ACKNOWLEDGMENTS

The majority of the financial support for this investigation was furnished by the Joint Highway Research Project of the Civil Engineering School, Purdue University.

Special thanks are expressed to Dr. Bayard E. Quinn, Professor of Mechanical Engineering, who as my major professor and project director furnished moral encouragement during this investigation. His long range plans made in the past for the project greatly expedited this particular investigation.

The loan of the test vehicle by the Indiana State Highway Commission was appreciated. The wonderful cooperation of the Commission personnel during the tests is acknowledged.

Thanks are due my fellow members of the Vehicle Dynamics Group; Kjell Hagen, Doug Veenstra for helping with the data processing and Ken Perry for preparing the illustrations for this thesis.

Special thanks are given to my wife, Catherine. Her patience and careful attention greatly facilitated the typing of the entire manuscript for this thesis.

TABLE OF CONTENTS

	Page
LIST OF ILLUSTRATIONS.	iv
ABSTRACT	ix
I. INTRODUCTION	1
II. FUNDAMENTAL CONSIDERATIONS OF DATA PROCESSING	11
III. CALIBRATION OF EQUIPMENT	45
IV. RESULTS OF HIGHWAY TESTS	98
V. MEASUREMENT AND PREDICTION OF FORCE POWER SPECTRA.	115
VI. CONCLUSIONS AND RECOMMENDATIONS.	145
Measurement of Dynamic Tire Forces	145
Equipment.	145
Experimental Results	146
Prediction of Dynamic Tire Forces.	147
BIBLIOGRAPHY	149
APPENDIX 1	
Theoretical Frequency Response Relationships for Model in Figure 39	151
VITA	155

LIST OF ILLUSTRATIONS

Figure		Page
1.	Illustration of the Relationship Between Static and Dynamic Forces	2
2.	Force That a Small Region in the Pavement Experiences as a Vehicle Passes	3
3.	Response of a Second Order System to a Step Input	16
4.	Second Order System Response to a Decaying Exponential	22
5.	Frequency Response for a Second Order System.	25
6.	Magnitudes of the Fourier Transforms for the Input and Output of a Second Order System	26
7.	Illustration of Aliasing.	28
8.	Numerically Determined Fourier Transform Where Aliasing Has Occurred	29
9.	Numerical Integration Error Per Step as a Function of Frequency	31
10.	Comparison of the Frequency Response for a Second Order System	35
11.	Comparison of Input and Output Fourier Transforms of a Second Order System.	36
12.	Frequency Response from Data of Varying Degrees of Accuracy	38
13.	Fourier Transforms of the Step Response (Output) of a Second Order System for Varying Degrees of Data Accuracy	39
14.	Magnitude of Frequency Response Determined from Truncated Data.	42

Figure Page

15. Magnitude of Fourier Transforms Numerically Determined from Truncated Data 43

16. Phase Angle for the Fourier Transform of the Step Response (Output) of a Second Order System. 44

17. Pressure Measuring System. 48

18. Drop Beam Calibrator 50

19. Force and Pressure Records for Calibration Tests of Right Rear Inner Dual at Three Different Drop Heights. 52

20. Magnitude of Frequency Responses for the F/P Calibration Tests of the Right Rear Inner Dual . 53

21. Fourier Transforms of Force Records for F/P Calibration of Right Rear Inner Dual 55

22. Fourier Transforms of Pressure Records for F/P Calibration of Right Rear Inner Dual 56

23. F/P Test Results from a .671 Inch Drop Test of a Right Rear Inner Dual. 57

24. F/P Test Results from a .291 Inch Drop Test of the Right Rear Inner Dual. 58

25. F/P Test Results from a .086 Inch Drop Test of the Right Rear Inner Dual. 59

26. Averaged F/P Frequency Response for the Left Rear Inner Dual. 62

27. Averaged F/P Frequency Response for the Left Rear Outer Dual. 63

28. Force and Displacement Records for Calibration Tests of Right Rear Inner Dual at Three Different Drop Heights 65

29. Magnitude of Frequency Responses for the F/X Calibration Tests of the Right Rear Outer Dual . 66

30. Magnitude of Frequency Responses for the F/X Calibration Tests of the Right Rear Inner Dual . 67

31. Displacement Fourier Transform for F/X Calibration of Right Rear Duals 68

Figure		Page
32.	F/X Test Results from a .086 Inch Drop Test of the Right Rear Inner Dual	70
33.	Low Frequency F/X Frequency Response for Right Rear Inner Dual.	71
34.	Seven Degree Freedom Model of Test Vehicle . .	73
35.	Definition of Terms Used for Seven Degree of Freedom Model of Test Vehicle.	74
36.	Relative Displacement between Rear Axle and Truck Bed.	76
37.	Change in Static Load under Tires for Static Changes in Displacement.	78
38.	Comparison of F/X Frequency Response for Three Different Vehicles	80
39.	3 Degree of Freedom Model of a Truck	83
40.	Comparison of Transient Response of Model with Experimental Results	87
41.	Comparison of the Model Frequency Response with Experimental Results	88
42.	F_I/X_4 Frequency Curves for Case I.	91
43.	F_I/X_4 Frequency Response Curves for Case II at Various Speeds.	94
44.	F_I/X_4 Frequency Response Curves for Case III at Various Speeds.	96
45.	Force Records of Left Rear Tires on Wheel Paths Centered about Test Point.	101
46.	Force Records of Left Rear Tires on Wheel Paths Centered 11 Inches Right of Test Point	102
47.	Tire Forces and Pavement Deflection.	104
48.	Pressure Record and Fourier Series Approximation	109

Figure Page

49. Comparison of Force Records Obtained from Two Conversion Processes 111

50. Comparison of the Total Force of an Automobile and the Test Truck 112

51. Comparison of the Automobile and Truck Dynamic Tire Forces Expressed as a Percentage of the Static Wheel Load. 114

52. 80% Confidence Interval for the Ratio of the Value of a Chi-Square Random Variable to the Average Value. 118

53. Data Preprocessing and Power Filtering Characteristic for Data Preprocessing. 123

54. Comparison of Results Using Two Different Data Preprocessing Techniques. 125

55. Comparison of Elevation Power Spectra of the Same Pavement Section for the 1962 and 1964 Surveys. 127

56. Predicted Force Power Spectra for Truck and Model of Truck 128

57. Predicted Force Power Spectra for Nominal Speeds of 20, 30, and 40 MPH.. 130

58. Predicted Force Power Spectra for Nominal Speeds of 50 and 60 MPH. 131

59. Experienced Force Power Spectra for Nominal Speeds of 20, 30, and 40 MPH 133

60. Experienced Force Power Spectra for Nominal Speeds of 20, 50, and 60 MPH 134

61. Comparison of Experimental Results for an Automobile and the Test Truck. 136

62. Predicted and Measured Force Power Spectra . . 137

63. Comparison of Predicted and Experienced RMS Force. 139

64. Experienced Force Power Spectra for Right Rear Outer Tire. 141

Figure Page

65. Experienced Force Power Spectra for Right Rear Outer Tire. 142

66. Force Power Spectra for Left Rear Duals at 60 MPH 143

67. Force Power Spectra for Left Rear Duals at 50 MPH 144

ABSTRACT

Kibbee, Gary Willard. Ph.D., Purdue University, August 1965. Measurement of the Dynamic Tire Forces of a Large Truck. Major Professor: Bayard E. Quinn.

The study of the dynamic tire forces of a moving vehicle is a relatively new subject that is receiving increased attention from both automotive engineers and highway engineers. This investigation was part of a joint effort between these two groups. The primary concern of this investigation was the measurement of the dynamic tire forces of a large truck as it passed over an instrumented section of pavement. The results of the investigation that deal with the pavement are presented in a Purdue University Ph.D. Thesis, "An Experimental Analysis of Transient Vehicle Loads and Response of Flexible Pavement", by John Sanborn. The problems associated with the measurement of the dynamic tire forces are discussed in this thesis.

Instrumentation was developed to measure independently the tire inflation pressure of the inner and outer rear dual tires of a large truck. These measurements were converted to dynamic tire force records by appropriate conversion techniques.

Because of the large amounts of data that were re-

quired for this investigation, problems and criteria associated with the processing of discrete data were investigated.

The experimental calibration of the pressure system was determined by using transient excitation.

During the calibration tests, additional studies were conducted concerning the behavior of the vehicle suspension system. The results indicated that the system response was amplitude dependent. However, for very small displacements, the system may be approximated as a linear system.

Typical records of dynamic tire force versus distance are given for highway tests conducted jointly with the Stresses and Deflections Group of the Civil Engineering School. These tests also indicated that the distribution of force between inner and outer dual tires is strongly influenced by the transverse road profile.

A comparison was made of the tire forces of the truck with those of an automobile for the same pavement section. The dynamic forces of one wheel of the truck were in some cases as great as the total force of one wheel of an automobile.

By combining a pavement elevation power spectrum with the characteristics of the suspension, it was possible to calculate a predicted dynamic force power spectrum. These results were then checked by calculating an experimental force power spectrum for the forces recorded when the vehicle traversed this section of pavement. The predicted

values were generally higher than the experimental values.

An example is also given of the use of spectral techniques to determine a system malfunction.

As a consequence of this investigation it was possible to obtain the dynamic tire force measurements that were of interest to those who were concerned with pavement behavior.

CHAPTER I

INTRODUCTION

When a vehicle is parked on a perfectly level and flat pavement, the only force transmitted to the pavement through the tires is the weight of the vehicle. If the vehicle moves at a constant speed over this ideal pavement, each wheel will transmit the same force as when parked. If the pavement is not perfectly flat, a condition that usually exists in any normal road, each of the tires of the moving vehicle will exert on the pavement the sum of the static force and a dynamic force that produces the vertical accelerations of the vehicle. Since the dynamic force may be positive or negative, the total force will fluctuate above and below the static load of a tire when the vehicle is parked. A typical total force versus time record is shown in Figure 1.

This record can be made by recording the dynamic forces in a tire and then adding them to the static force. It is convenient to view this record as a history of the force exerted on the vehicle by the road. As the vehicle traverses one small region in the pavement, this region will experience a total force versus time relationship of a transient nature as shown in Figure 2. The initial and

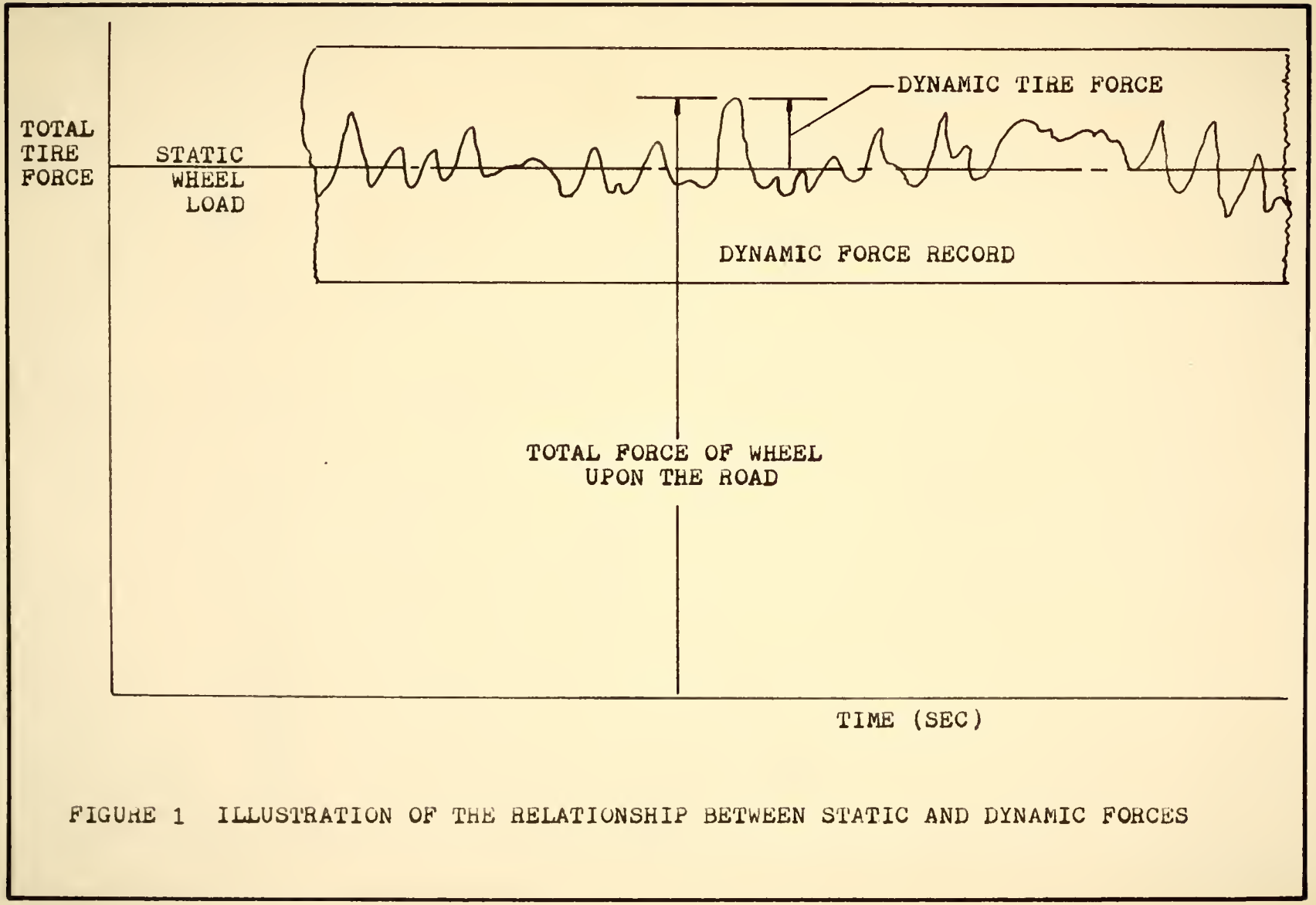

FIGURE 1 ILLUSTRATION OF THE RELATIONSHIP BETWEEN STATIC AND DYNAMIC FORCES

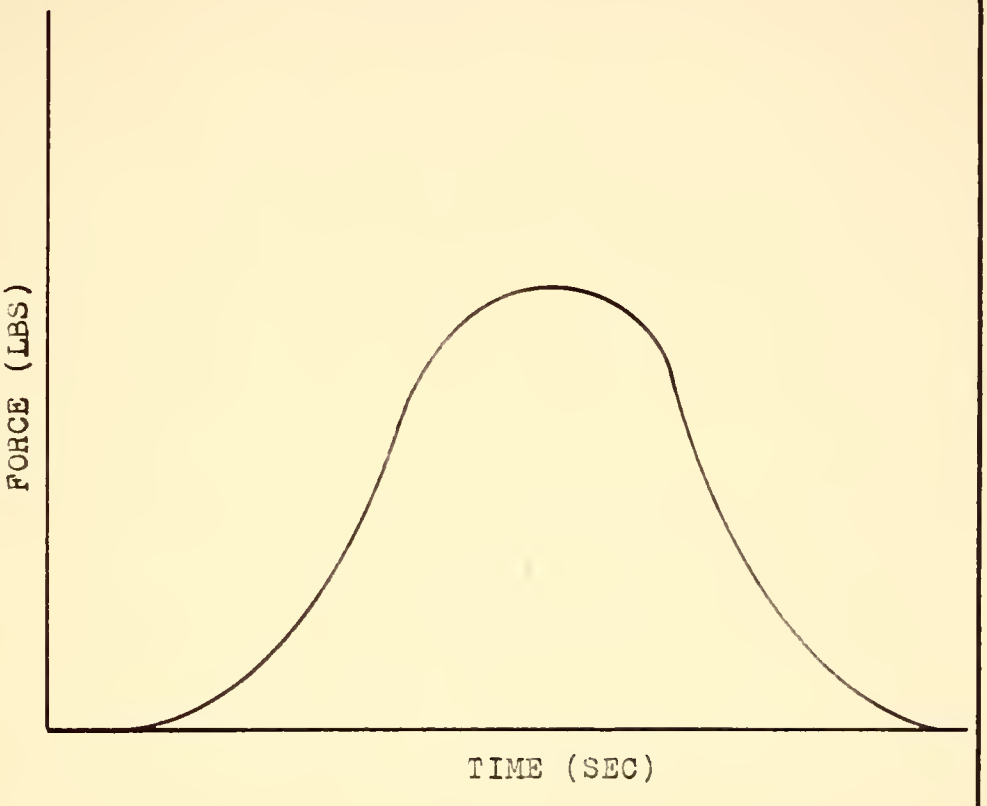

FIGURE 2 FORCE THAT A SMALL REGION IN THE PAVEMENT EXPERIENCES AS A VEHICLE TIRE PASSES

and final value of the force will be zero and the maximum value will usually occur when the tire is directly above the region under study. This maximum force is related to the total tire force.

Recently the Stresses and Deflections Group of the Civil Engineering School undertook an investigation of the pavement deflections caused by vehicles. One of the objectives of this investigation was to determine the effect that the dynamic vehicle forces had on the pavement deflections at one location.

The Vehicle Dynamics Group of the Mechanical Engineering School developed and calibrated the instrumentation necessary to measure the dynamic tire forces of a test vehicle in the form shown in Figure 1.

These two groups performed tests jointly on specific pavement sections. The Vehicle Dynamics Group then furnished the Stresses and Deflections Group with records of total force for pavement loading information. The results of the investigation that dealt with the pavement are presented in reference (1).

Since the vehicle had been instrumented for these tests, it afforded an excellent opportunity to check experimentally the results of certain procedures used to predict the dynamic force when the pavement condition (elevation profile) is known.

The measurement of the dynamic tire forces of a

moving vehicle is a relatively new field of interest. Various procedures have been applied, with varying degrees of success, to make these measurements.

The best method of measuring dynamic tire force would be to mount force transducers directly on the tire tread. However, instrumentation is not now available for this procedure. The procedures that have been used to experimentally determine these forces for a truck may be classified into three general categories:

1. Measurement of the strain in axle housing
2. Measurement of the tire sidewall deflection
3. Measurement of the tire inflation pressure

In 1957, Hopkins and Boswell[2] applied all three of these procedures simultaneously to a two axle truck with 9.00 x 20 tires to determine the most practical method for measuring dynamic tire force. The instrumentation was used with the right rear outer dual tire. The right rear inner tire was removed for the tests to permit installation of the equipment. To produce a 4500 lb rear wheel load, concrete blocks were used as ballast. Simultaneous recordings were made of the outputs of each of the three devices as the truck drove over an electric scale. By comparing

---

2. Superscripts refer to references listed in the Bibliography

these results with the forces measured by the scale, the authors concluded that the most practical method for measuring the weight variations involving all wheels of a vehicle was the tire pressure method. The disadvantage of the strain gage method was that the inertia of the vehicle suspension system affected the results. If both dual tires would have been used, the changing moment arm would be a problem in finding the total dynamic force of both tires. Furthermore, it would not be easy to separate the dynamic force of the inner tire and outer tire.

The measurement of tire sidewall deflection was subject to errors caused by small imperfections in the tire sidewall. It would be difficult to construct this type of equipment for simultaneous measurement of both inner and outer tire sidewall deflection because of space limitations between the tires.

The pressure measuring system used by Hopkins and Boswell employed a 0 - 50 psig pressure transducer mounted on the wheel. Electrical slip rings were used to transfer the pressure transducer output to recording instruments in the truck. The severe acceleration environment of the pressure transducer when it was mounted on the wheel may have caused errors in the results. Also the electrical resistance of the slip rings changed with wheel rotation speed. Further, the pressure gage sensitivity was not adequate for the small pressure changes that occur.

The authors recommended several refinements for the system. The most important recommendation was to mount a differential pressure transducer on the side of the truck and use a rotating pressure slip joint and flexible tubing to carry the pressure from the tire to the transducer.

In 1962, Fisher and Huckins[3] reported the results of an improved pressure measuring system. These investigators had followed the recommendations of Hopkins and Boswell[2] and had used a differential pressure transducer mounted on the side of the truck. A rotating pressure joint and flexible tubing were used to bring the pressure from the rotating wheel. This device was used on certain trucks that were operated as part of the AASHO Road Tests[4]. The pressure measuring system could be used with either a front tire or one rear dual tire. Calibration of the pressure system was performed by placing the test tire on an electric scale and using a mechanical oscillator lashed to the truck bed to produce a sinusoidal force. In this manner, the frequency response that related the dynamic force to the tire inflation pressure was determined for frequencies up to 10 cps.

Wilson[5] in 1964 developed further the pressure measuring system for an automobile. He developed certain system design criteria to minimize resonant effects of the pneumatic system.

Hamilton[6] developed a procedure that could be employed

to calibrate a passenger car suspension system together with a pressure measuring system. Using this technique, the frequency response of the system in question could be determined from the transient response of the system to an experimental excitation.

McLemore[7] developed the necessary equipment for the calibration of large vehicles. With this equipment, it was possible to apply a tire displacement disturbance to a set of dual truck tires. The resulting transient force under the tire and the transient differential tire inflation pressure supplied the information necessary to determine the frequency response of the pressure measuring system that could be used to relate dynamic force to tire pressure. This equipment was also used to calibrate the vehicle suspension system to determine the relationship between vertical tire displacement and tire force.

Hamilton[6] developed digital computer programs for use in processing calibration data and the conversion of pressure records to force records. An investigation of the integration procedures of these programs and other aspects of data processing was conducted to determine the errors that are introduced in numerical calculations.

De Vries[10] developed the necessary techniques required to calculate power spectra for highway profiles.

Several investigators[9,11,12] have worked with the relationship among elevation power spectra, vehicle

characteristics, and power spectra of experienced tire forces or center of gravity accelerations. However, the results obtained by these investigators indicated that further investigation should be conducted in this area.

In all previous investigations, no provision had been made for the simultaneous measurement of tire inflation pressure in the inner and outer tires on a truck rear axle. Special equipment was designed prior to this investigation for measuring these two pressures independently. An independent pressure measuring system was connected to each tire of a dual set. The pressure transducers were mounted on the side of the truck and were connected to the tires by flexible tubing and a special double pressure joint.

In order to conduct the proposed investigation, it was decided to make maximum use of the experience and equipment that had been developed by previous investigators. It was necessary, however, to develop a special double rotating pressure joint that was necessary to transfer the pressure disturbances from the rotating tire to the pressure transducers.

Prior to the investigation, the pressure systems and the auxiliary equipment were installed in the test vehicle. The two electrical amplifiers were mounted inside of the cab of the truck on the passenger side. The instrument operator sat on a small seat above the amplifiers. An

MG set for 110 vac power was mounted on the front of the truck.

The calibration procedure was improved in order to apply to large vehicles. A method for finding the static wheel load for various wheel dispositions was developed. A procedure of operation for the calibration of large vehicles by transient excitation was developed since the available equipment had not been used with a vehicle of the size used in this investigation.

The numerical accuracy of the data processing techniques was determined. These techniques were extended and improved.

A test procedure had to be developed for the tests that were conducted jointly with the Stresses and Deflections Group. This included a method for correlating the records obtained by each group.

The significant problems associated with this effort are described in the subsequent chapters.

CHAPTER II

FUNDAMENTAL CONSIDERATIONS OF DATA PROCESSING

Under certain conditions a time function can be transformed into the frequency domain by one of several methods. The methods that transform the time function directly will result in a frequency domain description in the form of a complex function of frequency. The magnitude of this function gives an indication of the extent to which various frequencies are present in the time function and can thus be used to indicate the frequency content of the time function. For example, a periodic wave of infinite extent in time can be represented in the frequency domain by complex Fourier coefficients. Each coefficient indicates the extent that a particular frequency is present in the time record. An aperiodic time function can be represented in the frequency domain under certain conditions by its Fourier transform. The magnitude of the Fourier transform expresses the frequency content as a function of frequency. This magnitude is sometimes referred to as the spectral distribution of the time function.

A direct Fourier transformation can not be made on a random function of infinite extent in time. However, when these functions satisfy certain requirements they can be represented in the frequency domain by the power spectrum. The power spectrum shows the distribution of the mean square

value of the time function over frequency.

Just as it is possible to describe in the frequency domain the input and output time function of a linear dynamic system, it is also possible to describe the dynamic system in the frequency domain by the frequency response of the system. The frequency response, also called the transfer function, describes the steady state response of the system to sinusoidal inputs. The magnitude of this complex function represents the attenuation or magnification of the sinusoidal input by the system. The phase angle represents the phase shift between the output and input sinusoids.

For a system that can be described by linear ordinary differential equations with constant coefficients, the response to an arbitrary time function can be found by using the response characteristics of the system. The time domain characteristic is the impulse response and the frequency domain characteristic is the frequency response. Results obtained by using either characteristic are equivalent.

The time response is obtained directly by convolution of the input with the impulse response of the system. If the frequency domain representation of the input is multiplied by the frequency response of the system, the frequency domain description of the time response is obtained.

A frequency response description was chosen to represent the vehicle suspension system and the pressure

measuring system used in this investigation. There are several reasons for adopting this viewpoint. One reason is that the integration associated with convolution in the time domain is more difficult than the multiplication used in the frequency domain. Another reason is that an experimental frequency response of a vehicle or pressure measuring system was easier to obtain than the impulse response. A method of applying a true impulse to a large vehicle was not available during the time that this investigation was conducted. A third reason is that with a frequency response description of the system, the effects of amplitude distortion and phase distortion may be examined independently.

The frequency response of a linear system can be found in an analytical form if all the parameters of the system are known. However, when the parameters are not known, as was the case with the vehicle and pressure measuring system used in this investigation, the frequency response may be found experimentally. The obvious way of doing this is to subject the vehicle to sinusoidal inputs and to compare the steady state output with the input. However, the vehicle used in this investigation was of such a nature as to require a very large and expensive device to produce sinusoidal inputs. Consequently, the experimental frequency response could not be obtained in this manner.

As has been indicated, the frequency characteristics of a system can be used to determine the response of the

system to an arbitrary input. Conversely, the response of the system to an arbitrary input can be used to determine the frequency characteristics. The use of this method does not require a detailed prior knowledge of the system. The determination of the frequency response characteristics of a vehicle suspension system will be referred to as the F/X calibration. For this frequency response, the vertical tire displacement X is considered the input and the change in force on the pavement is considered as the output. The determination of the frequency response characteristic of the pressure measuring system will be referred to as F/P calibration. Normally, the change in force would be considered as the input and the pressure change as the output, but since the pressure system is employed to indicate force, the inverse relationship is more convenient for this investigation. Thus pressure will be considered as input and force as output.

The systems used in this investigation were calibrated by subjecting them to a transient input x(t). The input and output y(t) were recorded on an oscillograph record. A Fourier transformation was made on y(t) and divided by a Fourier transformation that was made on x(t). This then was the frequency response Y(f).

$$Y(f) = \frac{\int_{-\infty}^{\infty} y(t)e^{-j2\pi ft}dt}{\int_{-\infty}^{\infty} x(t)e^{-j2\pi ft}dt} \qquad (1)$$

$j = \sqrt{-1}$

f: frequency (cycles per second)

t: time (seconds)

An analytical expression was, of course, not known for y(t). Nor was an analytical expression known for x(t).

Numerous problems were encountered when Equation 1 was applied to the transient records of the experimental tests of the vehicle and pressure systems used in this investigation. Several criteria had to be established in order to minimize inherent data processing errors. To best illustrate the need for these criteria, the response of a known linear second order system to a unit step input will be used. Although this system will not exactly represent the vehicle suspension system or the pressure measuring systems, it has some general properties that are common to both types of systems. A step input was chosen as a representative input since the displacement input produced by the testing device closely approximates this input. The differential equation that describes the system and the unit step response are shown in Figure 3. The analytical solution of the time response is easily found as is the analytical expression for the frequency response. The input and output can then be subjected to the same data processing procedures that were used for the actual system calibrations and the results compared to the analytical results to illustrate

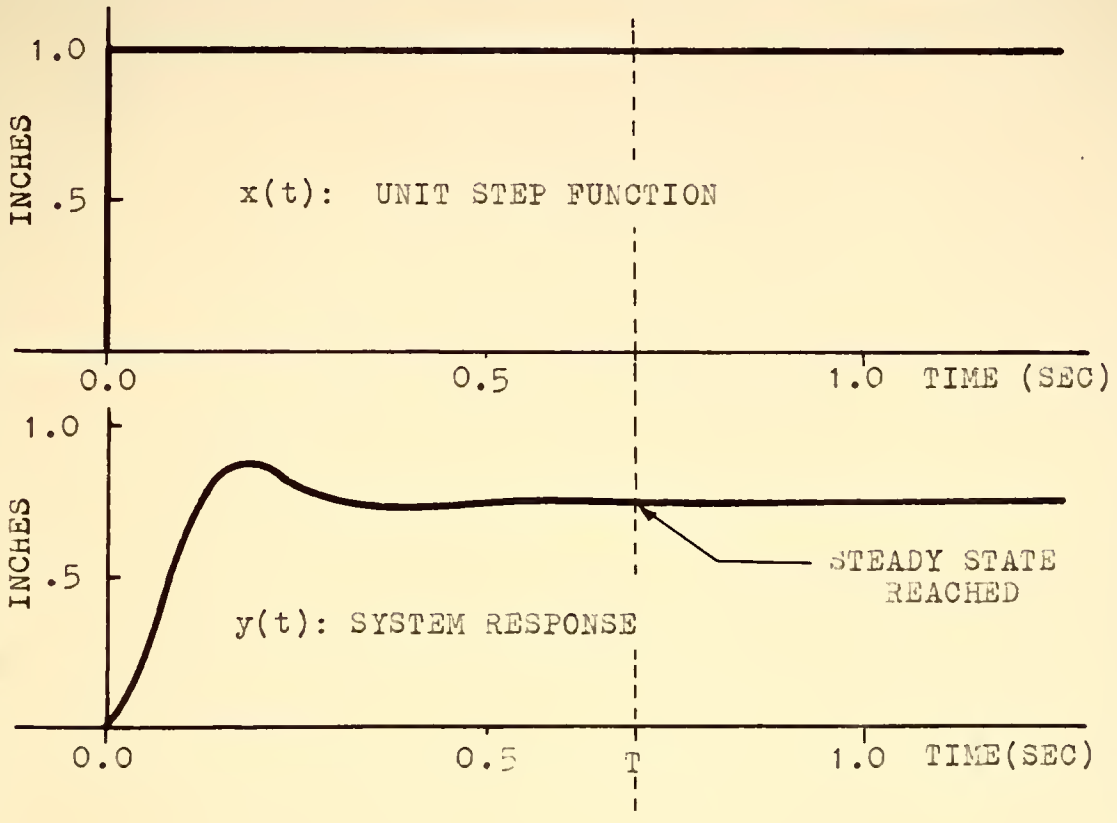

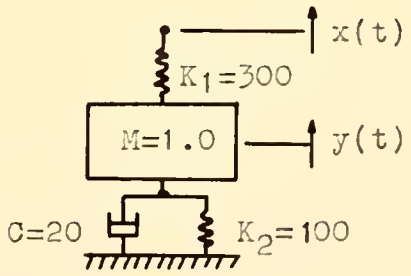

$$\frac{d^2y}{dt^2} + 20\frac{dy}{dt} + 400y = 300x$$

$$y(0) = 0; \quad \frac{dy}{dt}(0) = 0; \; x(t) = \text{UNIT STEP FUNCTION}$$

$$y(t) = .75(1-e^{-10t}(\cos 17.3t + .577\sin 17.3t))$$

FIGURE 3 RESPONSE OF A SECOND ORDER SYSTEM TO A STEP INPUT

why the criteria were chosen.

Using the input and response shown in Figure 3, there results

$$Y(f) = \frac{\int_0^T y(t)e^{-j2\pi ft}dt + \int_T^\infty .75e^{-j2\pi ft}dt}{\int_0^T e^{-j2\pi ft}dt + \int_T^\infty e^{-j2\pi ft}dt} \qquad (2)$$

T : Time at which response has reached steady state position.

The second integrals of the numerator and denominator of Equation 2 are meaningless in the form shown. An artifice that is used to overcome this difficulty is to multiply the integrands by the function $e^{-\beta(t-T)}$, integrate the product, and then pass β to a limit of zero in that order.[13,14] Following this procedure gives

$$Y(f) = \frac{\int_0^T y(t)e^{-j2\pi ft}dt + \lim_{\beta\to 0}\int_T^\infty .75e^{-\beta(t-T)}e^{-j2\pi ft}dt}{\int_0^T e^{-j2\pi ft}dt + \lim_{\beta\to 0}\int_T^\infty e^{-\beta(t-T)}e^{-j2\pi ft}dt} \qquad (3)$$

$$Y(f) = \frac{\int_0^T y(t)e^{-j2\pi ft}dt + \lim_{\beta \to 0} \frac{.75}{\beta + j2\pi f} e^{-j2\pi fT}}{\int_0^T e^{-j2\pi ft}dt + \lim_{\beta \to 0} \frac{1}{\beta + j2\pi f} e^{-j2\pi fT}} \qquad (4)$$

$$Y(f) = \frac{\int_0^T y(t)e^{-j2\pi ft}dt + \frac{.75}{j2\pi f} e^{-j2\pi fT}}{\int_0^T e^{-j2\pi ft}dt + \frac{1}{j2\pi f} e^{-j2\pi fT}} \qquad (5)$$

This method was employed to determine the integrals of Equation 1 when the input and response did not return to the initial value as was the case for both the F/P and F/A calibration tests.

The mathematical details which show that the original time functions are recovered when the Fourier integrals are obtained from these Fourier transforms are given in references (13) (14).

For the representative system described by the differential equation in Figure 3, the analytical expression for the frequency response may be written at once by substituting $j2\pi f$ for d/dt in this differential equation. The result is

$$Y(f) = \frac{.75}{1 - .0986f^2 + j.314f} \tag{6}$$

When evaluated by the method under consideration, the Fourier transforms $X(f)$ and $Y_i(f)$ of the unit step input and response of the system of Figure 3 are

$$X(f) = \frac{1}{j6.28f} \tag{7}$$

$$Y_i(f) = \frac{.75}{6.28f(j(1-.0986f^2)-.314f)} \tag{8}$$

Division of Equation 8 by Equation 7 gives

$$\frac{Y_i(f)}{X(f)} = \frac{.75}{(1-.0986f^2+j.314f)} \tag{9}$$

which is identical to Equation 6.

Although this method of calculating the Fourier transform is justified mathematically in reference (13) and (14), and the resulting Fourier transforms produced the correct frequency response for the system of Figure 3, a physical explanation of the situation will be given to aid in the understanding of the validity of this procedure when finding a frequency response. A physical explanation can be given when the problem is considered in a different manner. This explanation holds in particular for the system shown in Figure 3, and in general for many systems.

This problem would not have occurred if the aperiodic function would have returned to zero. If at some time T after the system had reached a practical steady state, the input were brought back to the initial position according to the relation

$$x(t) = e^{-\beta(t-T)}, \quad (t > T) \tag{10}$$

β : real constant greater than zero

the system output would also approach zero displacement. For the system of Figure 3, the exact analytical expression

for the system response is given by the relation

$$y(t) = \frac{.75}{(.0025\beta^2 - .05\beta + 1)} \left[e^{-10(t-T)} \left[(.0025\beta^2 - .05\beta)\cos 17.3(t-T) + \frac{(.025\beta^2 + .5\beta)}{17.3} \sin 17.3(t-T) \right] + e^{-\beta(t-T)} \right] \qquad (11)$$

This expression is shown in Figure 4 for various values of β. Notice that for small values of β , $y(t)$ may be expressed approximately by the term

$$y(t) \cong .75e^{-\beta(t-T)} \qquad (12)$$

This is because there is not an abrupt change of the input displacement as at time t = 0 and a relatively small discontinuity in the velocity of the input. Consequently, the system transients decay quickly and the output approaches the steady state decaying condition.

Using 10 and 12, Y(f) may be expressed approximately by

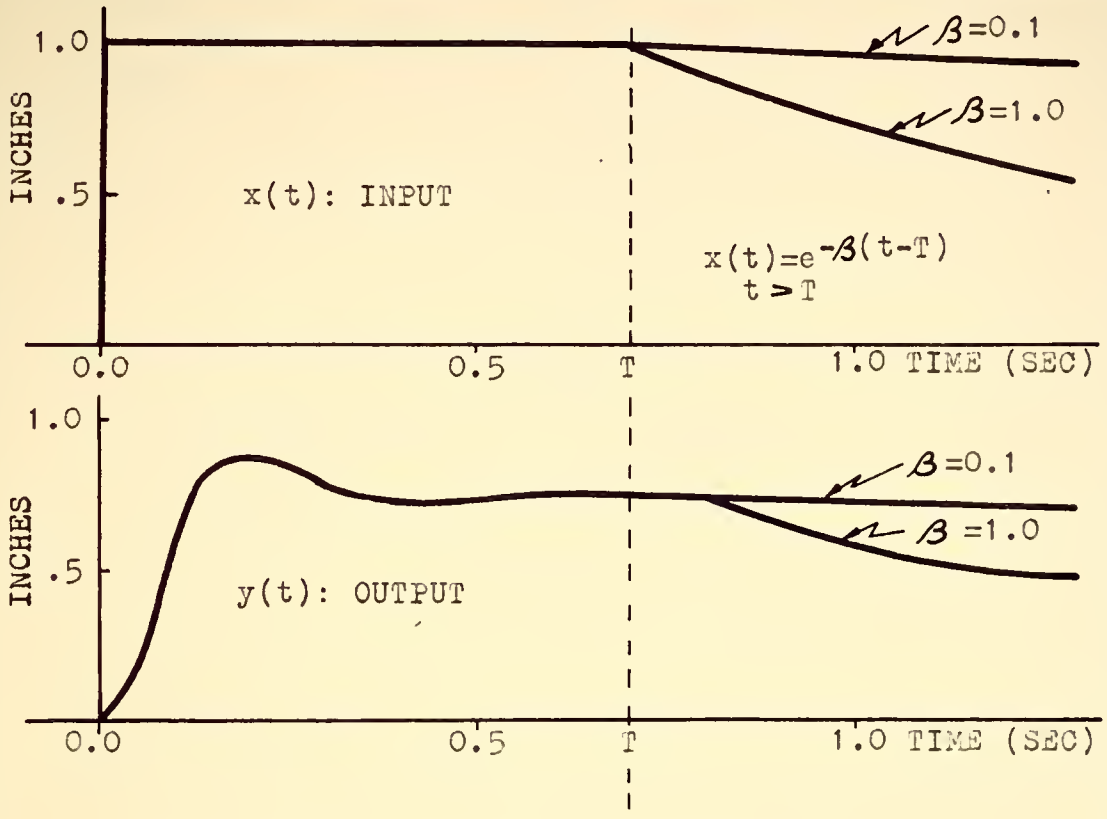

RESPONSE OF THE SYSTEM OF FIGURE 3 FOR t > T

$$y(t)=\frac{.75}{(.0025\beta^2-.05\beta+1)}\left[e^{-10(t-T)}\left|(.0025\beta^2-.05\beta)\cos 17.3(t-T)\right.\right.$$
$$\left.\left.+\frac{(.025\beta^2+.5\beta)}{17.3}\sin 17.3(t-T)\right|+e^{-\beta(t-T)}\right]$$

FIGURE 4 SECOND ORDER SYSTEM RESPONSE TO A DECAYING EXPONENTIAL

$$Y(f) \cong \frac{\int_0^T y(t)e^{-j2\pi ft}dt + \int_T^\infty .75e^{-\beta(t-T)}e^{-j2\pi ft}dt}{\int_0^T e^{-j2\pi ft}dt + \int_T^\infty e^{-\beta(t-T)}e^{-j2\pi ft}dt} \qquad (13)$$

$$Y(f) \cong \frac{\int_0^T y(t)e^{-j2\pi ft}dt + \frac{.75}{\beta+j2\pi f}e^{-j2\pi fT}}{\int_0^T e^{-j2\pi ft}dt + \frac{1}{\beta+j2\pi f}e^{-j2\pi fT}} \qquad (14)$$

The smaller β is taken the more nearly the equality of 12 will hold and hence those of 13 and 14. β can be taken as small as needed in 14 for all f of practical interest except f = 0. Thus instead of considering $e^{-\beta(t-T)}$ as an mathematical artifice, it may be viewed as an experiment that could be performed but was not. In other words, all the information about the dynamics of the system is contained in the first T seconds. No additional information is obtained after T, except possibly a constant gain.

Although a completely known second order system was used to demonstrate this point, similar reasoning may be applied to unknown systems that have a constant steady state step response.

When an unknown physical system is experimentally subjected to transient excitation, the analytical expression for the output is unknown. The input is sometimes known, but generally it is any available disturbance that has proper frequency content. During the test the input and output are recorded on an oscillograph record. The values of these traces at uniformly spaced increments of the time scale are tabulated at a later time. The tabulation of output describes $y(t)$ in Equation 1 and the input tabulation is $x(t)$. To evaluate the integrals of Equation 1, a numerical integration is performed on these tabulations. For illustration, a frequency response was made using the tabulations of the step input and the step response of the example linear second order system of Figure 3 following the same procedures as were used in the actual data processing of the records of input and output for the vehicle suspension and pressure systems used in the investigation. The magnitude of this frequency response and the magnitude of the analytical expression for the frequency response are illustrated in Figure 5. The difference between the curves illustrates the inaccuracies that result from this method of data processing. The data used for $y(t)$ was sampled at .005 second intervals and contained 3 significant figures. The errors of the frequency response are primarily due to the Fourier transform of the output. The Fourier transform of the input agreed well with

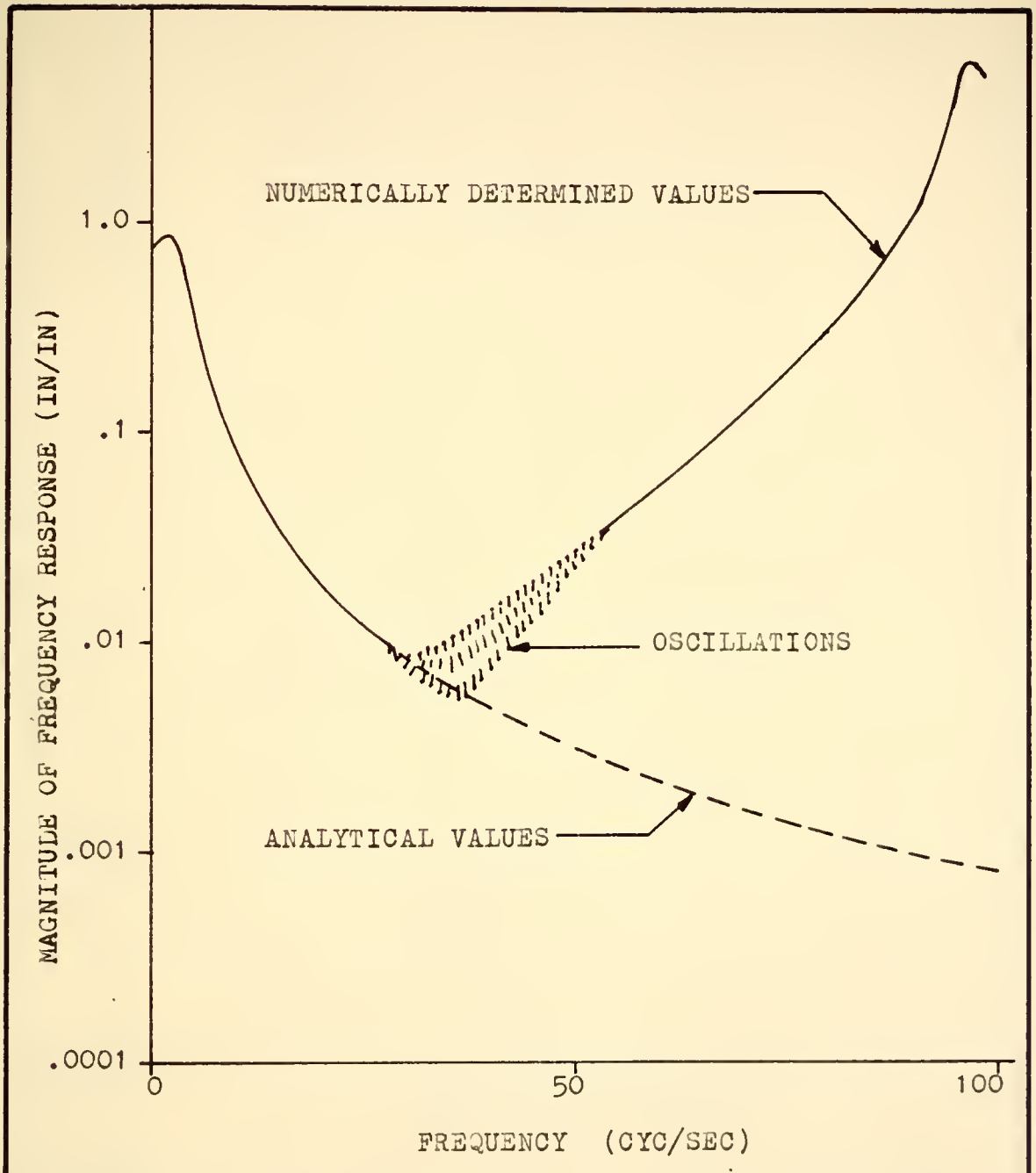

DATA SPACING=.005 SEC NYQUIST FREQUENCY=100 CYC/SEC

FIGURE 5 FREQUENCY RESPONSE FOR A SECOND ORDER SYSTEM

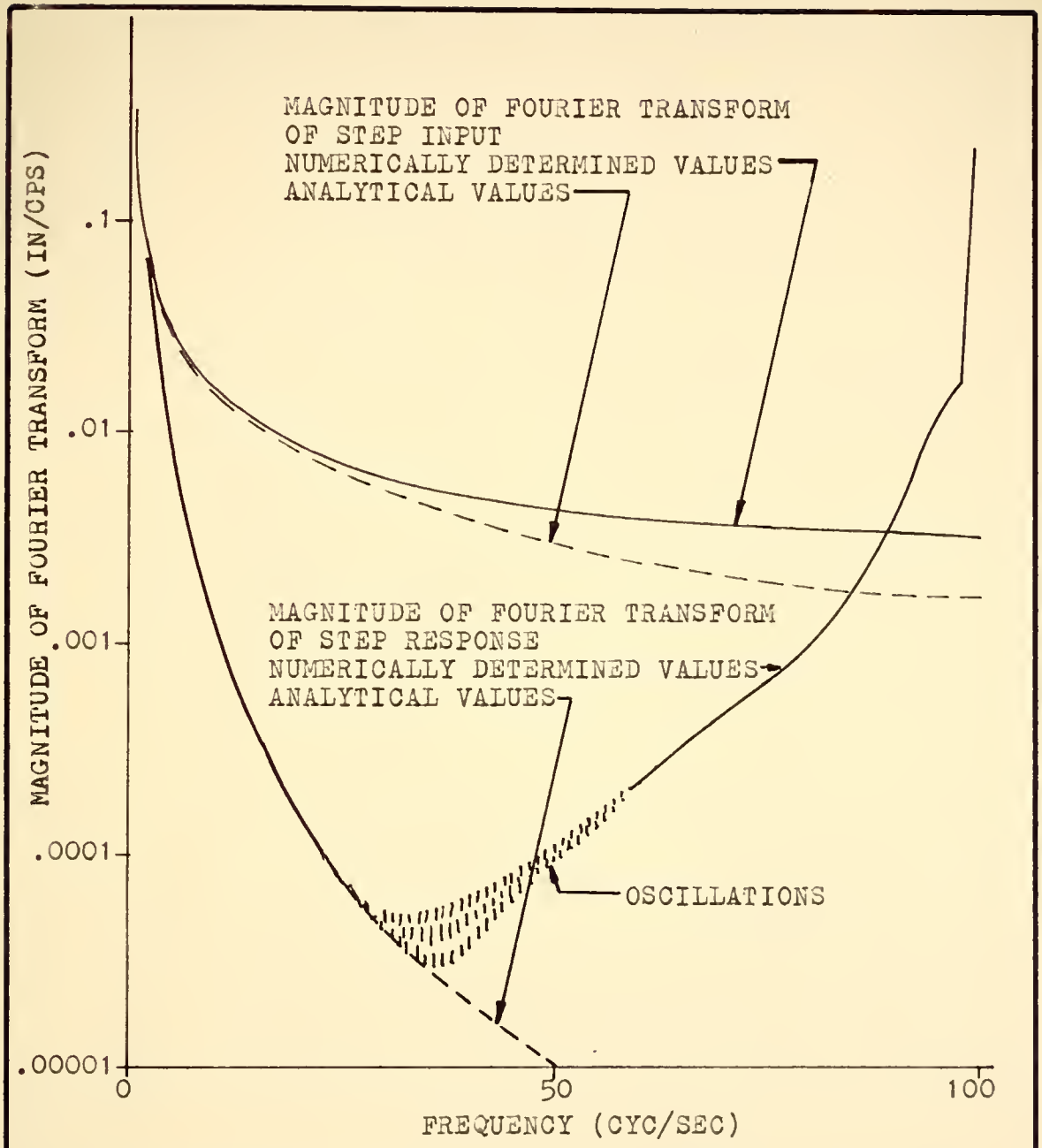

DATA SPACING=.005 SEC NYQUIST FREQUENCY= 100 CYC/SEC

FIGURE 6 MAGNITUDES OF THE FOURIER TRANSFORMS FOR THE INPUT AND OUTPUT OF A SECOND ORDER SYSTEM

the analytical transform as is shown in Figure 6. The scale of Figure 5 was chosen to accentuate the errors that do occur. The representation is good to 30 cps. There are many possible causes for the errors above 30 cps and these will be discussed. Criteria will be obtained that will minimize these errors.

One of the first problems that must be recognized when working with sampled data is aliasing.[15] If a function $z(t)$ is sampled at uniformly spaced time intervals of width Δt, then the maximum frequency f_m that can possibly be detected from the sample is

$$f_m = \frac{1}{2\Delta t} \tag{15}$$

This frequency will be referred to as the Nyquist frequency. What happens to frequencies in the original record that are higher than f_m? The answer is that they are confused with frequencies between 0 and f_m. This confusion, called aliasing, is illustrated in Figure 7. When a Fourier transform is made on the data, part of the frequency content of the high frequencies appears in the lower frequencies.

The data used to numerically calculate the Fourier transforms for Figure 5 had a Nyquist frequency well above any expected appreciable frequency content. To better illustrate the effect of aliasing on a Fourier transform, a small amplitude 120 cps sine wave was added to the step

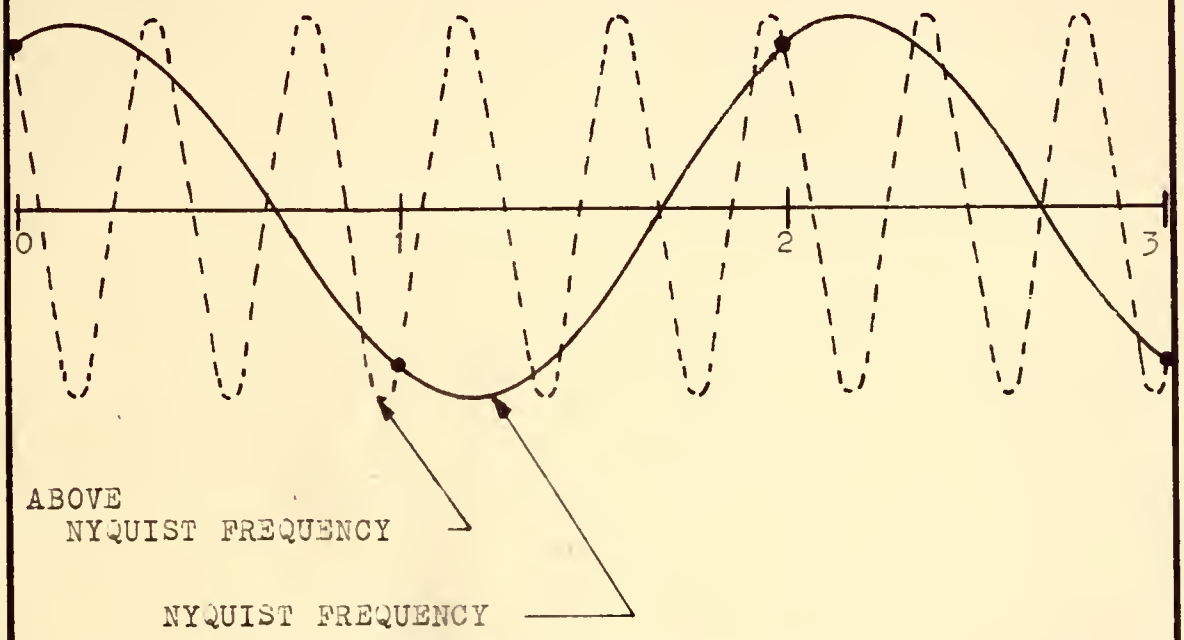

BOTH FUNCTIONS TAKE THE SAME VALUE AT t=0,1,2,3,.....

WHEN DATA IS SAMPLED AT t=0,1,2,3,.....THERE IS NO WAY TO DISTINGUISH BETWEEN THE TWO WAVES

THE NYQUIST FREQUENCY IS THE HIGHEST FREQUENCY THAT MAY BE RECOGNIZED IN A RECORD. THERE ARE TWO SAMPLES PER CYCLE.

FIGURE 7 ILLUSTRATION OF ALIASING

response function of the system of Figure 3 during the time from 0 to T. The data was then sampled at a rate that placed the Nyquist frequency at 100 cps which was below the high frequency sinusoid. Figure 8 shows the magnitude of the Fourier transform that was numerically calculated from this data. Also shown in Figure 8 is the plot of the magnitude of the analytical Fourier transform of the sum of the step response and the high frequency finite length sinusoid.

The numerically determined transform in Figure 8 exhibits two definite peaks that are not present in the transform obtained from data that did not contain the 120 cps sine wave. These peaks are caused by aliasing of the high frequency with frequencies between 0 and 100 cps.

Because there is only one finite length high frequency discrete sine wave present in the data, it is possible to qualitatively explain the peaks at 20 and 80 cps. When a 120, 80, or 20 cps sine wave is sampled at .005 second intervals starting at zero, the magnitude of all waves at each interval will be equal. The polarity of the 80 cps wave will always be opposite to the polarity of the 120 cps sine wave. This fact can be shown to account for the peak at 80 cps. The polarity of the 20 cps wave will be the same as the 120 cps wave at even time increments and opposite at odd time increments. This property and the Simpson integration coefficients will cause a peak to occur at 20 cps.

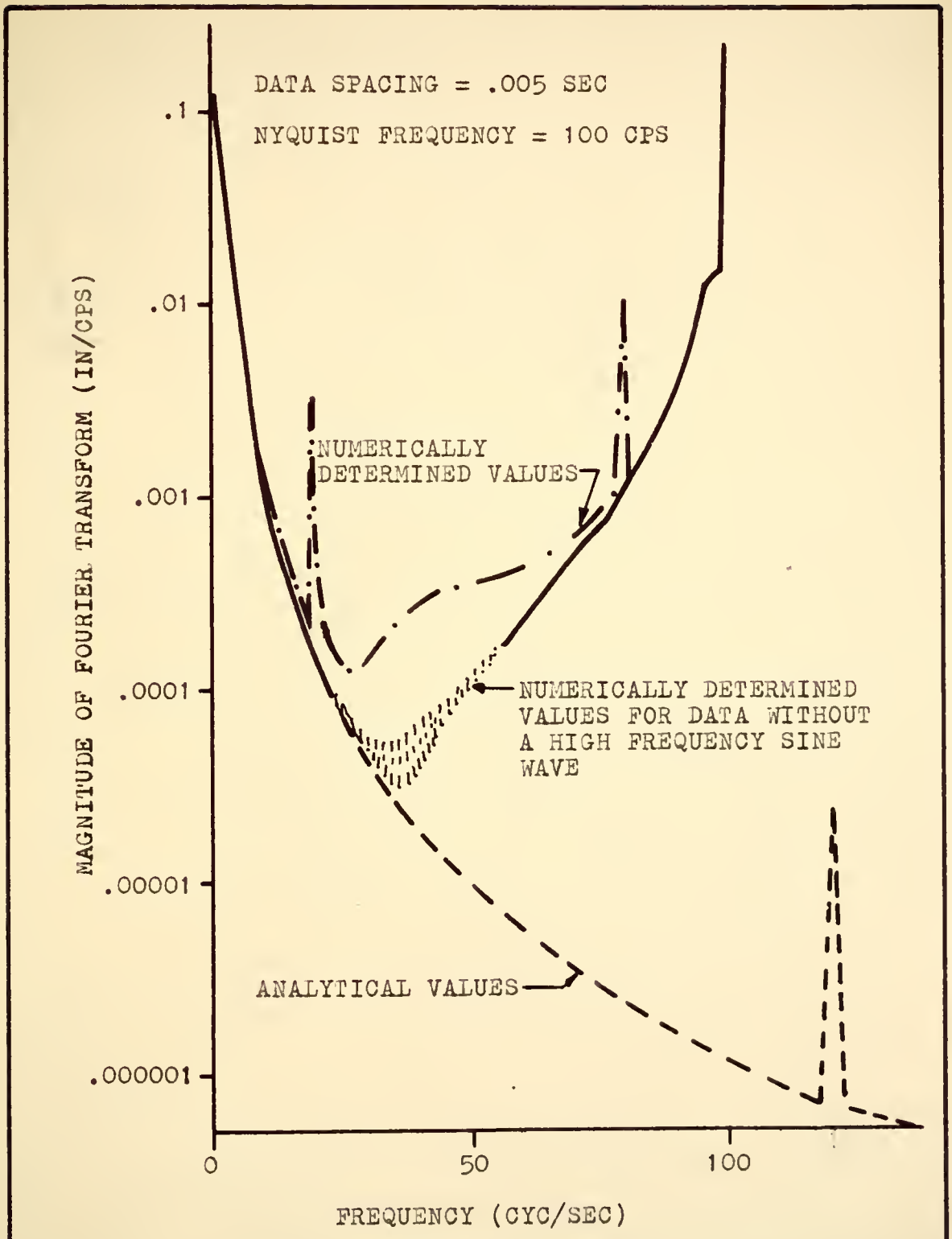

FIGURE 8 NUMERICALLY DETERMINED FOURIER TRANSFORM WHERE ALIASING HAS OCCURED

The criterion that may be stated from these results is that the sample spacing must be small enough to cause the Nyquist frequency to fall at a higher frequency than any appreciable true frequency content of the time record.

A second problem encountered in the evaluation of Equation 1 is the error produced by the numerical integration procedure. Simpson's rule integration procedure was used to integrate the product $f(t)e^{-j2\pi ft}$. This procedure will give exact results when a polynomial of degree not greater than three is integrated.[16] When the function to be integrated is only the sinusoid $e^{j2\pi ft}$, the error per step of integration can be expressed as a function of frequency.[15] The error per step of integration for Simpson's rule and the trapezoidal rule are shown as a function of frequency in Figure 9. Note that at high frequencies, the Simpson's procedure magnifies the result and the trapezoidal procedure attenuates the result.

It is not possible to apply the results shown in Figure 9 directly to the evaluation of the integrals of Equation 1 because the product $f(t)e^{-j2\pi ft}$ is to be integrated. However, Figure 9 does give an indication that Simpson's rule can not possibly give accurate results, even if f(t) were a constant, for sample rates below 5 samples per cycle. This is confirmed in Figure 5 and Figure 6 by the divergence of the numerically determined values from the analytical values at 40 cps. The transform of the step

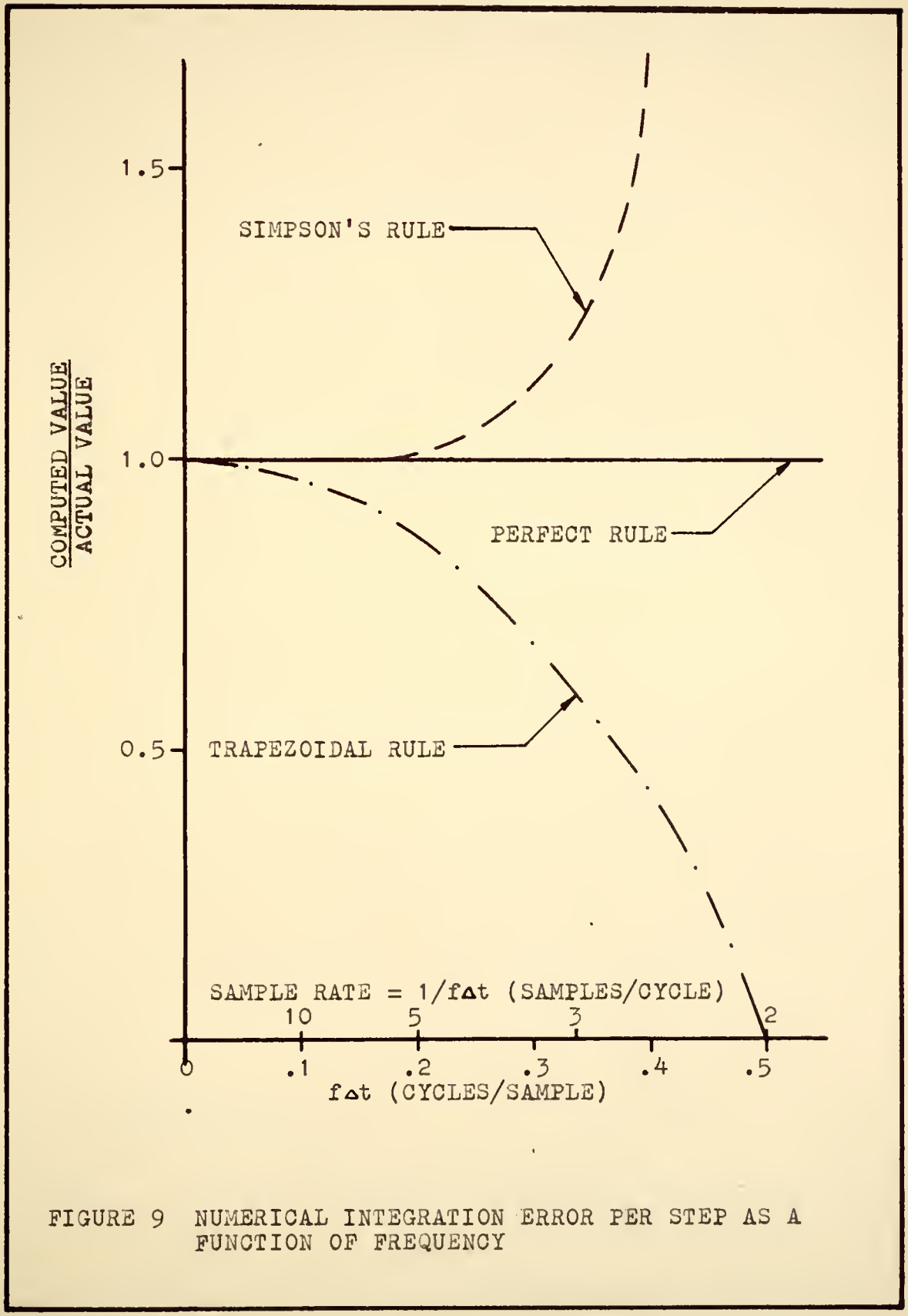

FIGURE 9 NUMERICAL INTEGRATION ERROR PER STEP AS A FUNCTION OF FREQUENCY

input does not exhibit this distortion because only 3 data values were used to determine it. The primary information for the step comes from the $1/j2\pi f$ term which results from the step not returning to zero. This is to be contrasted with the Fourier transform of the output which was calculated using 200 data values.

The criterion developed to minimize the error due to Simpson's rule distortion is to use only that part of the frequency response from zero to f_5 cps, where f_5 can be expressed by

$$f_5 = \frac{1}{5\Delta t} \tag{16}$$

Filon's method[17,18] is an alternative numerical integration procedure. Although not used extensively for the calculation of Equation 1 in this investigation, the results obtained by using this procedure will be discussed as they are an improvement on Simpson's rule. The method is an extension of Simpson's rule for the special case of evaluating integrals associated with Fourier transforms (or coefficients) of the form

$$\int_a^b f(t)\sin 2\pi ft\,dt$$

and

$$\int_a^b f(t)\cos 2\pi ft\,dt$$

The method will give exact results if f(t) is of the form

$$f(t) = A + B(t - t_o) + C(t - t_o)^2$$

where A,B,C, and t_o are constants.

Figures 10 and 11 illustrate the results of the Filon procedure compared with the analytical values. The tabulated input and output data was the same data as was used to calculate the results in Figures 5 and 6. Figure 10 shows a major improvement over the frequency response obtained by Simpson's rule integration in Figure 5. Also the oscillations between 30 and 40 cps have disappeared. Extreme distortion only occurs near the Nyquist frequency.

Dreifke[19] investigated the data processing errors incurred when finding a system frequency response from transient data. He used a numerical integration procedure to evaluate the integrals of Equation 1. While not as accurate as the Filon method, this procedure may be better than Simpson's rule. The following criteria were offered for

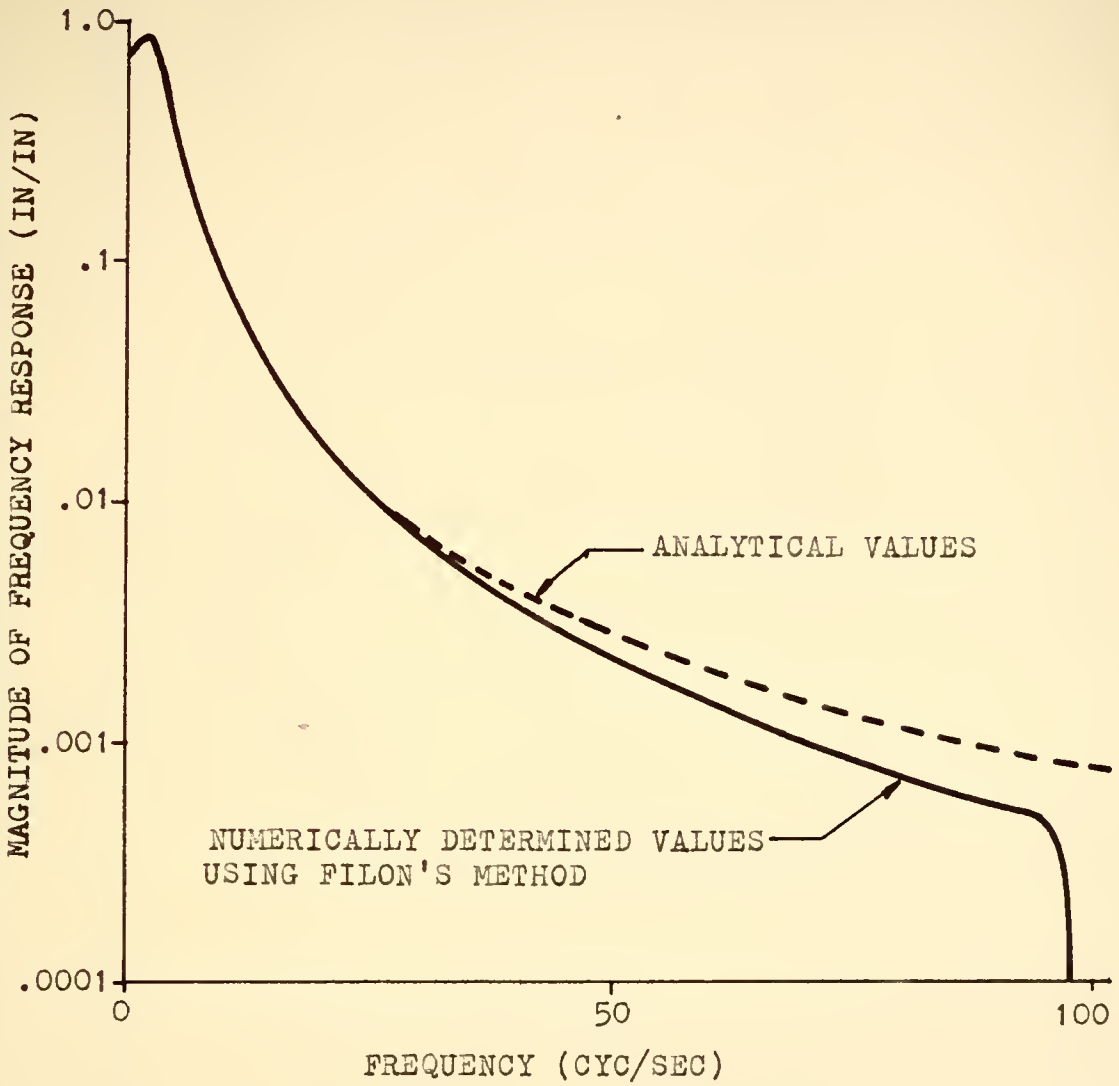

DATA SPACING = .005 SEC NYQUIST FREQUENCY = 100 CYC/SEC

FIGURE 10 COMPARISON OF THE FREQUENCY RESPONSE FOR A SECOND ORDER SYSTEM

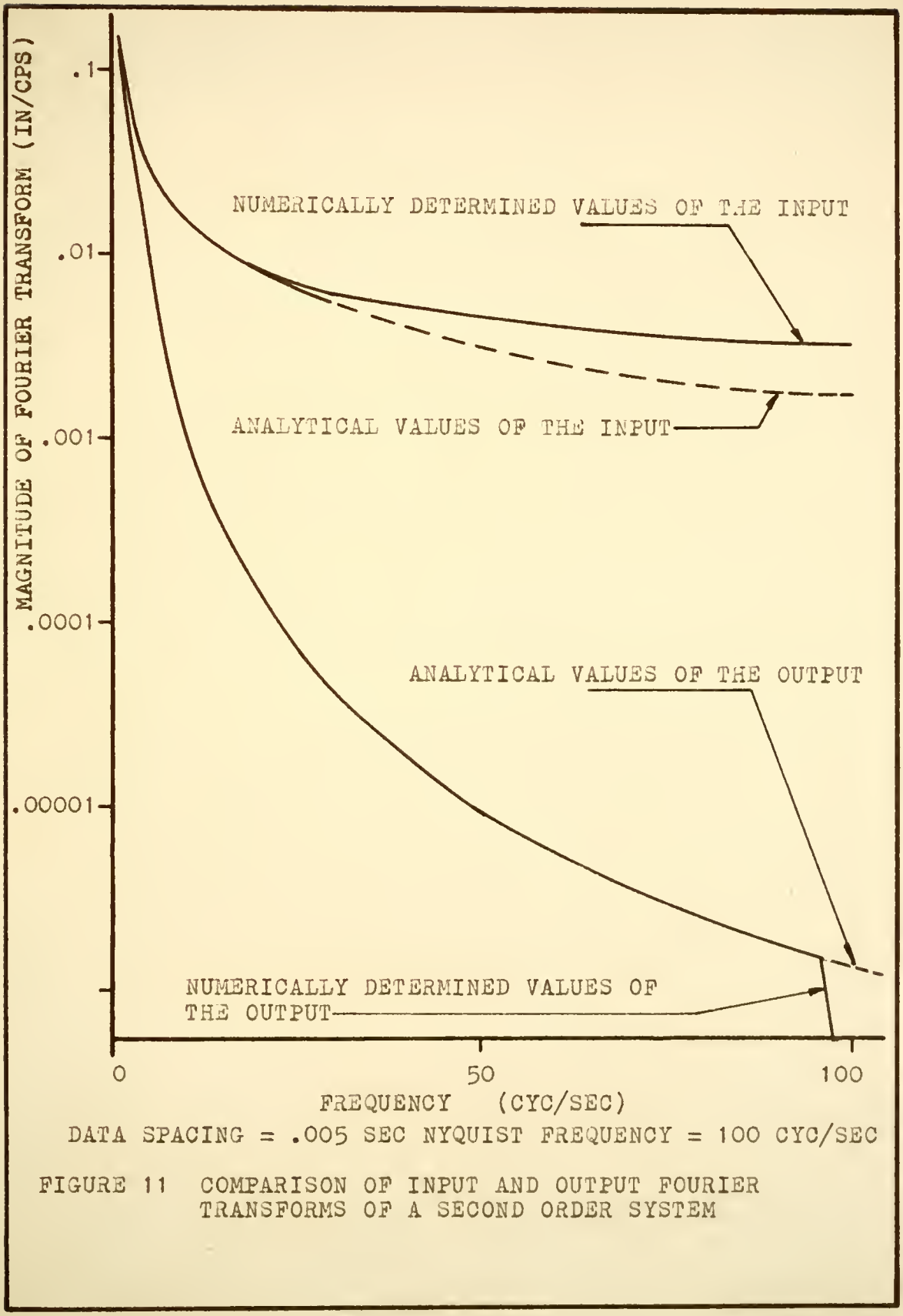

FIGURE 11 COMPARISON OF INPUT AND OUTPUT FOURIER TRANSFORMS OF A SECOND ORDER SYSTEM

approximately 25 per cent maximum error in the frequency response:

$$\omega_{max}\Delta t < \pi/2$$

$$|F(j\omega)| > 2e$$

$$\Delta t < T_1/10$$

where

T_1 = smallest characteristic time of interest in the system

e = estimated ordinate reading error in the time domain

ω_{max} = maximum angular frequency to be used

$F(j\omega)$ = either input or output Fourier transform

The first criterion suggests that the maximum usable frequency is one-half the Nyquist frequency.

The second criterion is pertinent to this investigation and will be considered in detail. The application of this criterion can be shown in the following example. The data that was used to obtain the results for Figure 5 and 6 was rounded off by various amounts and then processed by use of Simpson's rule. Figures 12 and 13 illustrate the frequency responses and output Fourier transforms obtained from this data.

Since the input function consisted of only three data

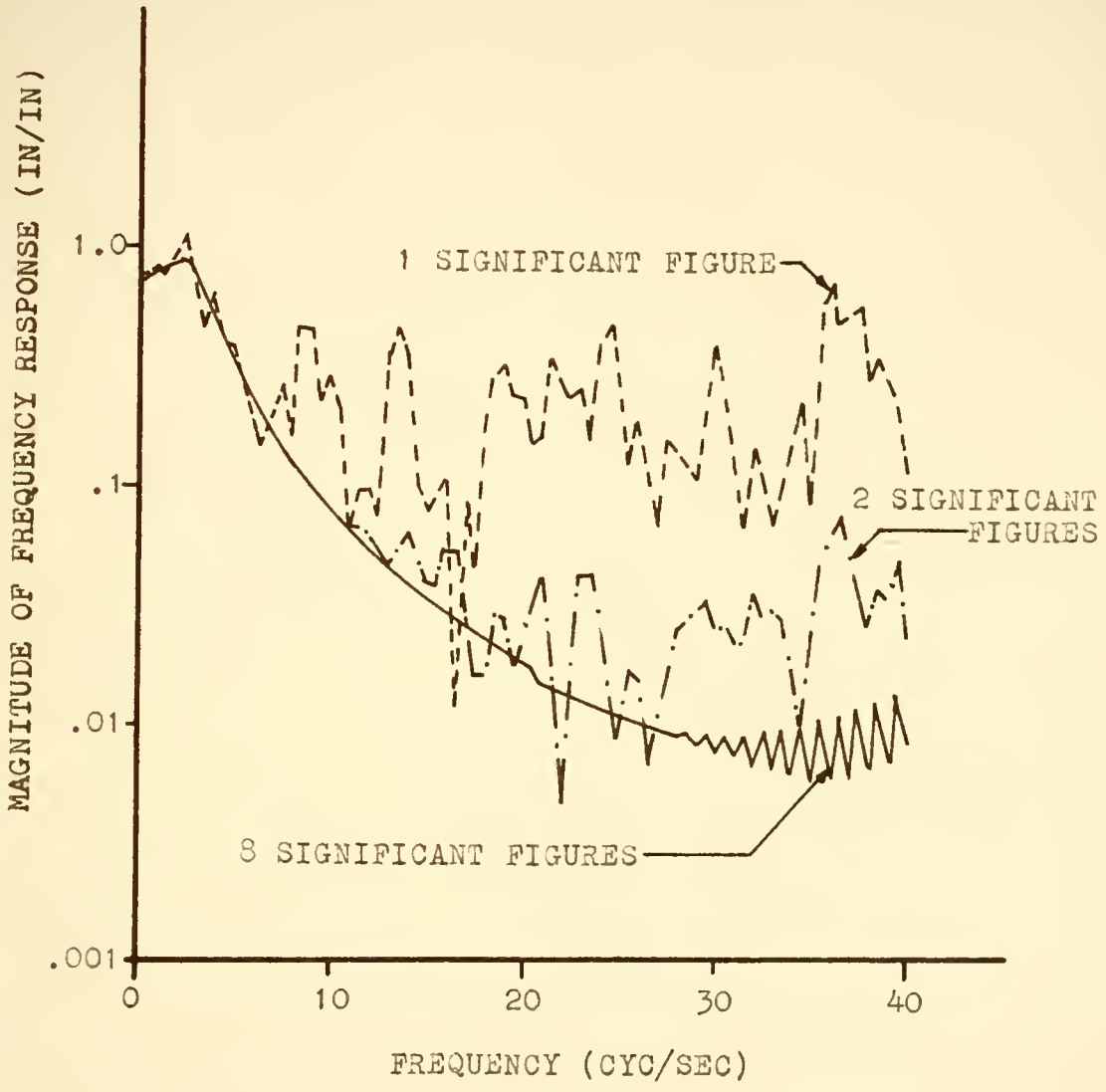

DATA SPACING = .005 SEC NYQUIST FREQUENCY = 100 CYC/SEC

FIGURE 12 FREQUENCY RESPONSE FROM DATA OF VARYING DEGREES OF ACCURACY

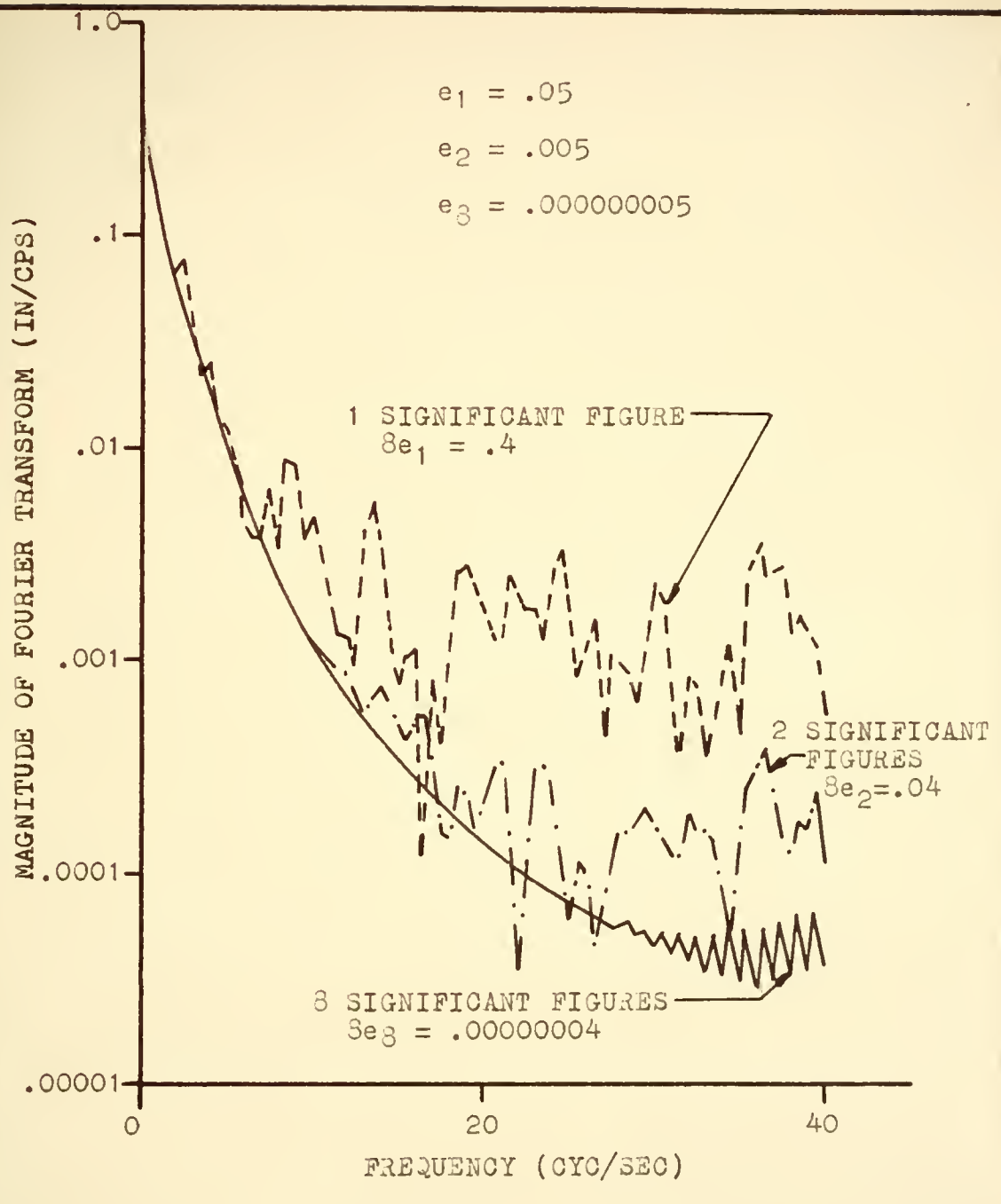

DATA SPACING = .005 SEC NYQUIST FREQUENCY = 100 CYC/SEC

FIGURE 13 FOURIER TRANSFORMS OF THE STEP RESPONSE (OUTPUT) OF A SECOND ORDER SYSTEM FOR VARYING DEGREES OF DATA ACCURACY

values (0.0, 1.0, 1.0), the scatter of points of the frequency response is due entirely to the scattering of the output Fourier transform. If the second criterion were applied to the three transforms in Figure 13 with e being taken as the round off error in the last significant figure of the data, the resulting three frequency responses would be expected to be accurate in the following ranges:

From data of one significant figure accuracy 0 - .5 cps
From data of two significant figure accuracy 0 - 5 cps
From data of eight significant figure accuracy entire range.

The analytical frequency response function for this system is given in Figure 5. Comparison of the various results shown in Figure 12 with Figure 5 indicates that the criterion holds for the results obtained from data of one significant figure accuracy, conservative results for the data of two significant figure accuracy, and is not correct for the results obtained from data of eight significant figure accuracy. The reason that the criterion fails in the last case is that Simpson's rule integration distortion overshadows the effects of data inaccuracy.

The length of transient data read and tabulated must be considered as an additional source of error in evaluating the Fourier transform. Total information can be obtained

only if the transient record is read to the point in time where the trace has reached a steady state value. But if the sampling interval is to be made as small as possible, it may not be economical to read the record this far. Figures 14 and 15 show the results when the data of the second order system shown in Figure 3 is truncated at 1.0 and .75 second. The transient had practically died out at 1.0 second but it was still present at .75 second. It appears as if no large errors will result if the records are read only to 75 per cent of the length of time until the transient has practically decayed.

Thus far the phase angle of the Fourier transforms and frequency responses have not been discussed. In power spectrum work phase angle information is not needed. However, for deterministic calculations, the phase angle of the frequency response as a function of frequency is required. Figure 16 illustrates the phase angle of the Fourier transform of the second order system step response illustrated in Figure 3. Above 20 cps the phase angle that results from Simpson's rule analysis exhibits a large oscillation. Again Filon's method shows much better results than Simpson's rule. Up to 20 cps the results from Simpson's rule fall on the analytical results. The Filon's results fall on the analytical results to 65 cps.

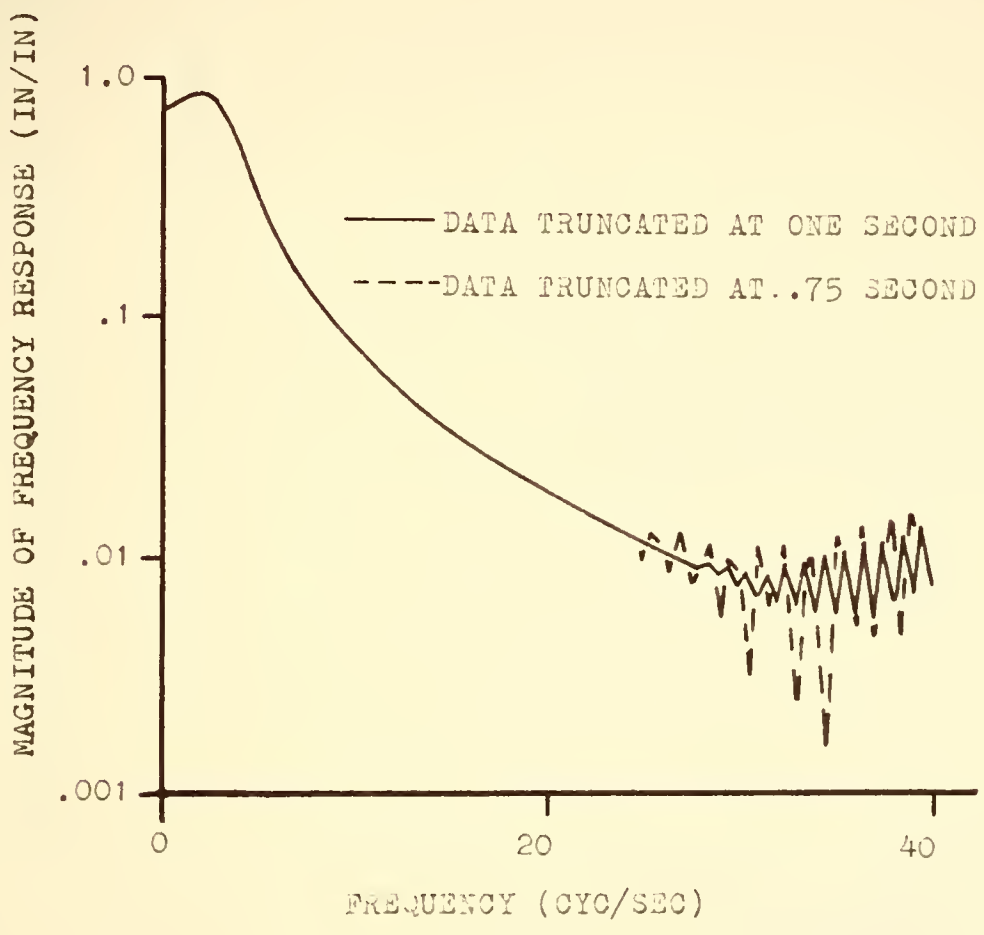

DATA SPACING = .005 SEC NYQUIST FREQUENCY = 100 CPS

FIGURE 14 MAGNITUDE OF FREQUENCY RESPONSE DETERMINED FROM TRUNCATED DATA

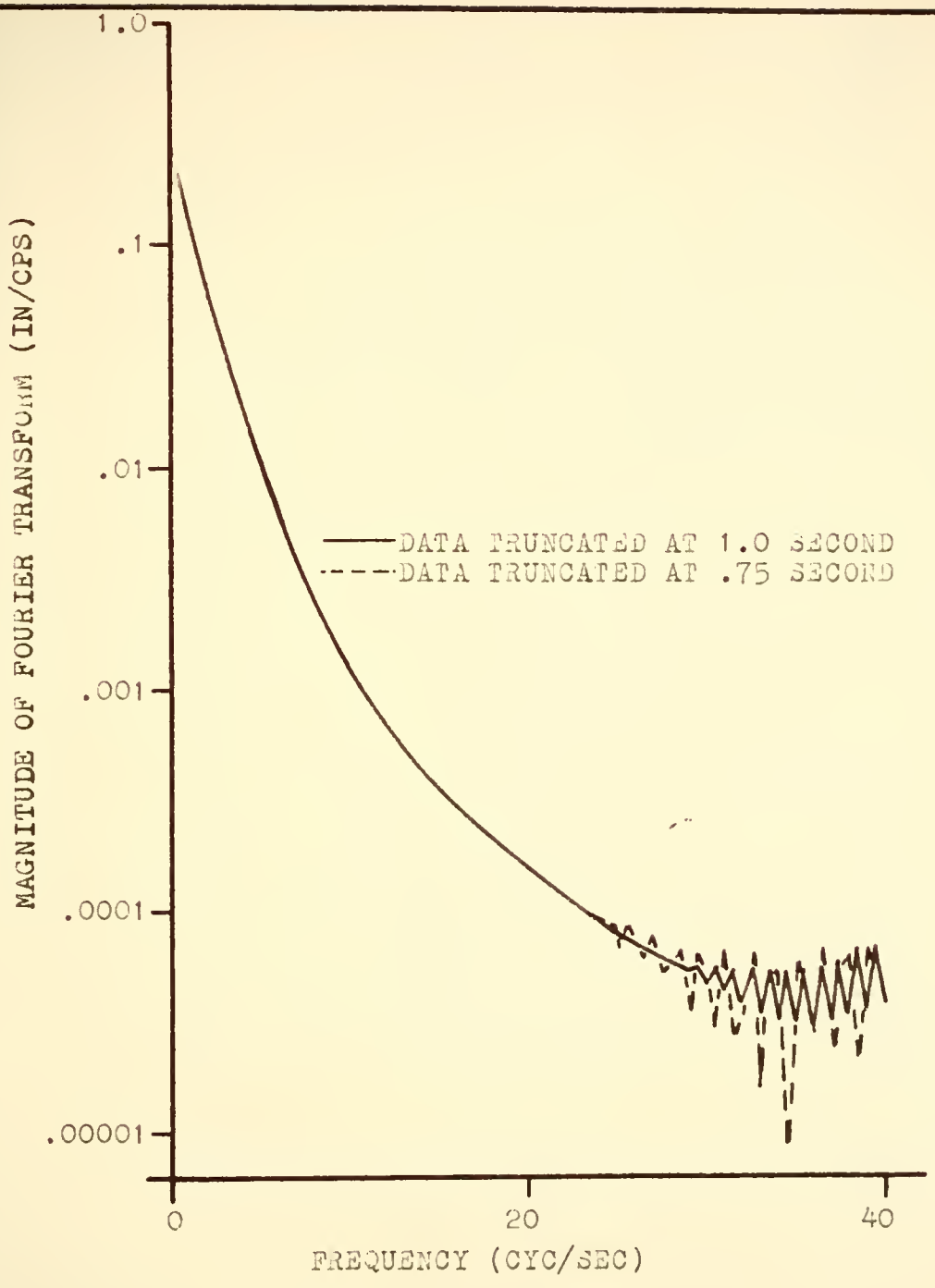

DATA SPACING = .005 SEC NYQUIST FREQUENCY = 100 CYC/SEC

FIGURE 15 MAGNITUDE OF FOURIER TRANSFORMS NUMERICALLY DETERMINED FROM TRUNCATED DATA

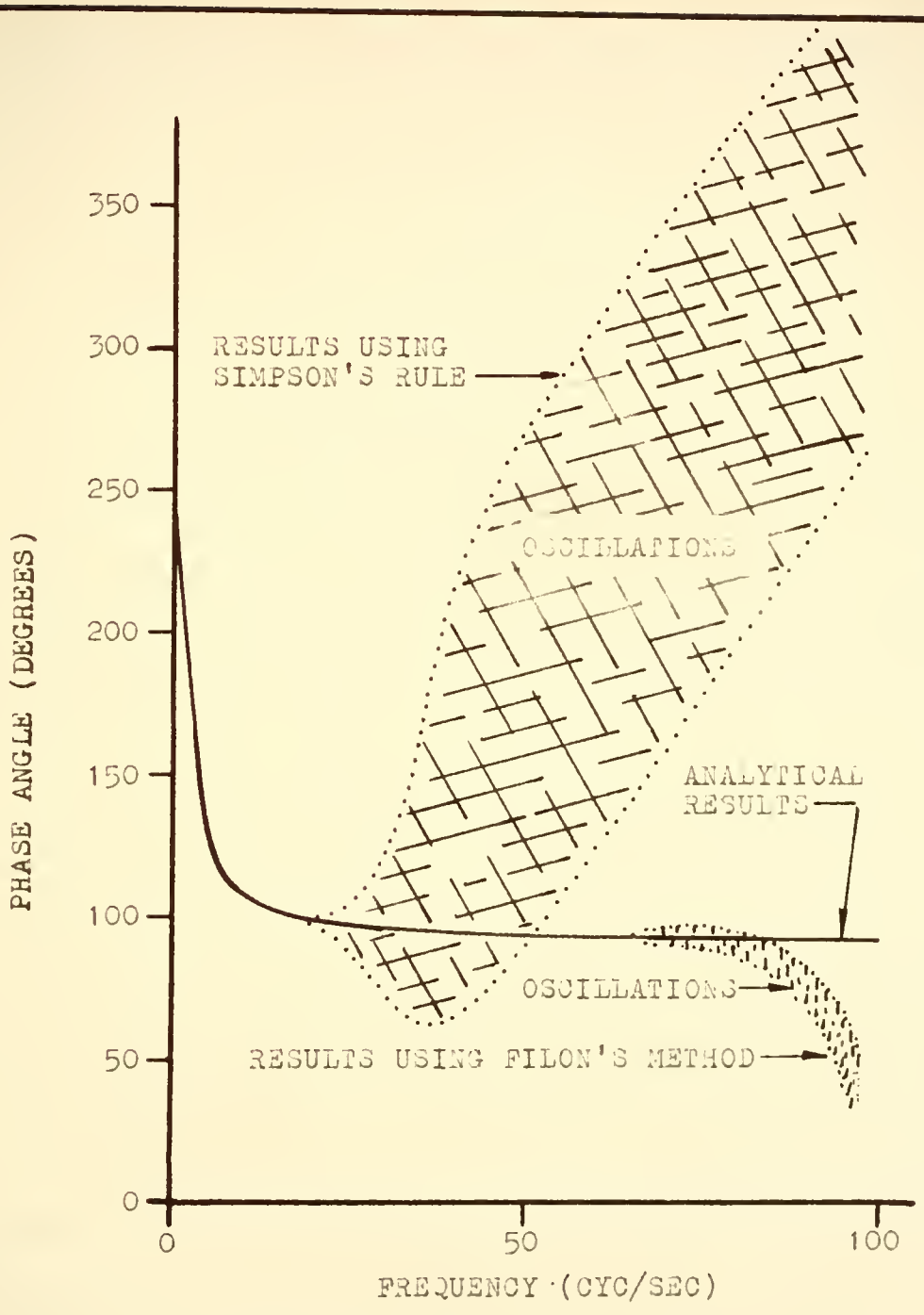

DATA SPACING = .005 SEC NYQUIST FREQUENCY = 100 CYC/SEC

FIGURE 16 PHASE ANGLE FOR THE FOURIER TRANSFORM OF THE STEP RESPONSE (OUTPUT) OF A SECOND ORDER SYSTEM

CHAPTER III

CALIBRATION OF EQUIPMENT

The vehicle used for this investigation was a single rear axle dump truck. The front tires and the dual rear tires were size 11.00/20-12 ply nominally inflated to 75 psi. Gravel was used as ballast to obtain a total static load on the rear axle of 18000 lbs and a gross vehicle weight of 26000 lbs.

In order to determine the dynamic tire forces exerted on the pavement by each tire of either set of dual tires, the dynamic air pressure in these tires was measured.

To overcome the difficulties listed in Chapter I, the pressure transducers were mounted on the side of the truck and were connected to the tires by flexible tubes and a rotating joint. The pressure measuring systems used for this investigation were specially designed and built since there were none available commercially. Part of this investigation dealt with the forces on the left side of the truck and part dealt with the forces on the right side of the truck. Thus the pressure measuring systems were designed for interchangeable use on either the left or right

set of rear duals.

The principal design objective of the pressure measuring systems was to have the first natural frequency of the pneumatic components as high as possible. To meet this objective, a design procedure similar to that developed by Wilson[5] was used.

In order to measure the tire pressure of the inner and outer dual independently, it was necessary to bring the two pressures through a rotating joint without cross-leakage. There were no commercially available rotating joints that could meet this requirement. This necessitated a rotating joint being designed and built to meet the following specifications:

1. Continuous operation at 600 rpm
2. Continuous operation at 100 psi
3. Maintain a 60 psi pressure differential between channels
4. Produce negligible wheel unbalance
5. Produce no mechanical resonances that would excite the pressure system
6. Easily adapted to either left or right side operation
7. Produce no safety hazards

The pressure measuring system for one tire is shown in Figure 17. Valves 1 and 2 are open prior to testing as the system comes to an equilibrium temperature and pressure. During a test, valve 1 is closed and the pressure transducer then indicates the difference in pressure between the reference tank pressure and the pressure at the transducer which is related to the actual tire pressure.

The equalization restriction was provided to pass any slowly varying pressure components that would be caused by the heating and cooling of the tire. To minimize the resonant peaks of the pneumatic system, two damping restrictions were provided in each pressure system. The relief valve was included for over-pressure protection of the transducer. In the event that the differential pressure across the transducer would become excessive, the relief valve would rupture and reduce the differential pressure to zero.

In order to relate the recorded differential pressure P to the tire force F, the system was experimentally calibrated. The results of this type of calibration will be referred to as F/P.

To predict the dynamic tire force F beneath a set of dual tires from highway elevation measurements, it is necessary to know the dynamic relationship between the displacement X of the tread of the tires and the dynamic tire force F under each of these tires. It was thus necessary to calibrate the truck itself to determine the relationship

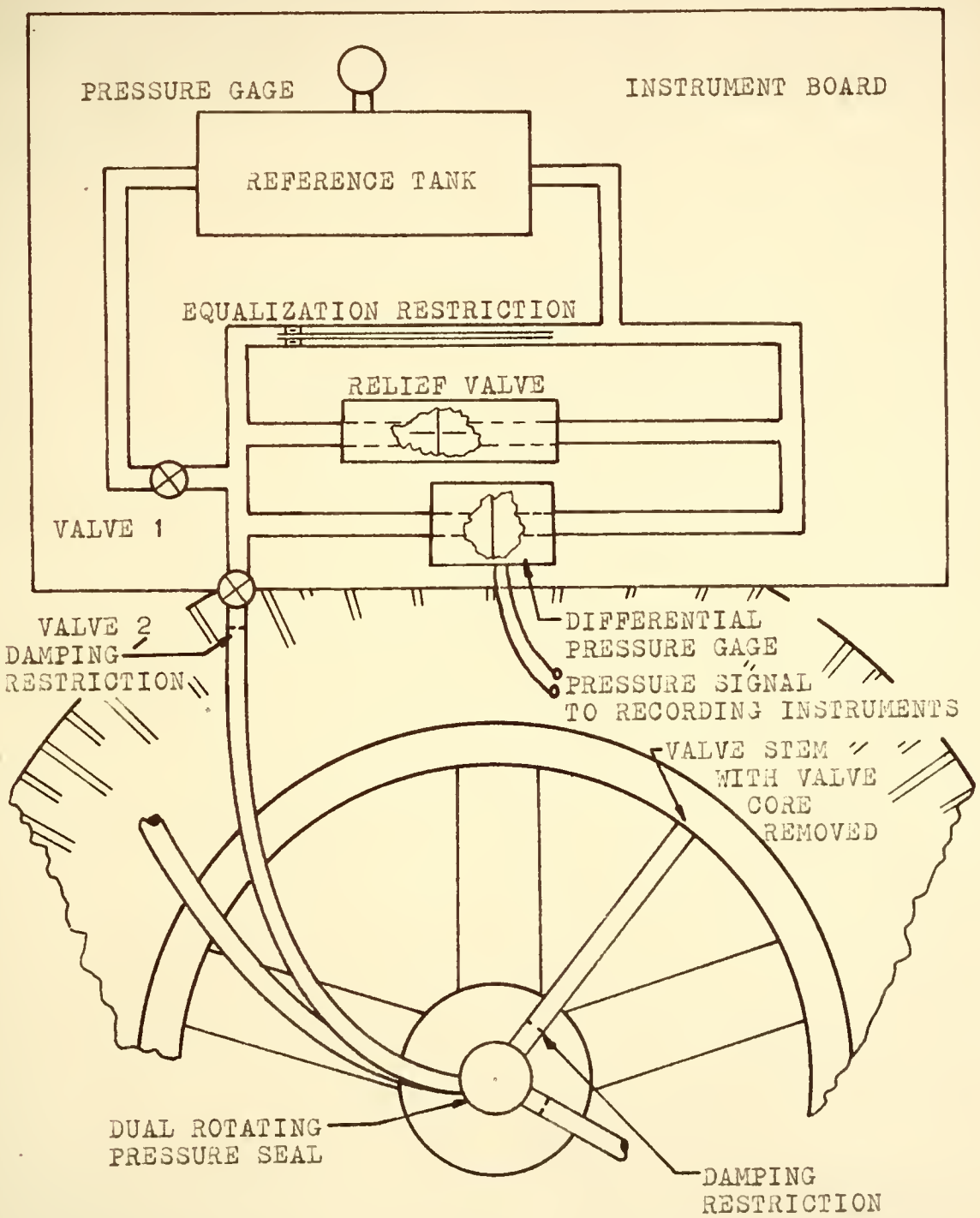

FIGURE 17 PRESSURE MEASURING SYSTEM

between tire displacement and tire force. This type of calibration relationship will be referred to as F/K.

Both the F/P and F/K relationships were found from recorded transient data of tests performed on the truck with a drop beam calibrator. This calibrator is illustrated in Figure 13. Construction details of this device are given in reference (7). The drop beam calibrator will produce a substantially vertical tire displacement input that approximates a step function. This input is applied simultaneously to both tires of the dual set. The test procedure was as follows: With the truck in position on the drop beam, the beam was raised to a preselected height. The release device was operated and the beam dropped to the down position. This transient displacement input resulted in a tire force transient and a tire pressure transient. For an F/K calibration test, tire force and displacement were measured simultaneously. The F/P calibration test required simultaneous measurement of tire force and tire pressure.

The dynamic tire force was measured with two load cells, one under each tire of the dual set. The placement of these load cells is shown in Figure 13. Each load cell had a 7000 pound capacity and a sensitivity of approximately 0.2 mm per pound at maximum amplifier sensitivity. Full scale deflection at this amplifier setting was approximately 100 pounds.

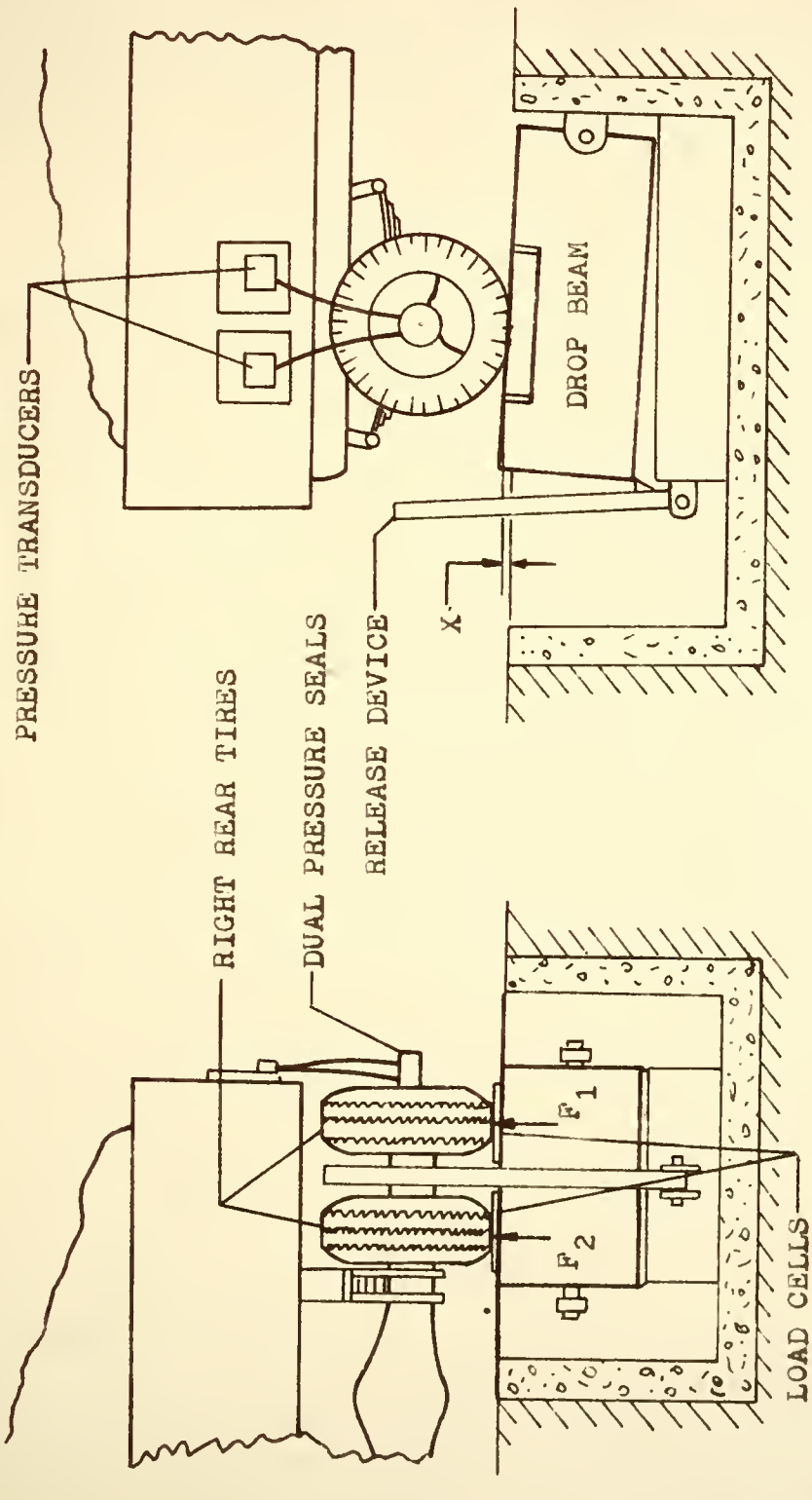

FIGURE 18 DROP BEAM CALIBRATOR

The displacement of the drop beam at the tires was the input tire displacement. This displacement was indicated during the transient testing with a potentiometer arrangement. Since the largest tire displacement was of the order of 5/8 inch, the motion of the beam beneath the tires was susstantially vertical since the distance from the beam pivot to the load cells was 36 inches. For all the calibration tests, all of the truck wheels were at the same level when the beam was down.

The sets of tire displacement-tire force and tire pressure-tire force records were read, tabulated and processed by using Equation 1 to obtain the F/X and F/P frequency responses.

The initial portions of the three sets of force and pressure records are shown in Figure 19. These are records for the F/P calibration test of the right rear inner dual tire pressure measuring system. Taree different drop heights were used in order to determine the dependence of the pressure response upon the magnitude of the input.

By using the complete transient records, the F/P frequency response curves shown in Figure 20 were obtained. Simpson's rule was used for the numerical integration. Note that, for the data spacing used in reading the records, f_5 (the maximum recommended frequency to use the results from this integration procedure) is 62.5 cps. Duplicate results were obtained when Filon's procedure was employed

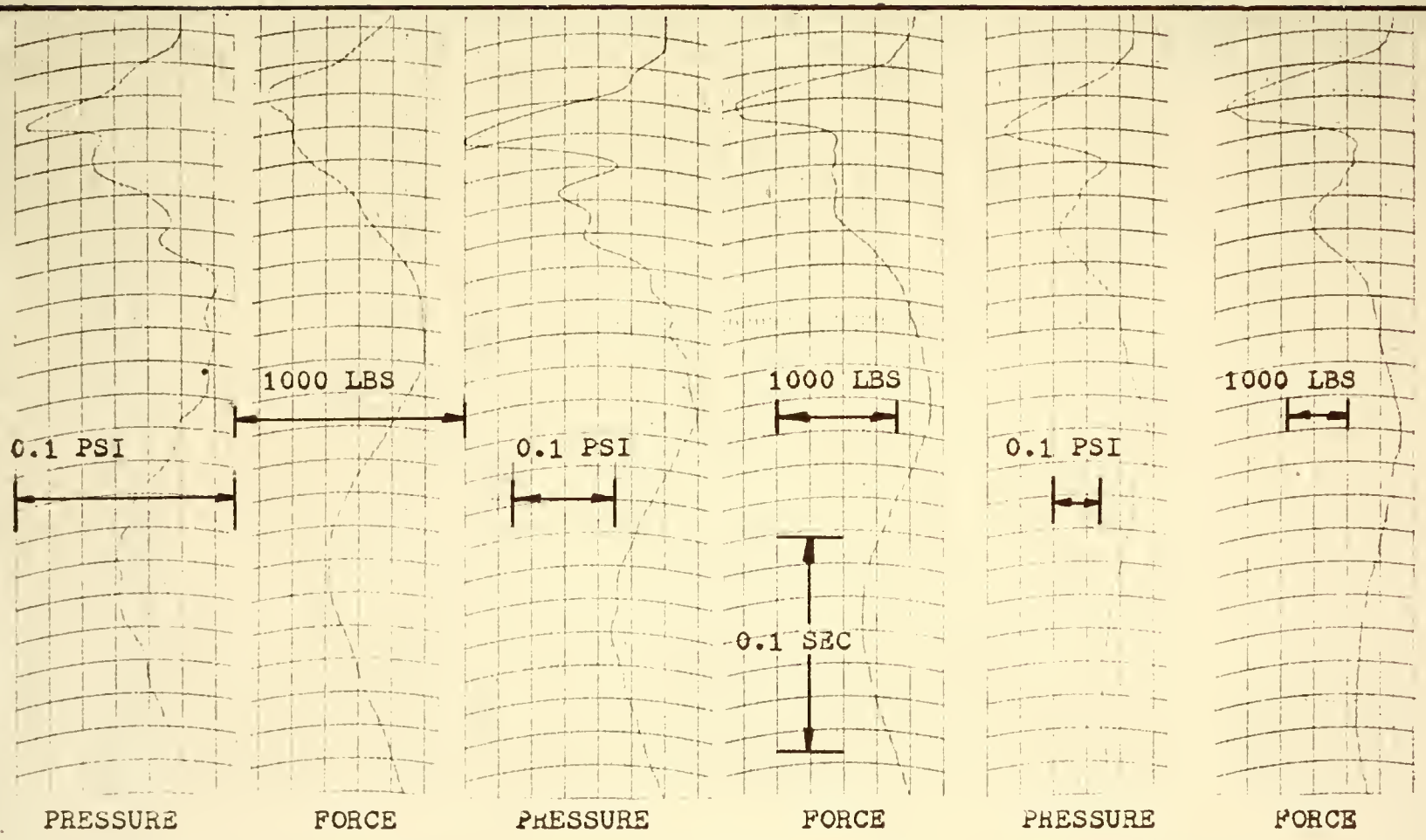

FIGURE 19 FORCE AND PRESSURE RECORDS FOR CALIBRATION TESTS OF RIGHT REAR INNER DUAL AT THREE DIFFERENT DROP HEIGHTS

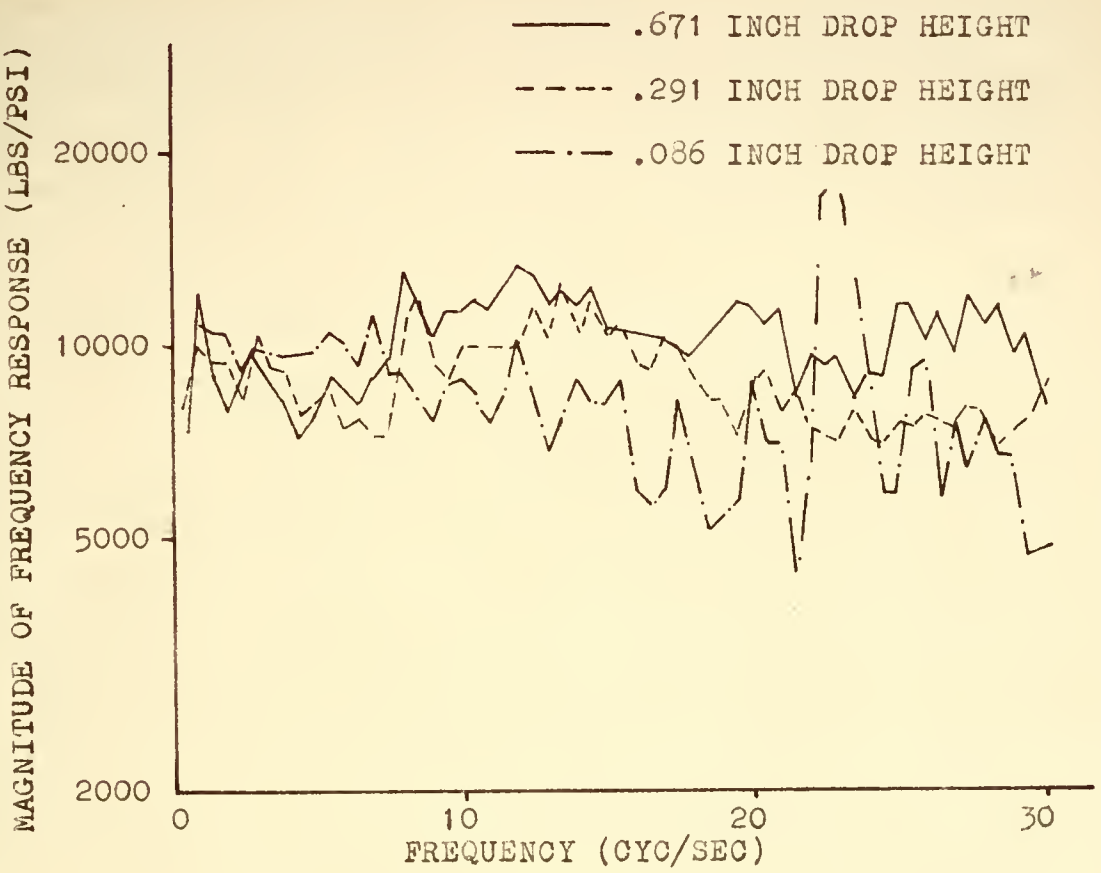

DATA SPACING = .003205 SEC

NYQUIST FREQUENCY = 156 CYC/SEC

f_5 = 62.5 CYC/SEC

FIGURE 20 MAGNITUDE OF FREQUENCY RESPONSES FOR THE F/P CALIBRATION TESTS OF THE RIGHT REAR INNER DUAL

for the numerical integration. Evidently the numerical integration procedure was not the reason for the erratic results illustrated. Aliasing may be also ruled out since the record traces were recorded on an oscillograph that had an 30 cps bandwidth.

Figures 21 and 22 illustrate the apparent reason for the questionable results indicated in Figure 20. These figures show the magnitudes of the Fourier transforms of the transient force and pressure records. The transforms are used as the numerators and denominators of Equation 1 to determine the frequency response curves shown in Figure 20. The 3e error criterion suggested by Driefke[19] is indicated for each transform. This criterion is in some respects analogous to a signal-to-noise ratio criterion where the signal would correspond to the transform and the noise would correspond to the data reading error. It is apparent in Figure 21 and 22 that for both the force and the pressure transforms there is only a small portion of the Fourier transforms that fall above the 3e line. Hence only in a small region of frequency will the criterion be satisfied, i.e. the signal-to-noise ratio is in general too small.

The frequency scale was magnified to clearly depict the low frequency region from 0 to 3 cps in Figures 23, 24, and 25. These figures illustrate the magnitude of the pressure transform, force transform, and frequency response

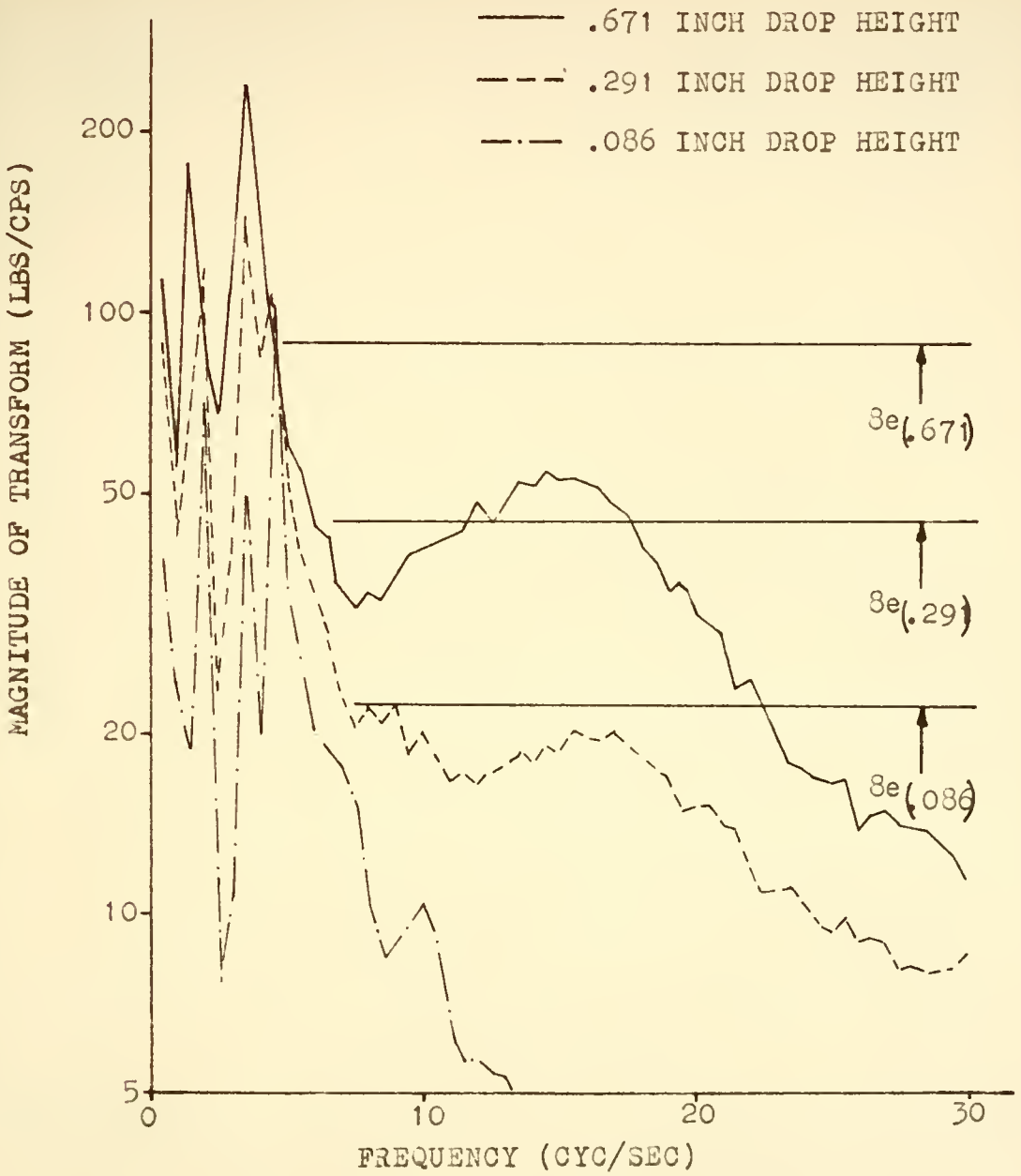

DATA SPACING = .003205 SEC NYQUIST FREQUENCY = 156 CPS
f_5 = 62.5 CPS

DATA ACCURACY (e):

$e_{(.086)} = \pm 2.8$ LBS	$8e_{(.086)} = 22.4$
$e_{(.291)} = \pm 5.6$ LBS	$8e_{(.291)} = 44.8$
$e_{(.671)} = \pm 11.2$ LBS	$8e_{(.671)} = 89.6$

FIGURE 21 FOURIER TRANSFORMS OF FORCE RECORDS FOR F/P CALIBRATION OF RIGHT REAR INNER DUAL

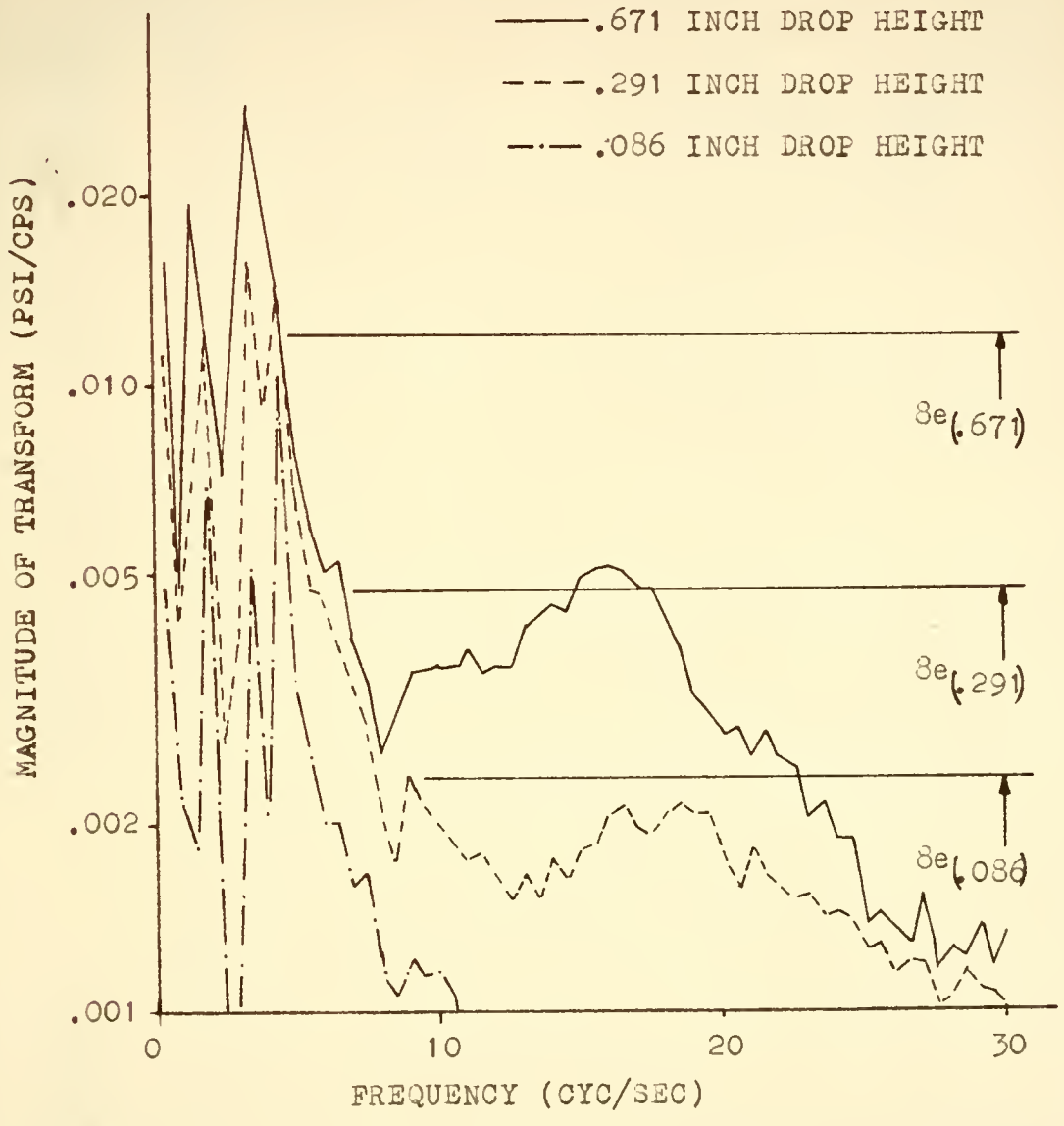

DATA SPACING = .003205 SEC NYQUIST FREQUENCY = 156 CYC/SEC
f_5 = 62.5 CYC/SEC

DATA ACCURACY (e):

$e_{(.086)} = \pm .000297$ PSI	$8e_{(.086)} = .00238$
$e_{(.291)} = \pm .000594$ PSI	$8e_{(.291)} = .00476$
$e_{(.671)} = \pm .001485$ PSI	$8e_{(.671)} = .01188$

FIGURE 22 FOURIER TRANSFORMS OF PRESSURE RECORDS FOR F/P CALIBRATION OF RIGHT REAR INNER DUAL

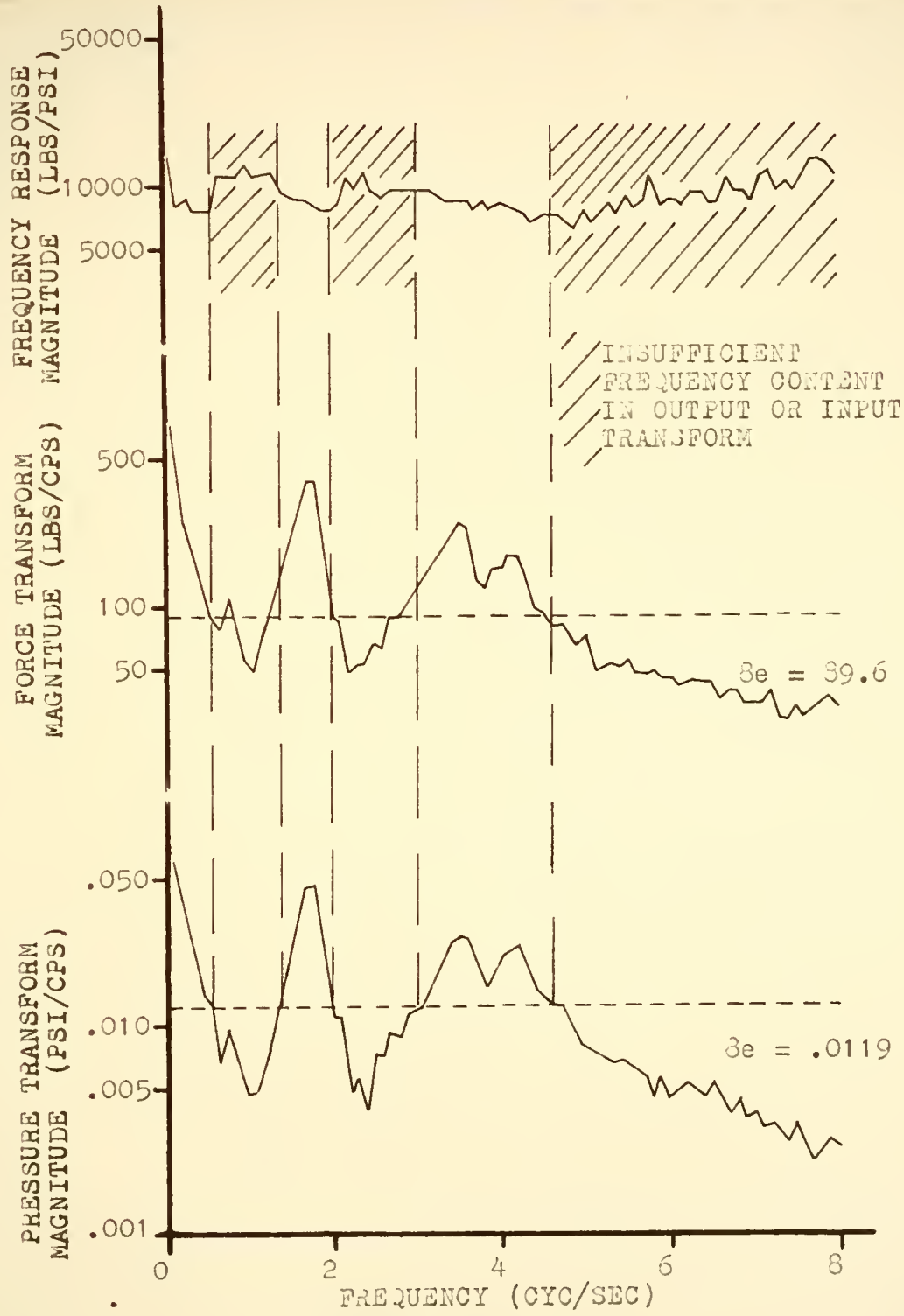

FIGURE 23 F/P TEST RESULTS FROM A .671 INCH DROP TEST OF THE RIGHT REAR INNER DUAL

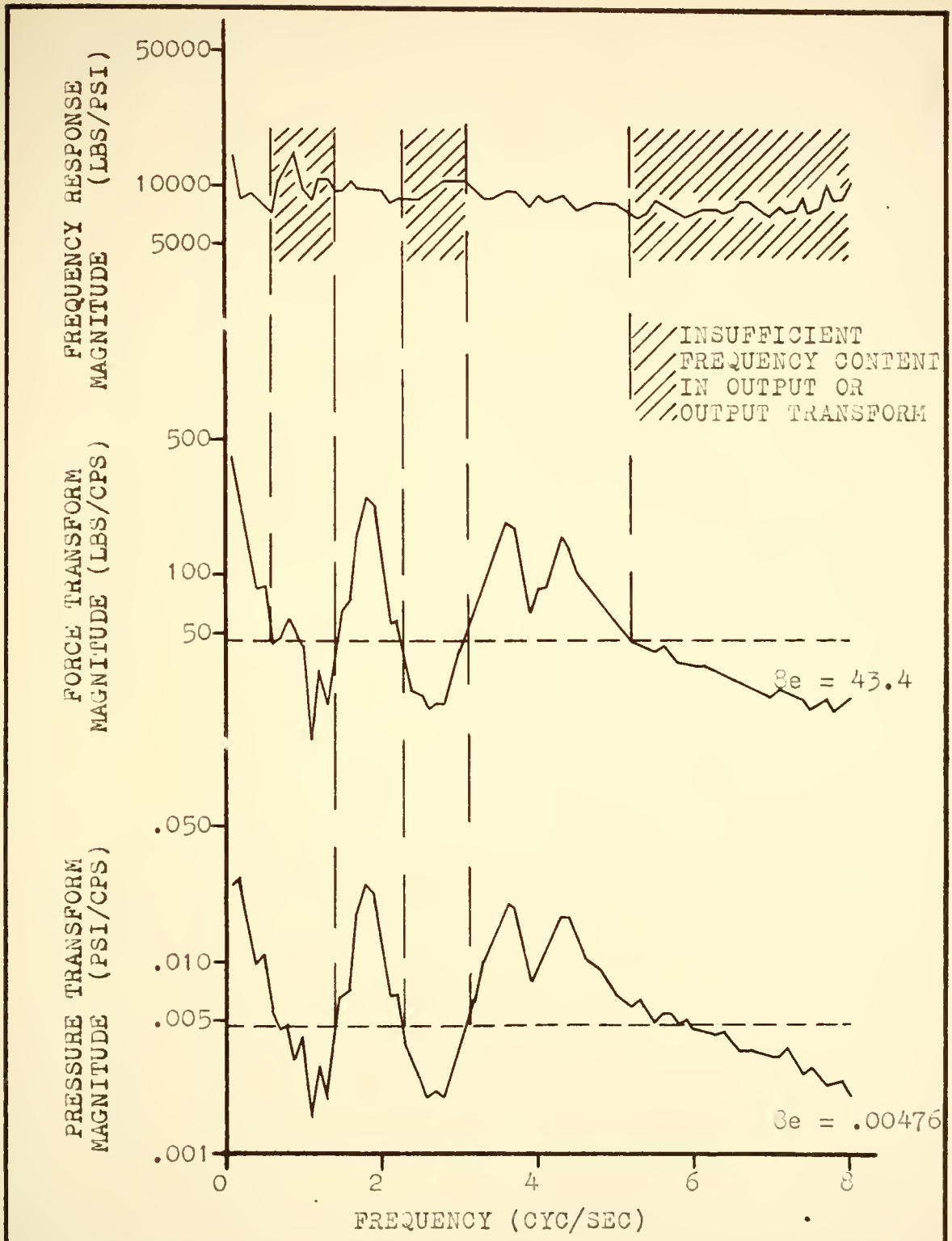

FIGURE 24 F/P TEST RESULTS FROM A .291 INCH DROP TEST OF THE RIGHT REAR INNER DUAL

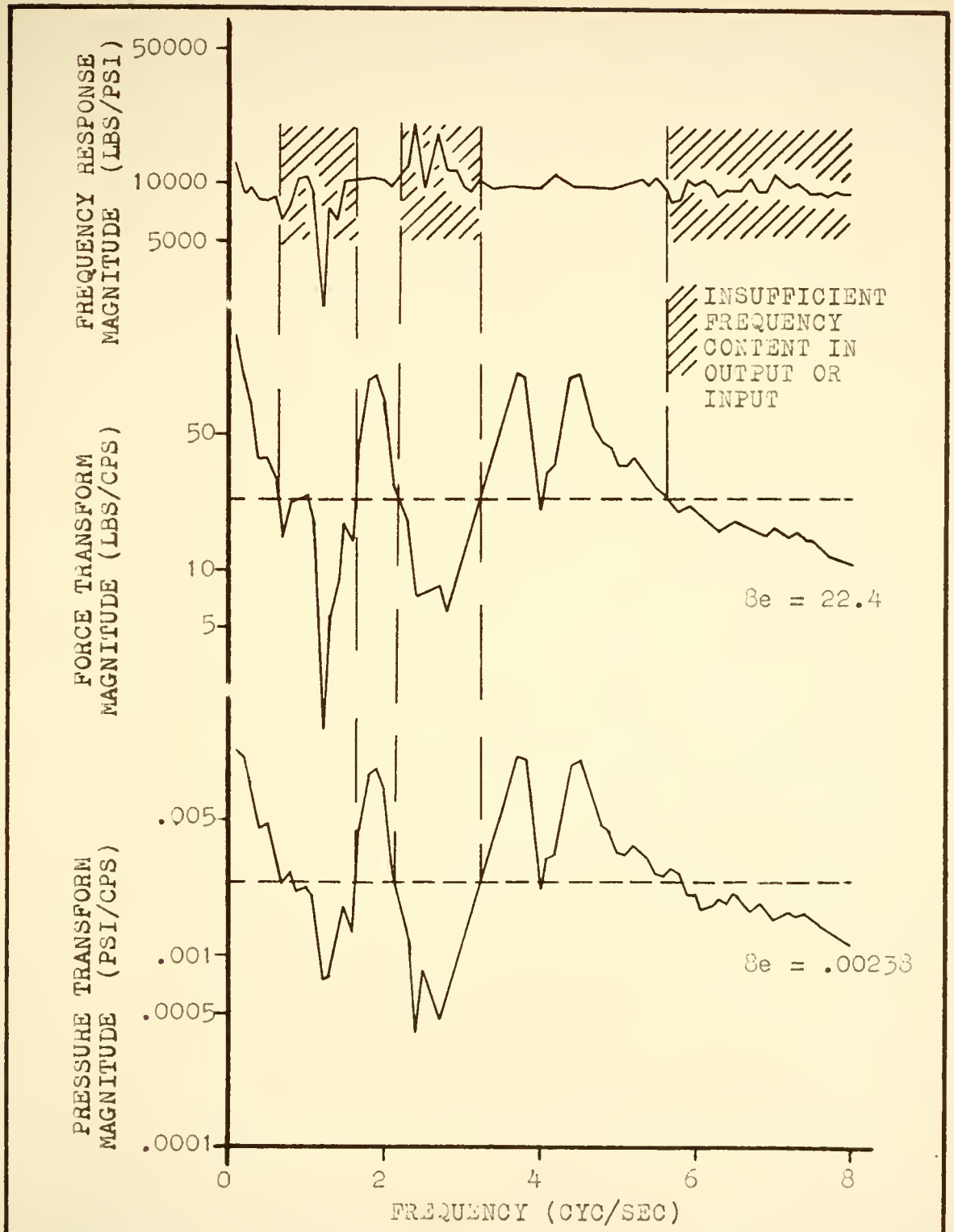

FIGURE 25 F/P TEST RESULTS FROM A .086 INCH DROP TEST OF THE RIGHT REAR INNER DUAL

for each drop height. The regions of the frequency response curve where either the input or output transform falls below the 3e criterion are not as smooth as when this criterion is satisfied.

This condition could not be detected until after the records had been processed. It is a direct result of inadequate recording equipment since the pressure transducers, force cells, and amplifiers were not operated at their maximum sensitivity. If the signal could be recorded on a device that would reduce the reading error, a larger portion of the transforms would meet the 3e error criterion, provided of course, that their magnitudes are roughly correct in the present form.

The F/P frequency response curves thus obtained may not be accurate for frequencies greater than 6 cps. However, this does not pose as great a problem as may appear. The regions in which the transforms had adequate magnitude are precisely the regions that correspond to the resonant frequencies of the truck motion. The frequency content near these frequencies will be shown to be predominant in the test records when the truck was operated on the highway. Thus a good estimate is available for the predominant frequencies of the records.

Two procedures that may be used to convert the pressure records to force records will be discussed. One is to choose a constant value of F/P. The value of F/P in the

regions that satisfy the 3e error criterion would be used. In these regions the frequency response result for each drop height is approximately constant. There is approximately a 10 percent variation among the curves for the three drop heights in these regions which could be caused by the non-linearities in the system. For the right rear inner tire pressure measuring system an average value for F/P would be 9200 lbs/psi. However, it must be recognized that the pressure measuring system will not measure a constant pressure change because of the equilization bypass. Test results indicate that frequencies below 0.1 cps will not be measured accurately.

The second procedure that may be used when converting the pressure records to force records is to use a weighted average of the frequency response curves obtained from the three drop heights. This procedure will tend to smooth the irregular experimental results that are caused by the data processing. The averaged results of the left rear inner and left rear outer pressure measuring systems are given in Figures 26 and 27. To show the similarity of these pressure measuring systems to a pure time lead system, the phase angle for such a system with a .005 second lead is illustrated. The magnitude of the lead system frequency response would be a constant. This time lead corresponds to the average time it would take for a pressure pulse to travel from the pressure transducer to the tire-pavement contact point, an

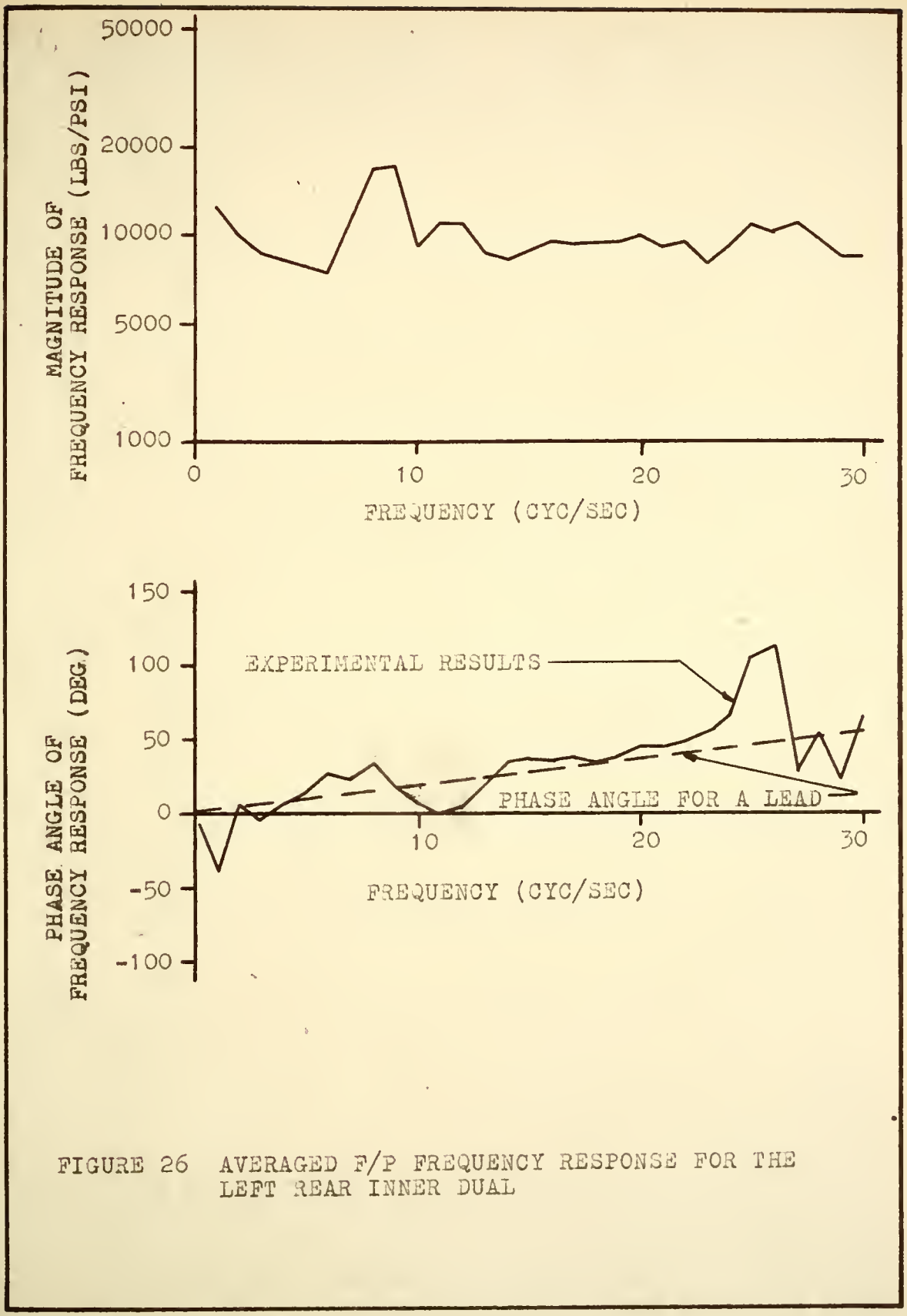

FIGURE 26 AVERAGED F/P FREQUENCY RESPONSE FOR THE LEFT REAR INNER DUAL

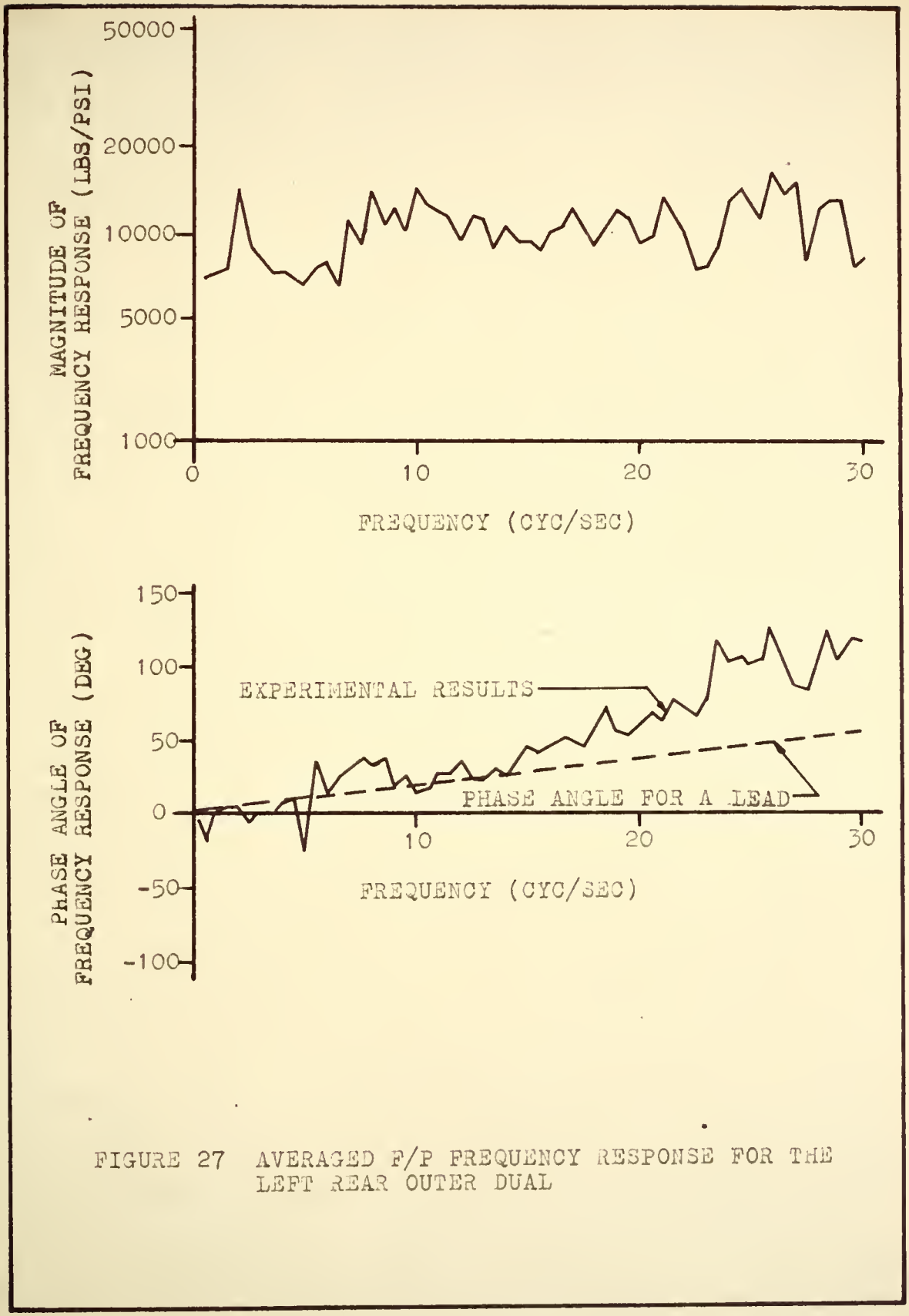

FIGURE 27 AVERAGED F/P FREQUENCY RESPONSE FOR THE LEFT REAR OUTER DUAL

average distance of approximately 6 feet. This distance is not constant since, as the tire rotates, the distance from the valve stem to the tire-pavement contact point varies.

Unlike the pressure measuring systems, where resonances could be minimized by proper design, the vehicle suspension system was to be used without any modifications. The frequency response relationship between the force and the tire displacement F/X will then be expected to exhibit resonances that correspond to certain modes of vehicle vibration.

Initial portions of three transient test records of force and displacement are shown in Figure 28. These records are for displacement of both right rear dual tires and the force under the inner right rear dual. Three tests at different drop heights were made in order to determine how the magnitude of the input affects the type of response. When the entire lengths of the transient records are processed and substituted into Equation 1, the results in Figure 29 and 30 are obtained. The force transforms of the inner tire force records are almost identical to those illustrated in Figure 21. The input displacement transforms are shown in Figure 31. For comparison, Fourier transforms of pure steps are also shown in Figure 31. The differences between each set of curves in Figure 31 apparently are not the result of data processing errors, but the fact that the inputs are not perfect steps as can be seen from the data of Figure 28.

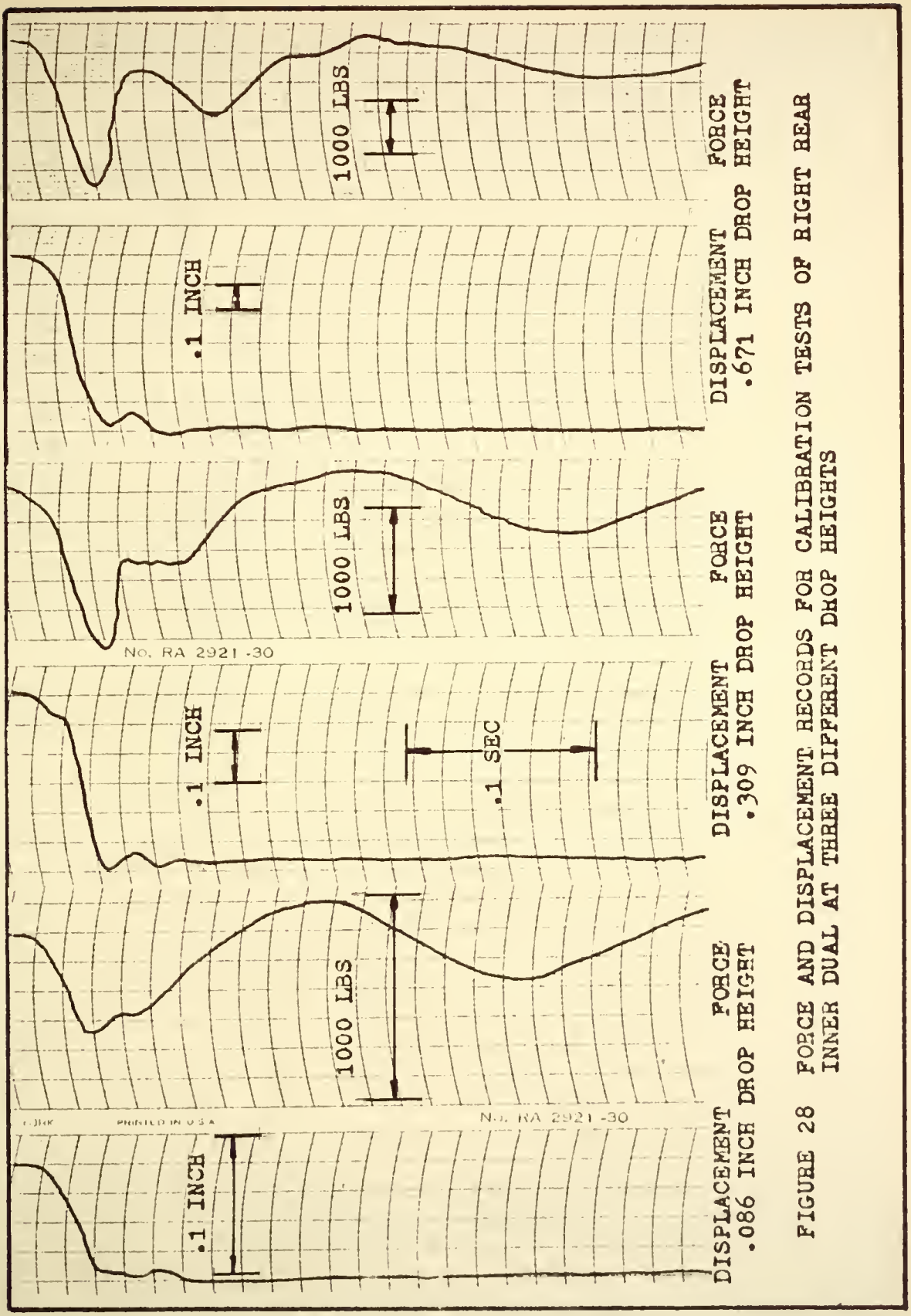

FIGURE 28 FORCE AND DISPLACEMENT RECORDS FOR CALIBRATION TESTS OF RIGHT REAR INNER DUAL AT THREE DIFFERENT DROP HEIGHTS

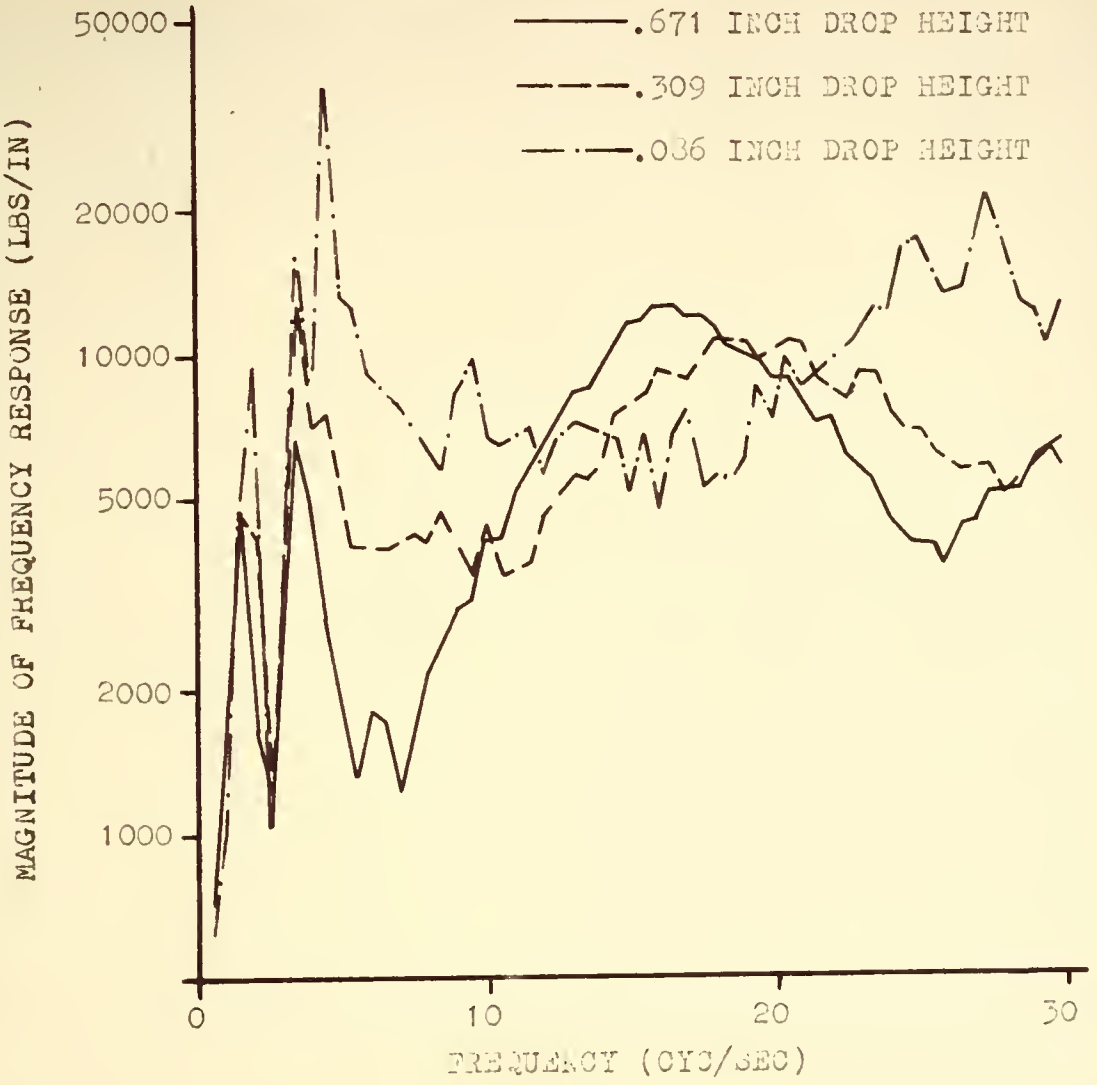

DATA SPACING = .003205 SEC

NYQUIST FREQUENCY = 156 CYC/SEC

f_5 = 62.5 CYC/SEC

FIGURE 29 MAGNITUDE OF FREQUENCY RESPONSES FOR THE F/X CALIBRATION TESTS OF THE RIGHT REAR OUTER DUAL

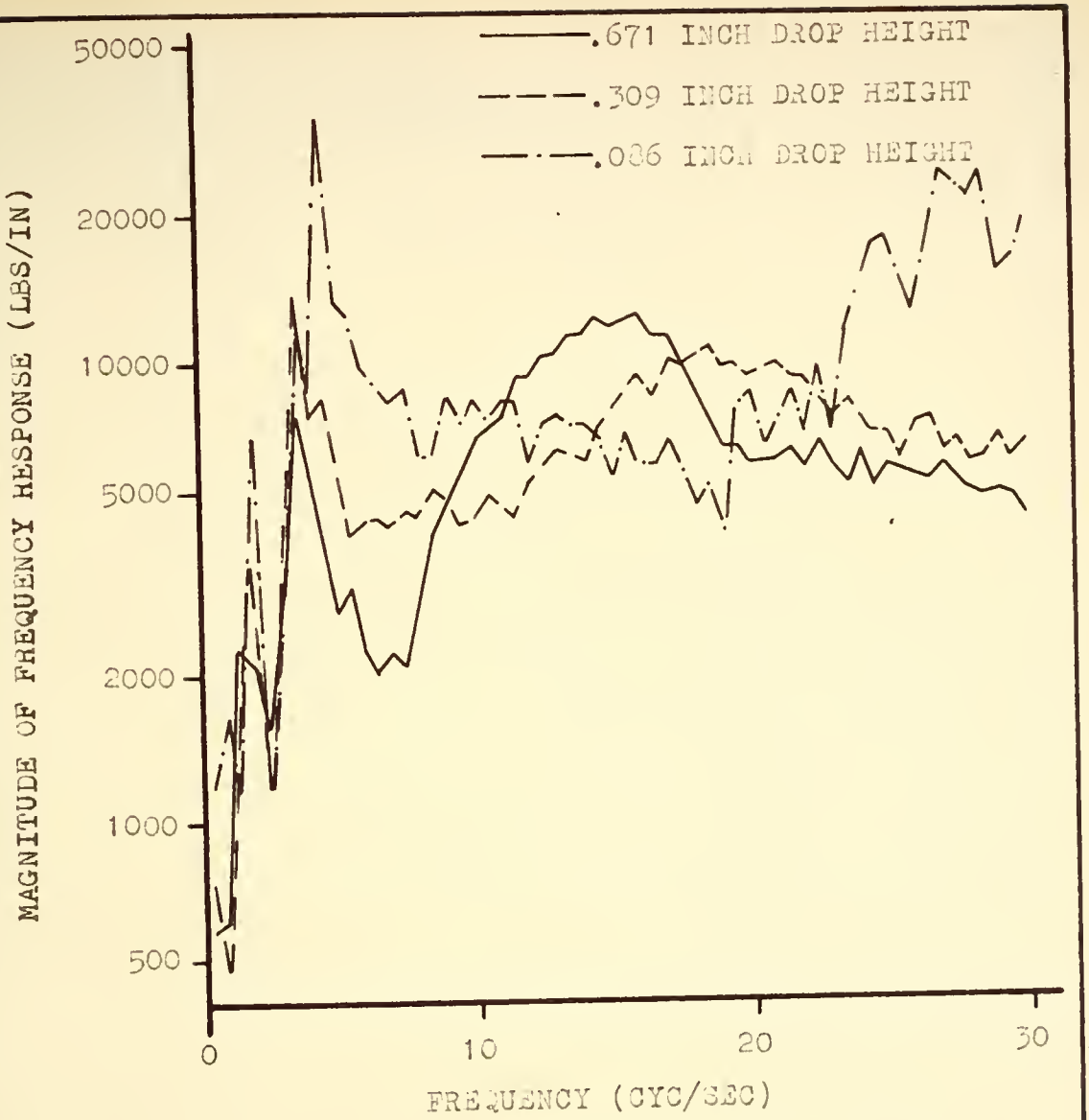

DATA SPACING = .003205 SEC

NYQUIST FREQUENCY = 156 CYC/SEC

f_5 = 62.5 CYC/SEC

FIGURE 30 MAGNITUDE OF FREQUENCY RESPONSES FOR THE F/X CALIBRATION TESTS OF THE RIGHT REAR INNER DUAL

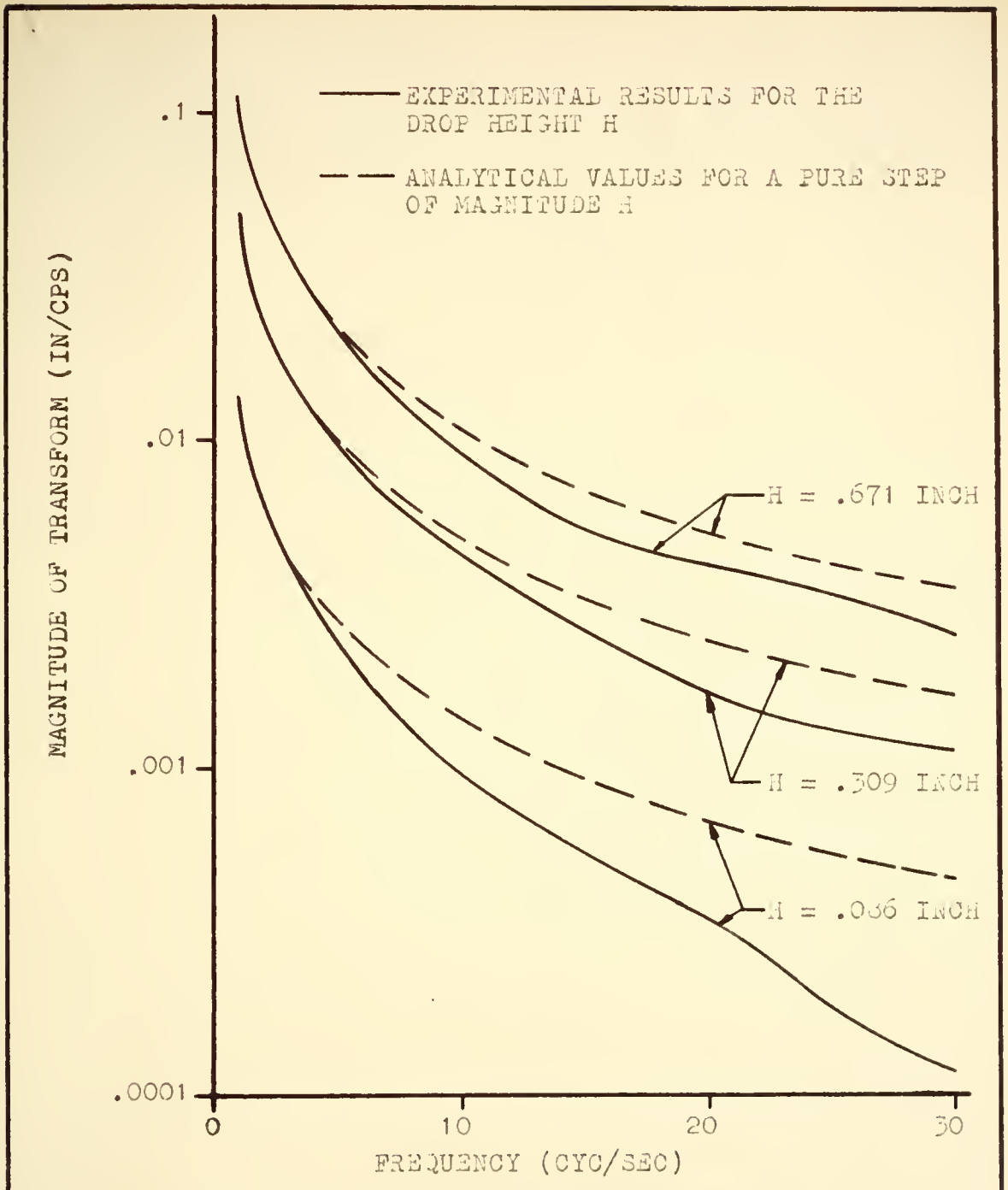

DATA SPACING = .003205 SEC NYQUIST FREQUENCY = 156 CPS
f_5 = 62.5 CPS

FIGURE 31 DISPLACEMENT FOURIER TRANSFORMS FOR F/K CALIBRATION OF RIGHT REAR DUALS

The low frequency portion of the .036 inch drop F/A frequency response and the transforms of the input and output are illustrated in Figure 32. The transform of the input does fall below the 5e line at about 4 cps but it does not exhibit the usual erratic behavior associated with a small transform magnitude compared to the reading error. The magnitude of the force transform would appear to be a more logical choice to which to apply the 5e criterion since it does exhibit this behavior when the magnitude is small. However, the deficiency of the frequency content is not the reason for the deviation among the F/A frequency response curves at the lower frequencies. The low frequency results of all three F/A frequency response curves are given in Figure 33. Below about 3 cps the curves give relatively consistant results while they deviate to some degree above this frequency. Especially note that the resonance at 3.6 cps does not reach the same magnitude for each drop height. This also is evident for the peak at 4.4 cps. These peaks correspond to portions of the force transforms of sufficient magnitude to satisfy the 5e error criterion. The apparent reason that these curves deviate can be found by inspection of Figure 28. Note that all of the input displacement records are similar in shape but of different magnitude and hence all of the Fourier transforms of these records would be expected to be similar in shape

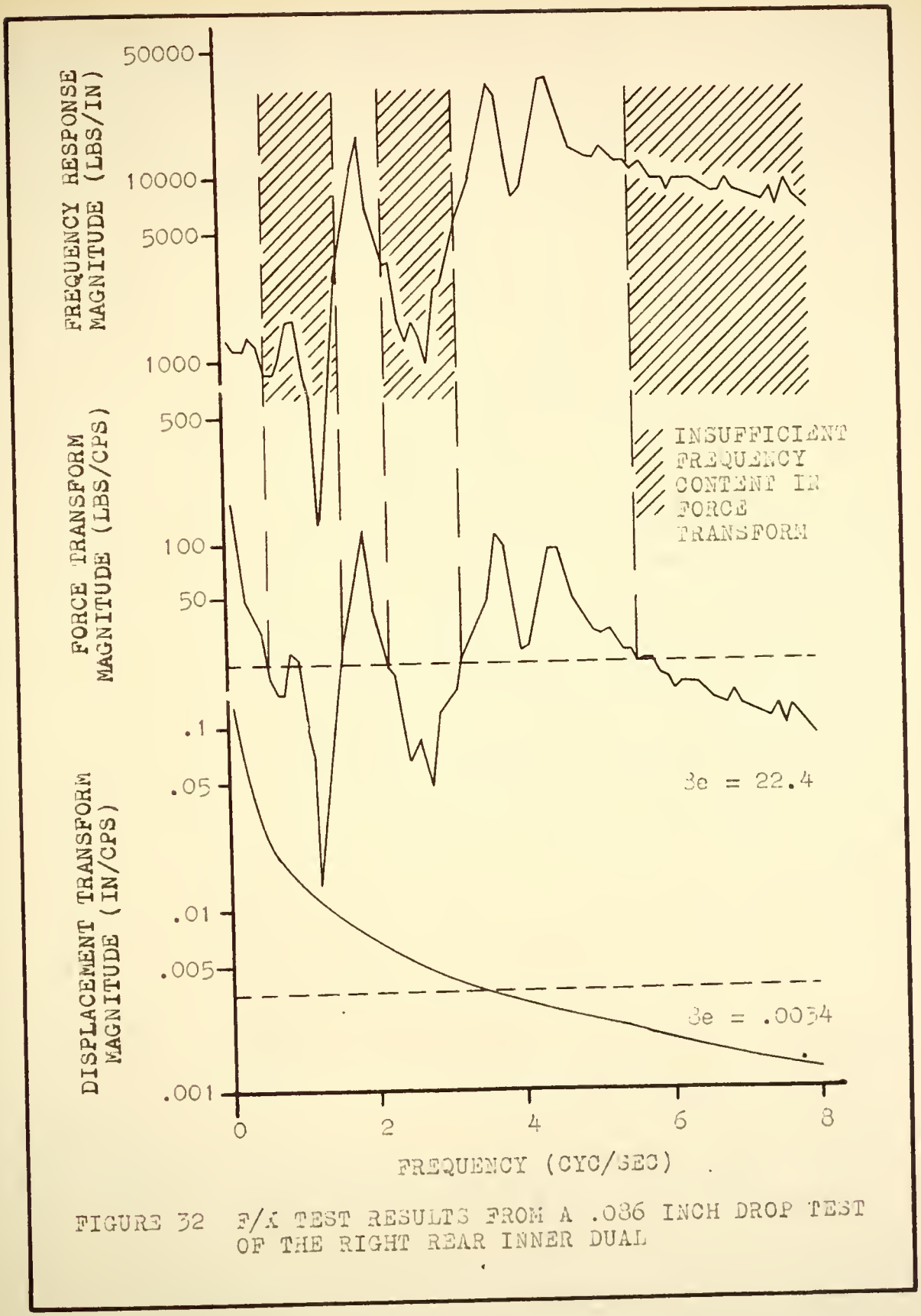

FIGURE 32 F/A TEST RESULTS FROM A .086 INCH DROP TEST OF THE RIGHT REAR INNER DUAL

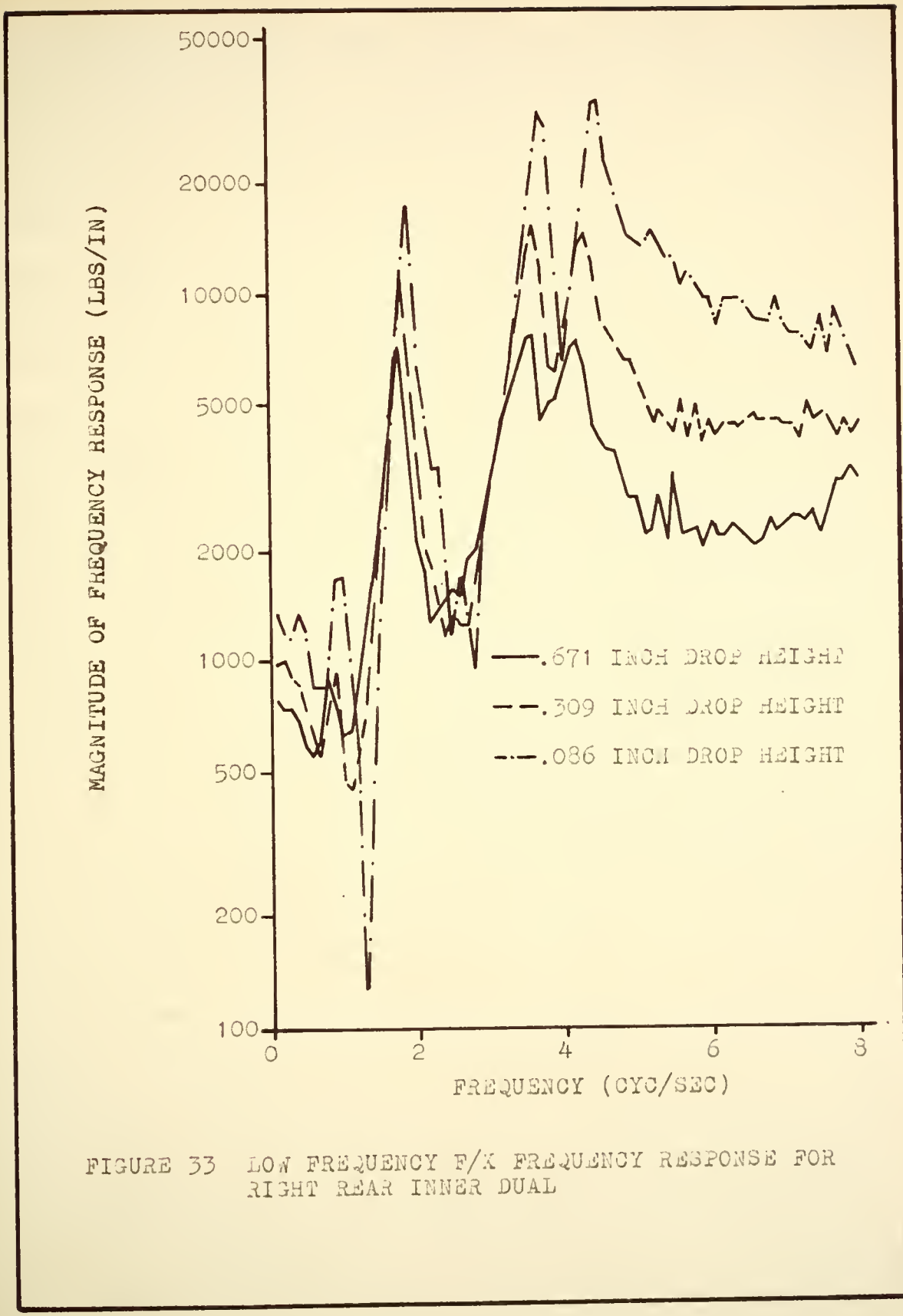

FIGURE 33 LOW FREQUENCY F/X FREQUENCY RESPONSE FOR RIGHT REAR INNER DUAL

but of different magnitude. The results in Figure 31 concur with this expectation. For a linear vehicle suspension system, all of the force records would be expected to be of similar shape but different magnitudes. This would also be expected of all the Fourier transforms of the force output. Note, however, that all of the force records in Figure 20 are not similar in shape near time zero. For the .671 inch drop there are several distinct cycles of a 15 cps decaying sinusoid, in the .309 inch drop record there is one cycle of this transient, and in the .056 inch drop record the transient did not occur. This type of result would be expected in certain types of nonlinear systems. This effect is more clearly indicated in the force transforms of Figure 21 where at 15 cps there is a high relative magnitude of the transform for the .671 inch results and a low relative magnitude of the transform for the .056 inch results.

The most probable cause for obtaining this type of force response is Coulomb friction in the leaf springs of the suspension system. Figures 34 and 35 illustrate a possible seven degree of freedom model of the truck for motions of Z, θ_1, θ_2, Z_F, θ_F, Z_R, and θ_R. The Coulomb dampers are indicated by B_1, B_2, B_3, and B_4. For large displacement inputs, the dynamic forces are large enough to overcome these damping forces and to permit the rear axle to vibrate between the sprung mass and ground. This mode

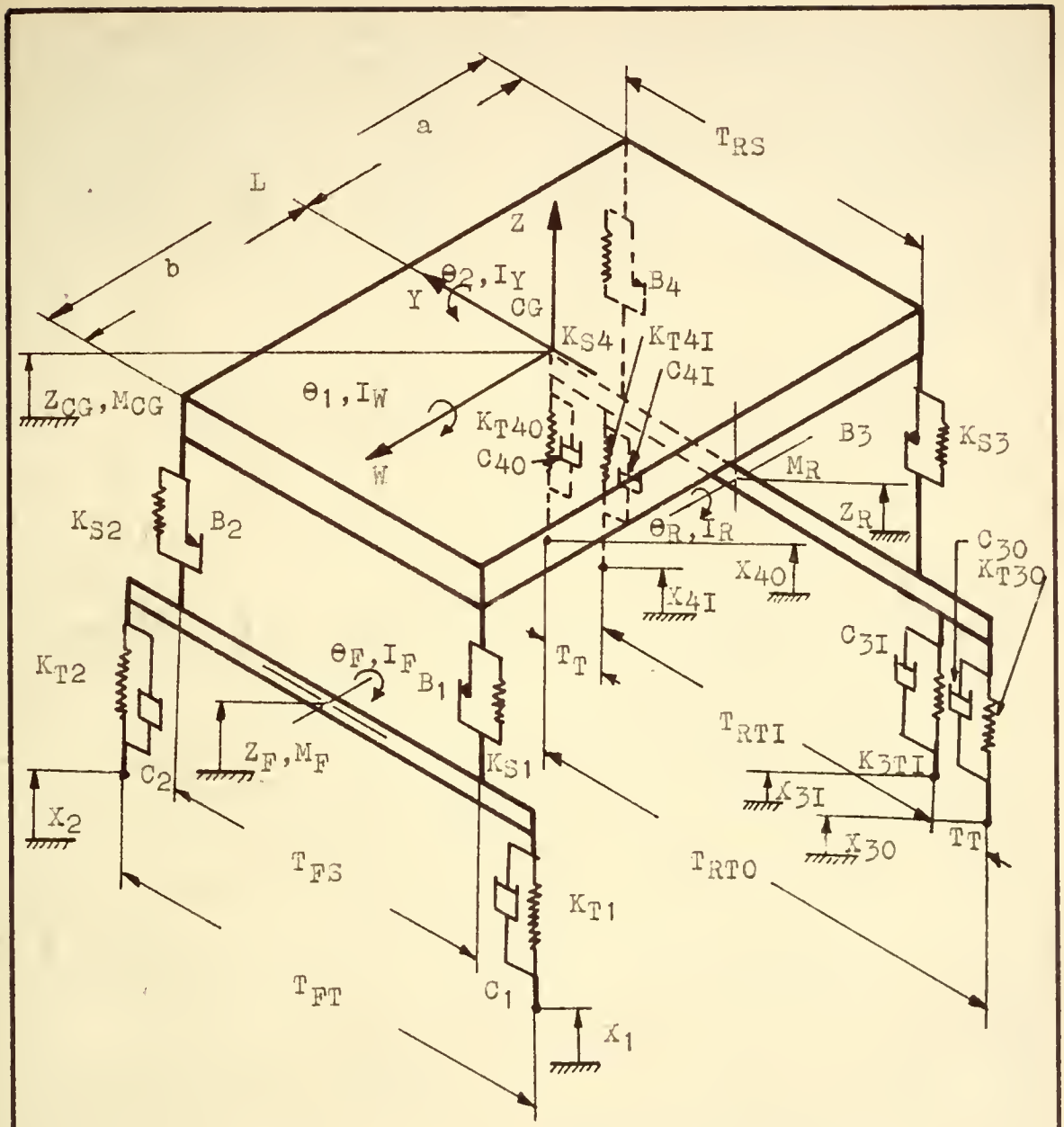

FIGURE 34 SEVEN DEGREE OF FREEDOM MODEL OF TEST VEHICLE

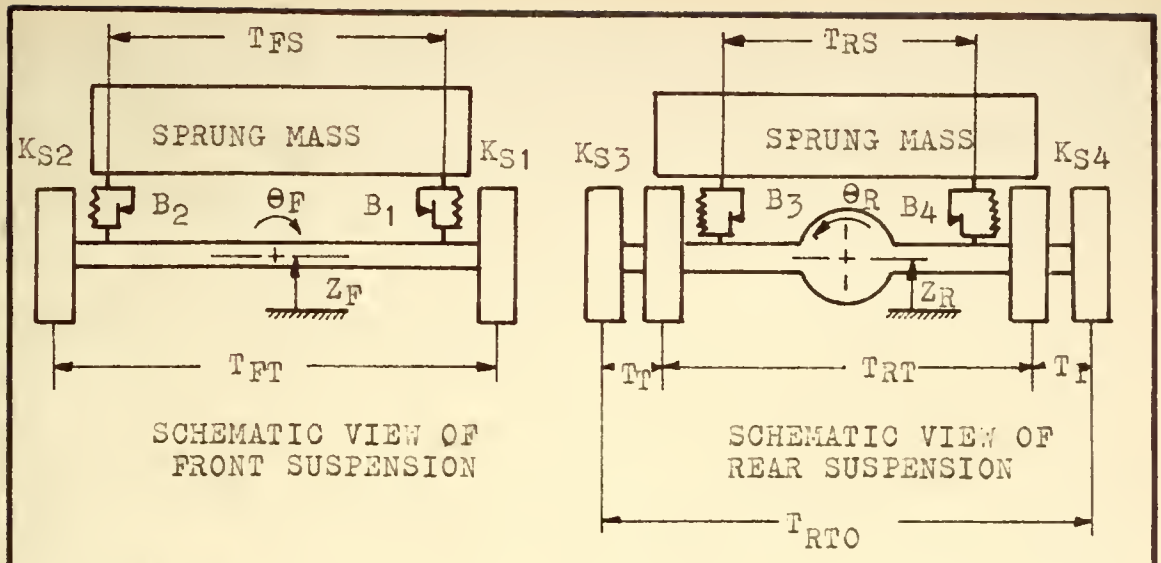

K_{T1}, K_{T2}, K_{T3O}, K_{T3I}, K_{T4I}, K_{T4O} - TIRE SPRING CONSTANTS (LBS/IN)

C_1, C_2, C_{3O}, C_{3I}, C_{4I}, C_{4O} - TIRE DAMPING COEFFICIENTS (LBS/IN/SEC)

M_F, M_R, M_{CG} - MASS OF FRONT AND REAR AXLES AND BODY (LB-SEC^2/IN)

I_F, I_R, I_Y, I_W - MASS MOMENTS OF INERTIA (LB-SEC^2-IN)

K_{S1}, K_{S2}, K_{S3}, K_{S4} - SUSPENSION SPRING CONSTANTS (LBS/IN)

B_1, B_2, B_3, B_4 - SUSPENSION COULOMB DAMPING (LBS)

X_1, X_2, X_{3O}, X_{3I}, X_{4I}, X_{4O} - TIRE DISPLACEMENTS (IN)

FIGURE 35 DEFINITION OF TERMS USED FOR SEVEN DEGREE OF FREEDOM MODEL OF TEST VEHICLE

is sometimes referred to as "axle hop" or "wheel hop." For small displacements the dynamic forces are not large enough to permit this mode of oscillation. It is not possible to state whether or not there was a relative displacement between the axle and the sprung mass for the smallest drop height by observing the force records directly. It is conceivable that the rear axle motion could be in phase with the motion of the sprung mass. This mode can not be recognized in the force records as readily as the wheel hop mode. Although there are several other elements of the suspension system that are nonlinear to a degree, the Coulomb friction in the leaf springs is considered as the most important.

No tests were made to determine if any relative displacement between the sprung mass and the rear axle occured during the calibration tests. However, several road tests were made where relative displacements of the rear axle relative to the truck bed were recorded. The experimental results would correspond to the displacement of K_{34} and B_4 in Figures 34 and 35. Some typical results of these tests are shown in Figure 36. At 20 mph there was virtually no relative displacement, while at higher speeds relative displacements were recorded. The peak at the left of each record is the result of passing over a one inch pipe used as an event marker. .

An interesting effect was noted during the calibration tests. As the beam was lifted to the initial height, the

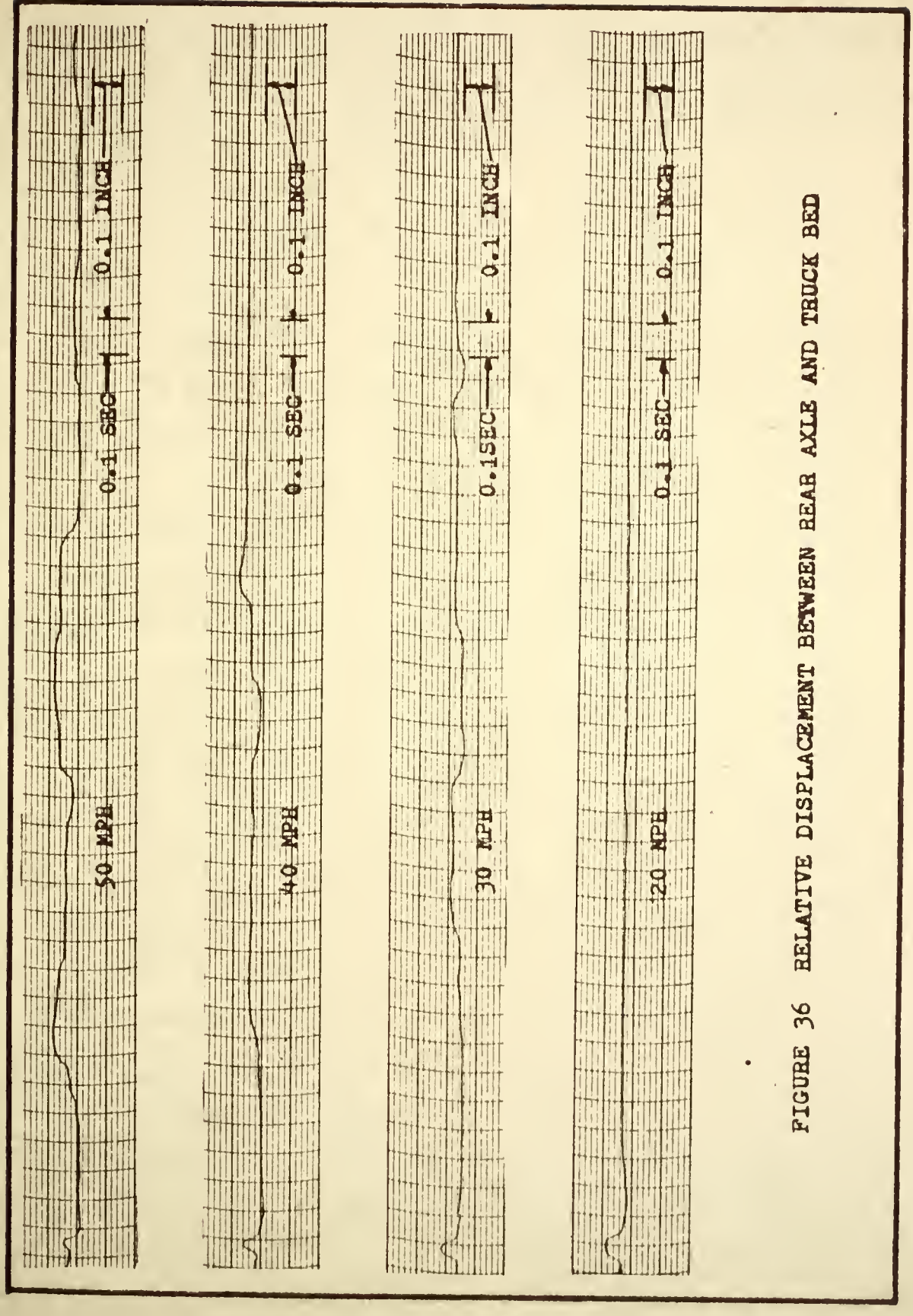

FIGURE 36 RELATIVE DISPLACEMENT BETWEEN REAR AXLE AND TRUCK BED

static force would change under each dual tire. The force under the inner tire would increase while the force under the outer tire would decrease. Figure 37 illustrates these observations for the right rear set of duals. The force change is due to several causes. The reason that the inner tire force increases and the outer tire force decreases is due to the relative angle between the rear axle and the bottom of the two tires. This is the angle θ_1 in the Figures 34 and 35. Apparent in Figure 37 is the fact that, as the beam is lifted, there is a net increase in force at the right rear corner of the vehicle. This results from the resistance offered by the other springs at the other corners of the vehicle. There is a further effect that would tend to cause a net reduction of the total force transmitted by the tire, that is, as the truck is tilted in the θ_1 direction the center of gravity will lie slightly closer to the left side than to the right, similar to an inverted pendulum. A change in force due to the latter two reasons has been observed when testing automobiles. An attempt was made to experimentally measure the total force distribution among the right and left rear duals for various truck dispositions, but due to instrumentation difficulties and time limitations, the exact total force beneath each tire was not determined.

For purposes of comparison, the frequency response curves for an automobile, a small truck, and the test vehicle are

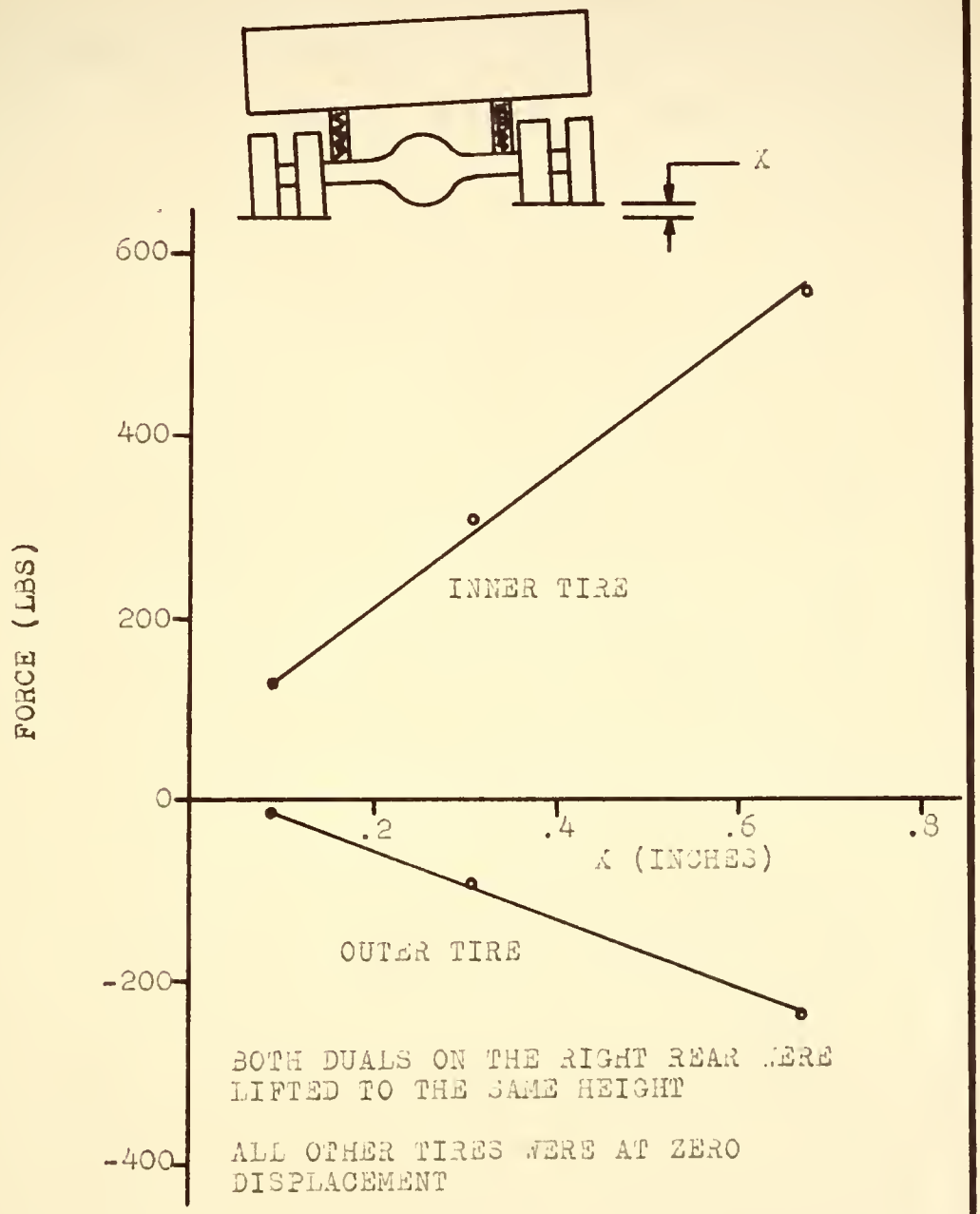

FIGURE 37 CHANGE IN STATIC LOAD UNDER TIRES FOR STATIC CHANGES IN DISPLACEMENT

shown in Figure 38. The automobile had a gross vehicle weight of 4400 lbs and the tires were inflated to 30 psi. The automobile F/X characteristic shown is the result of a transient test where displacement and force were recorded at the right front tire when the right front tire was subjected to a .17 inch drop on a calibrator similar to that shown in Figure 13. The small truck had a gross vehicle weight of 7800 lbs and the tire inflation pressure was 45 psi. The F/X characteristic shown is for a .5 inch drop displacement of the right rear dual tires and the force under the outer right rear tire. The results for the test truck are from the .036 inch drop test. The F/X characteristic is for the outer right rear dual. The peaks in the characteristics at 17 cps for the 7800 G.V.W. and the automobile correspond to the wheel hop modes.

Since the 26000 G.V.W. truck used in this investigation was on loan from the Indiana State Highway Commission, the time that it was available for testing was limited. For this reason, the major effort of the investigation was directed toward developing the pressure measuring systems and conducting road tests with the Stresses and Deflections Group. Consequently, there was little time available to investigate the vehicle suspension system. Information obtained pertaining to the truck suspension system was mainly in the form of F/P and F/X calibration records. The load on the front and rear axle and various vehicle dimensions were

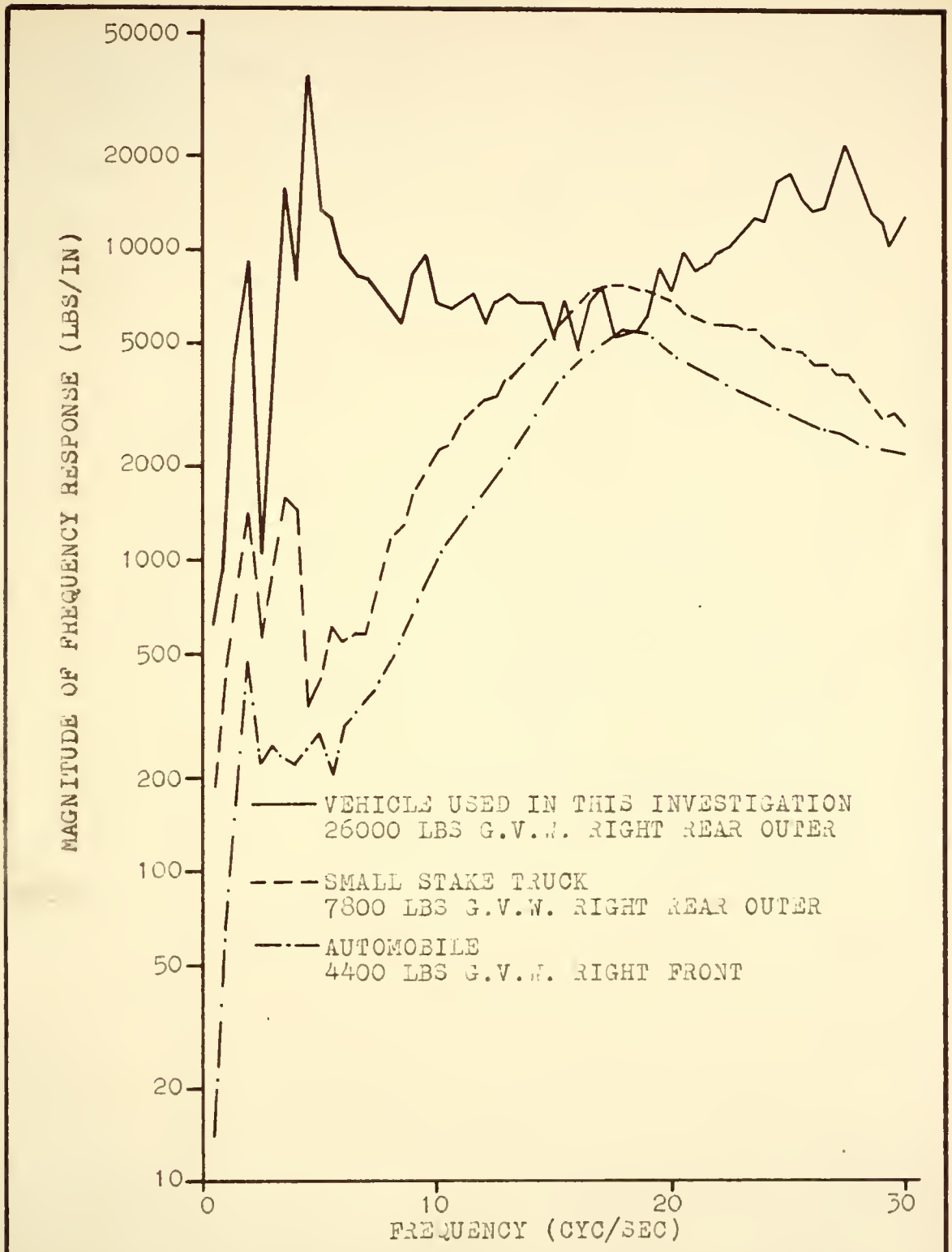

FIGURE 38 COMPARISON OF F/X FREQUENCY RESPONSE FOR THREE DIFFERENT VEHICLES

also determined, however.

With this limited information, it is difficult to choose an experimental characteristic that will best describe the truck. If nonlinear theory were to be used to predict the dynamic forces from highway elevation measurements, a more detailed study of the suspension system is in order. However, if linear theory is to be employed for an approximate prediction of the dynamic tire forces from elevation measurements, it appears from the results shown in Figure 36 and 28 that for low speeds the calibration results from the .036 inch drop tests would provide the best information about the truck that is experimentally available. For the higher speeds, the truck becomes more nonlinear and the results of the .036 inch drop tests would be expected to be less accurate.

Since both the vehicle suspension system and the pressure measuring systems were calibrated when the vehicle was parked, the question arises as to the effect that vehicle speed has on the F/X and F/P calibration. The tire tread has mass and hence the pressure measuring system performance would depend on the wheel rotation speed. This problem is beyond the experimental facilities that are currently available. Other possible problems of the pressure measuring system that may not be detected during the calibration are: (1) eccentricity of the tire or wheel assembly, (2) mechanical vibrations of the pressure tubing

(3) a rock in the tire tread. However, the existance of any of these problems may sometimes be found from a power spectrum analysis of the actual road test records.

The velocity dependence of the dynamic force exerted on the pavement by the truck is an important problem that must be considered in detail. Experimental facilities are not available to thoroughly investigate this problem. This problem will be discussed with reference to a mathematical model of the vehicle suspension system. The model shown in Figures 34 and 35 could be used except that the numerical values of 34 parameters are required. The values of only six of these parameters were determined during the time that the truck was available. Because of the extended nature of the corresponding equations of motion, they are not listed. Substantial simplification can be realized if the assumption is made that the leaf springs in the suspension system do not deflect. This assumption is justified for low vehicle speeds by the results of Figure 36. The assumption completely ignores the possibility of the axle hop mode, but road test records indicate that this mode is not usually excited at any speed. The primary effect of the leaf springs would be to produce a smaller effective spring constant at each corner of the vehicle. The model based on this assumption is shown in Figure 39.

For this model, knowledge of 10 parameters is needed. Of these, six are known. Approximate values of the other

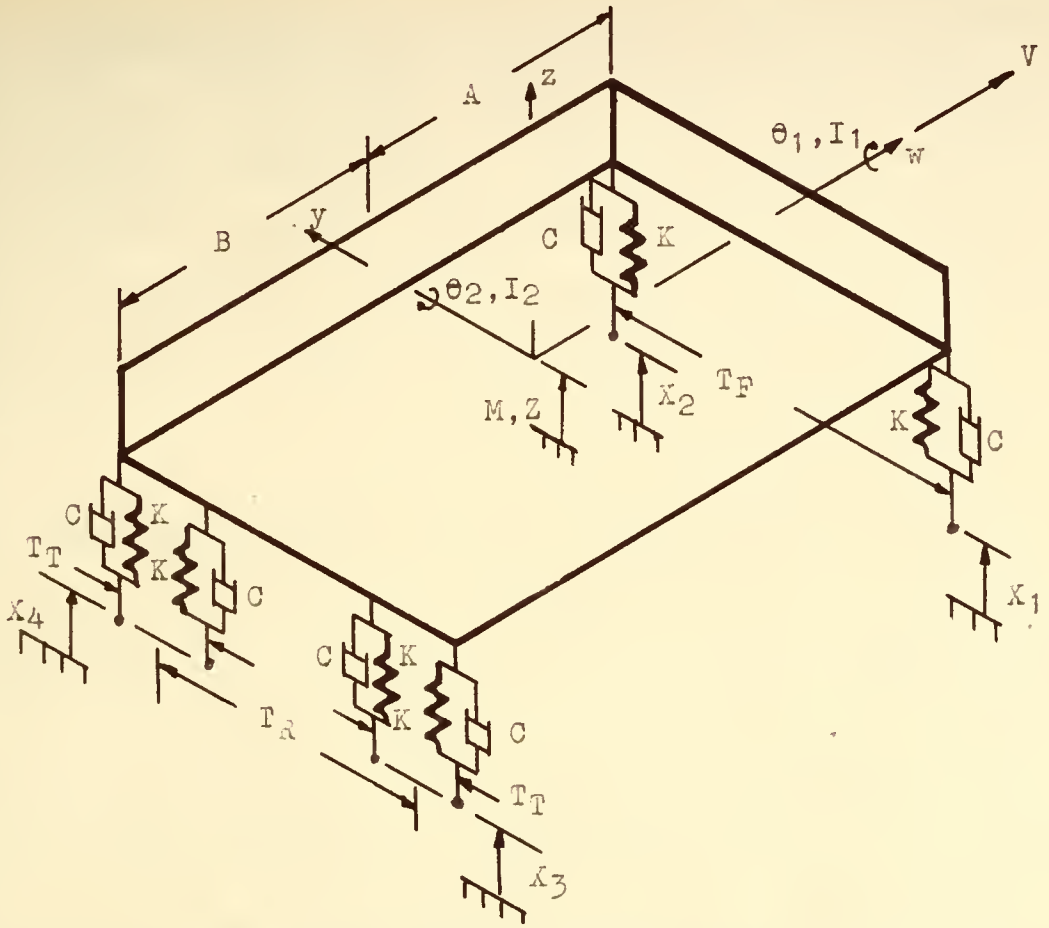

K: TIRE SPRING CONSTANT (LB/IN)
C: TIRE DAMPING CONSTANT (LB-SEC/IN)
I_1, I_2; MASS MOMENTS OF INERTIA (LB-IN-SEC^2)
M: VEHICLE MASS (LB-SEC^2/IN)
Z: VERTICAL DISPLACEMENT OF CG (IN)
X_1, X_2, X_3, X_4: VERTICAL TIRE DISPLACEMENT (IN)
V: VEHICLE VELOCITY IN w DIRECTION (IN/SEC)

FIGURE 39 3 DEGREE OF FREEDOM MODEL OF A TRUCK

four constants were obtained from references (4) (20). In Figure 39 the wyz axis is fixed to the center of gravity. The equations of motion are similar to those in reference (21). There is a small difference between these equations and those derived in reference (22). For small deflections about the static equilibrium position, the equations of motion are:

$$M\ddot{Z} + 6C\dot{Z} + 6KZ + 2C(2B - A)\dot{\theta}_2 + 2K(2B - A)\theta_2$$

$$= KX_1 + C\dot{X}_1 + KX_2 + C\dot{X}_2 + 2KX_3 + 2C\dot{X}_3 + 2KX_4 + 2C\dot{X}_4 \qquad (17)$$

$$I_1\ddot{\theta}_1 + C(\frac{T_F^2}{2} + T_R^2 + T_T^2)\dot{\theta}_1 + K(\frac{T_F^2}{2} + T_R^2 + T_T^2)\theta_1$$

$$= -\frac{T_F}{2}KX_1 - \frac{T_F}{2}C\dot{X}_1 + \frac{T_F}{2}KX_2 + \frac{T_F}{2}C\dot{X}_2 - T_RKX_3 - T_RC\dot{X}_3$$

$$+ T_RKX_4 + T_RC\dot{X}_4 \qquad (18)$$

$$I_2\ddot{\theta}_2 + 2C(A^2 + 2B^2)\dot{\theta}_2 + 2K(A^2 + 2B^2)\theta_2 + 2C(2B - A)\dot{Z}$$

$$+ 2K(2B - A)Z = - AKX_1 - AC\dot{X}_1 - AKX_2 - AC\dot{X}_2$$

$$+ 2BKX_3 + 2BC\dot{X}_3 + 2BKX_4 + 2BC\dot{X}_4 \qquad (19)$$

The dynamic forces exerted at the right rear inner and outer wheels are:

$$F_I = K\left[X_4 - Z - B\theta_2 - \frac{1}{2}(T_R - T_T)\theta_1\right] + C\left[\dot{X}_4 - \dot{Z} - B\dot{\theta}_2 - \frac{1}{2}(T_R - T_T)\dot{\theta}_1\right] \quad (20)$$

$$F_O = K\left[X_4 - Z - B\theta_2 - \frac{1}{2}(T_R + T_T)\theta_1\right] + C\left[\dot{X}_4 - \dot{Z} - B\dot{\theta}_2 - \frac{1}{2}(T_R + T_T)\dot{\theta}_1\right] \quad (21)$$

Two methods are available for checking the accuracy of this model. One is to determine the tire force from equations 17-21 when X_1, X_2, and X_3 are zero and X_4 is the tire displacement recorded during an experimental calibration test. The initial conditions for this procedure are:

$$\theta_1(0) = \frac{T_R X_4(0)}{\left(\frac{T_F^2}{2} + T_R^2 + T_T^2\right)} \quad (22)$$

$$\theta_2(0) = \frac{X_4(0)}{2(A + B)} \quad (23)$$

$$Z(0) = \frac{AX_4(0)}{2(A + B)} \quad (24)$$

A comparison is shown in Figure 40 of the force-time relationship computed from the model for the .086 inch drop input and the corresponding experimental values.

The other way to check the model, which would be equivalent to the first method if the truck were linear, is to compare the analytical frequency response of the model with the experimental frequency response of the truck. This comparison is made in Figure 41 with the .086 inch drop test results. From Figures 40 and 41 it is evident that the analytical transient response and frequency response do not exactly duplicate the experimental results although they are of a similar character. It does appear that the theoretical frequency response does agree with the results of the .086 inch drop in some regions as well as do those of experiments conducted using larger drop heights.

Although the model does not exactly represent the real system, it does approximate it closely enough so that some general conclusions may be reached concerning the vehicle velocity relationships. It is assumed that both the inner and outer rear dual wheels experience the same input. It is further assumed that when the input of a front tire is considered, the wheel path of the front tire is the same as the common rear wheel path.

The way that velocity enters into the vehicle response is the time lag involved for the rear tires to experience an input after the front tires have experienced input. This can be illustrated by the following hypo-

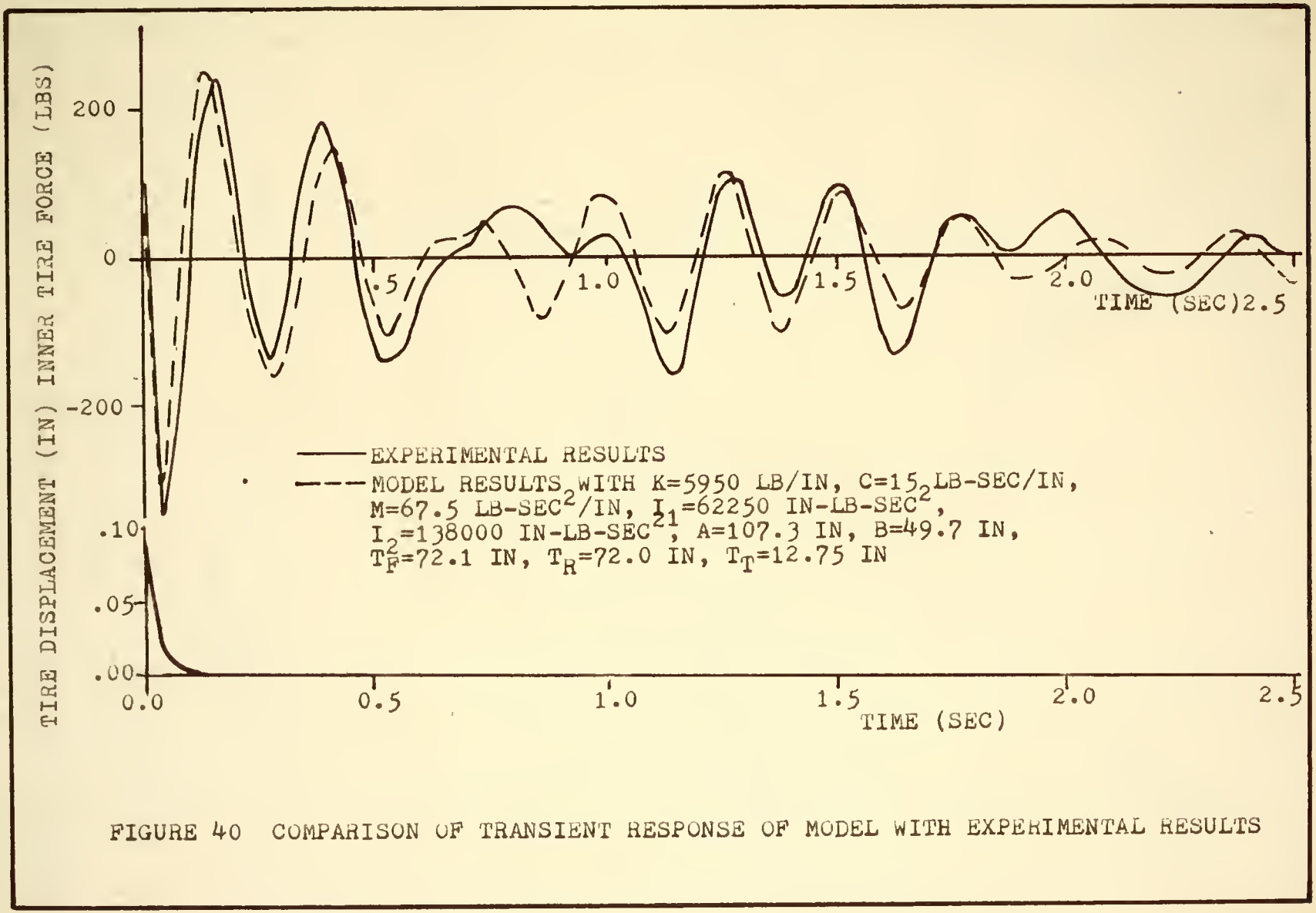

FIGURE 40 COMPARISON OF TRANSIENT RESPONSE OF MODEL WITH EXPERIMENTAL RESULTS

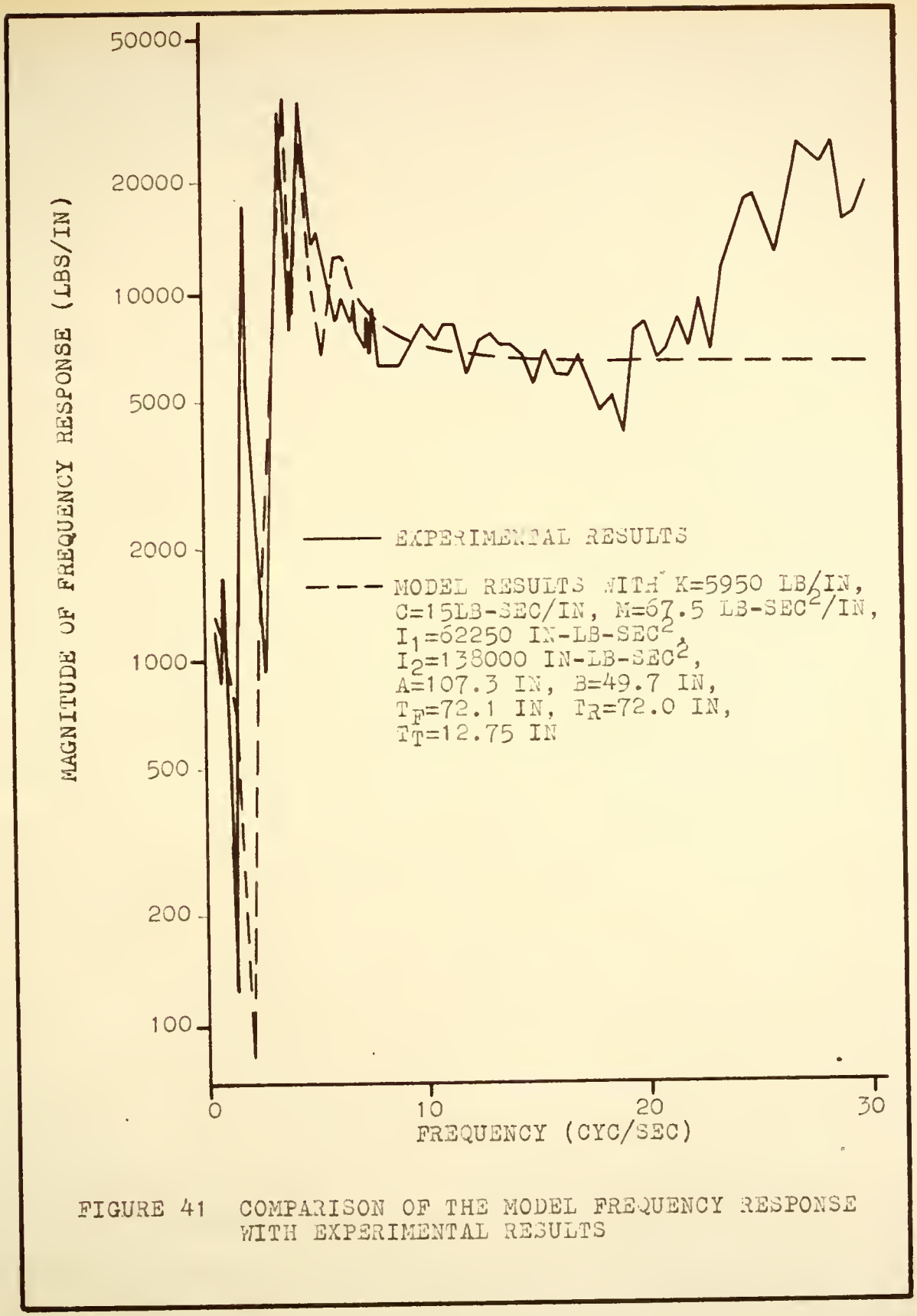

FIGURE 41 COMPARISON OF THE MODEL FREQUENCY RESPONSE WITH EXPERIMENTAL RESULTS

thetical example. Assume that two equal amplitude sinusoidal roadways are available--one with wave lengths 20 feet long and the other with wave lengths 10 feet long. Consider the excitation of a vehicle with a 10 foot wheelbase as it traverses either of these two roadways. When the vehicle traverses the road with the 20 foot wave lengths at a speed of 20 feet per second, it experiences a one cycle per second input. However, since the road wave length is twice the wheel base, the front wheels are exactly out of phase with the rear wheels, and the net result is a pure pitching input to the vehicle. When this same vehicle traverses the roadway with the 10 foot wave lengths at a speed of 10 feet per second, it still will experience an input of one cycle per second. On this pavement, since the road wave length is equal to the wheel base, the front and rear tires will be identically in phase and the net result is a pure vertical mode input to the vehicle. The vehicle would not be expected to respond to these two different types of inputs in the same manner.

These observations may be further studied by considering three cases involving the model and the appropriate inputs. These particular situations were chosen because they represent various assumptions that have been found in the literature. The various frequency response relationships are given in Appendix 1. The variable of interest will be the F_I/A_4 frequency response where F_I is the force under

the right rear inner dual and X_4 is the displacement of the right rear duals. Frequency is the product of the vehicle velocity and the reciprocal of the pavement wave length.

Case I illustrates the assumption[10] that the vehicle derives excitation from only one input, that being the displacement of the right rear dual tires. The other tires are implicitly assumed to be held at the zero level. The left tires and the right front tire are thus riding on a level track while the right rear dual tires are riding on a sinusoidal track. Since there is only one input for this case, there are no time lags. Thus the frequency response will not depend on vehicle velocity.

The frequency response curve for Case I together with an illustration of the vehicle excitation are shown in Figure 42. Frequency response curves obtained experimentally on the drop beam calibrator would correspond to this curve. Only the low frequency portion of the curve is shown since this curve shows the important low frequency resonances. These resonances will account for most of the dynamic forces when the vehicle is operated on the highway. As frequency increases the vehicle body is essentially motionless and the F_I/X_4 relationship is merely the tire spring constant. However, because of the tire damping, as the frequency becomes infinite, the F_I/X_4 ratio will also become infinite.

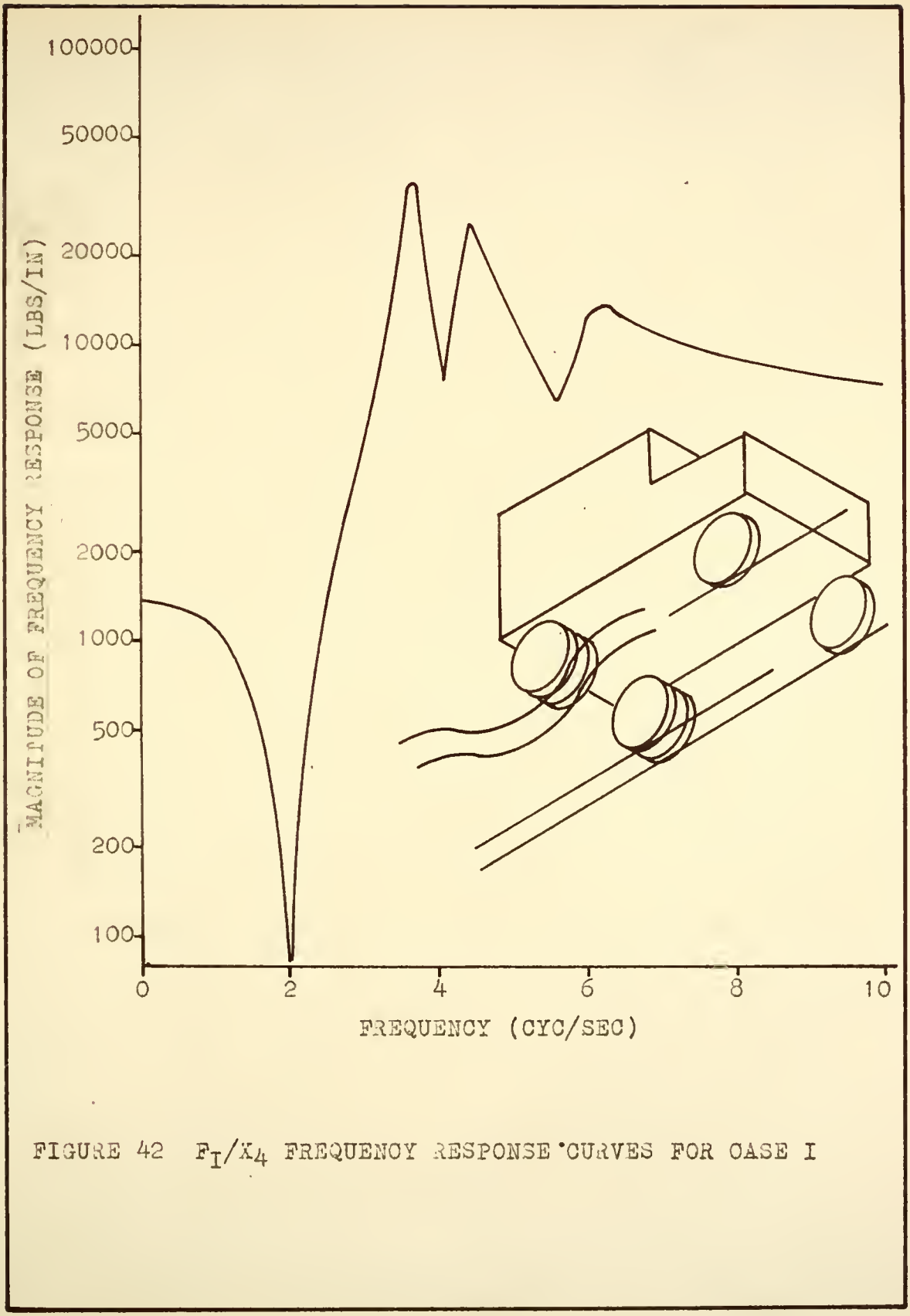

FIGURE 42 F_I/X_4 FREQUENCY RESPONSE CURVES FOR CASE I

At zero frequency the nonzero value of F_I/X_4 is the result of a force being necessary to move the mass from the static equilibrium position. This point is partially verified by Figure 37 where the experimental value of the static value of F_I/X_4 appears to be 800 lbs/in instead of the value of 1300 lbs/in as given for the model. Note that no account was made in the model for the center of gravity shift because of tilting. This would tend to make the zero frequency value of F_I/X_4 smaller. An automobile would also exhibit a nonzero F/X characteristic at zero frequency.

An important point here, and it applies to passenger cars as well as the truck, is that when the assumption is made that there is only one input it is implicitly assumed that the other tires are held at zero level. If an elevation profile is used as an input to one set of tires, misleading results may be obtained if there is a grade or a hill in the input data. The input wheel would follow the hill or grade and the other three inputs would remain at the zero level. Thus if this point is not recognized it would be possible to unknowingly have mathematical situations that would correspond to some unrealistic situation such as the input wheels at a 2 foot elevation while the other tires were at zero elevation. Very large forces would then be predicted incorrectly.

Some investigators have assumed a Case I situation for an automobile by reasoning from the following experi-

mental results for a vehicle that was not moving: When the input displacement is applied to one wheel and the dynamic force is measured at another wheel, the results are very small when compared to the results obtained when the input and output are at the same wheel. Thus they conclude that by neglecting the inputs at the other wheels, the final results will only change by a small amount. In actuality, by neglecting the other wheels they could impose an artificial condition that could alter the results when a grade or hill is present in the elevation data.

Case II was not found to be used by any investigators in the literature but it is a logical extension of Case I. The situation is that two displacement inputs are considered, one for the right front and the other for the right rear dual tires. The truck excitation and the frequency response curves for various speeds are given in Figure 43. The left wheels of the truck are traveling on a level track and the right wheels are on a sinusoidal track.

Since there are two inputs, velocity will alter the frequency response because of the time required for the disturbance to reach the rear wheels after reaching the front wheels. The frequency response at zero frequency, i.e. when the right front and rear tires are lowered or raised the same amount, takes a nonzero value because the vehicle has dual tires. As one side of the truck is raised, the force on the inner and

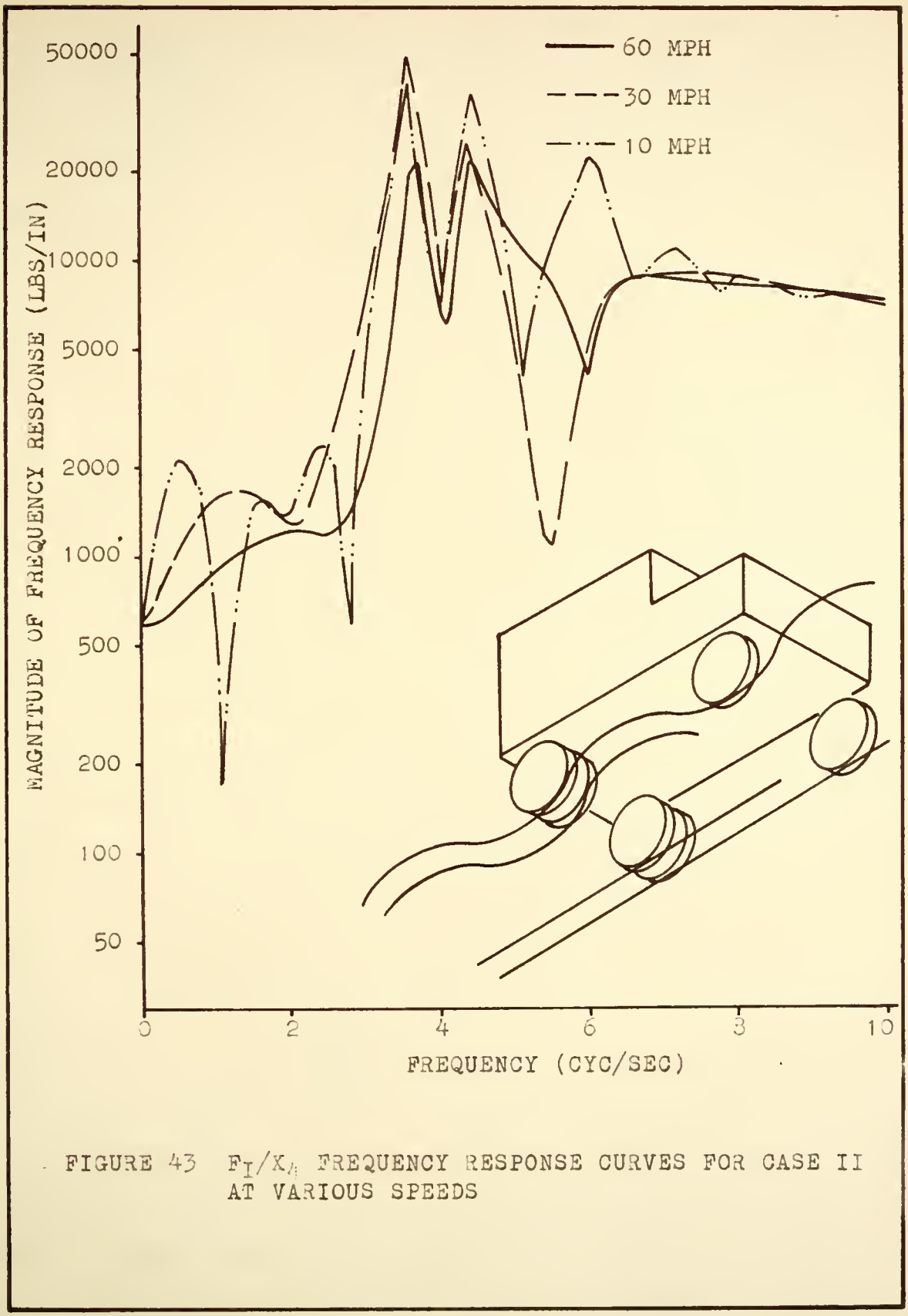

FIGURE 43 F_I/X_4 FREQUENCY RESPONSE CURVES FOR CASE II AT VARIOUS SPEEDS

outer right rear duals will change because of the relative angle, θ_1 in Figure 39, between the truck and the ground. For an automobile, the zero value ordinate would be zero if a similar model were used. However, the fact that the center of gravity shifts when the vehicle is tilted has not been accounted for in the model. In the actual vehicle, there will be a change in the static force due to the center of gravity shift as the vehicle is tilted.

Note that the frequency response magnitude at zero frequency for Case II is smaller than Case I. This is because the right front tire no longer is fixed. The high frequency region would be similar to Case I. Note, however, that the resonant peaks are higher for Case II than for Case I at low speeds.

Case III illustrates the assumption that all tires receive inputs, and the roadway is identical in the right and left wheel paths. This assumption was used in reference 23. The frequency response and truck excitation are shown in Figure 44. Note that the zero frequency ordinate is zero since there are no springs to resist when a displacement is simultaneously applied to all wheels. A passenger car would respond similarly at low frequencies. The high frequency portion is similar to Case I and II. The resonant peaks are higher for this case than the other cases. Also there are only two prominant peaks since the rolling mode, tilting from side to side, is not excited.

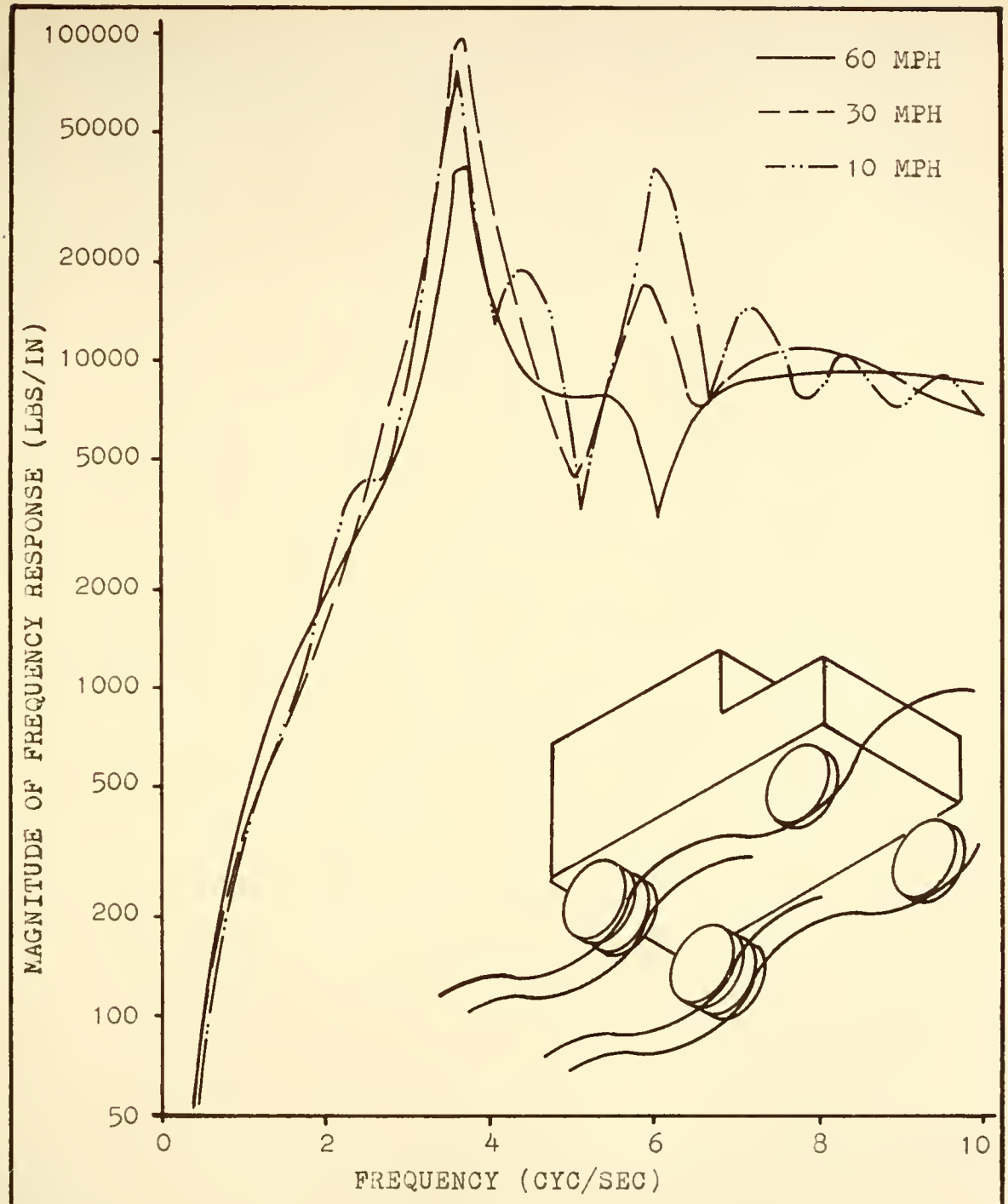

FIGURE 44 F_I/X_4 FREQUENCY RESPONSE CURVES FOR CASE III AT VARIOUS SPEEDS

A Case IV could be discussed where one frequency sine wave would be applied to one side and another frequency to the opposite side, but the results would not be such as to be easily presented and hence will not be discussed. Information about both wheel paths would be required.

CHAPTER IV

RESULTS OF HIGHWAY TESTS

The primary objective of this investigation was to measure the dynamic tire forces that a large vehicle exerted on the pavement during highway tests conducted jointly with the Stresses and Deflections Group of the Civil Engineering School. The pressure measuring systems were developed for this purpose. The force records obtained during these tests were used by the Stresses and Deflections Group as pavement loading information.

The highway tests were made with the test vehicle in the same condition as when the pressure measuring systems were calibrated. During these tests, the tire pressure in the inner and outer left rear dual tires was recorded as the truck traversed a region near a test point in the pavement. The truck driver maintained a given constant speed in the region near the test point. As the truck passed over this region, the Stresses and Deflections Group measured, among other things, seismic accelerations at various depths in the pavement and sub base.

In order to locate the test section on the pressure records, one inch pipes were placed across the left wheel

path at equal distances before and after the test point. These pipes produced characteristic impulses in the pressure records that were easily distinguishable from variations in the pressure caused by the normal road profile. The Stresses and Deflections Group used strip switches to activate an event marker on their oscillograph. These switches were usually placed in the left wheel path at equal distances before and after the test point and were activated when the truck passed over the switch. This switch would also produce a small characteristic pulse in the pressure record that was distinguishable in most of the records. These pulses were used to correlate the time base for the truck pressure records with the records obtained by the Stresses and Deflections Group.

At the start of each run, the truck was stopped and the tire pressure systems allowed to come to equilibrium. The output of the pressure instrumentation was balanced to a zero position. The truck would then accelerate to the given speed for the run and pass over the test section. After the truck had moved away from the initial position, the relative elevation of the initial contact point of each of the six tires was measured with a rod and level. It was intended to later place the truck in a similar disposition on the calibrator to determine the static value of the force at each of the left rear dual tires. In this way, the dynamic forces could be added to the initial static

force to obtain the total force. Because of time limitations and instrumentation difficulties these static tests were not performed. The static force under each tire of the rear axle was therefore assumed to be 4500 lbs.

Particular attention was given to this last detail because the vehicle did not use the normal wheel paths during the highway tests. The test point was located approximately 11 inches to the left of the pavement center line and in order for the left rear dual tires to be centered over the test point, the left wheels had to assume wheel paths in the left lane. When the left rear dual tires were centered over the test point, the left rear inner dual tire was almost on the crown of the road, and consequently, the left outer dual, spaced 12 inches to the left, was on a wheel path at a lower elevation than the inner tire wheel path. Thus for this condition the static load was larger on the inner tire and, as shown in Figure 45, the dynamic forces were also larger. These records are for various speeds and for the left rear wheel paths centered about the test point. The large forces near the test point are the result of a depression in the road caused from the installation of the instrumentation in the road. Figure 46 illustrates the force records at the same speeds but for wheel paths centered approximately 11 inches to the right of the test point. For these wheel paths, the static forces are more nearly equal since the left rear tires are

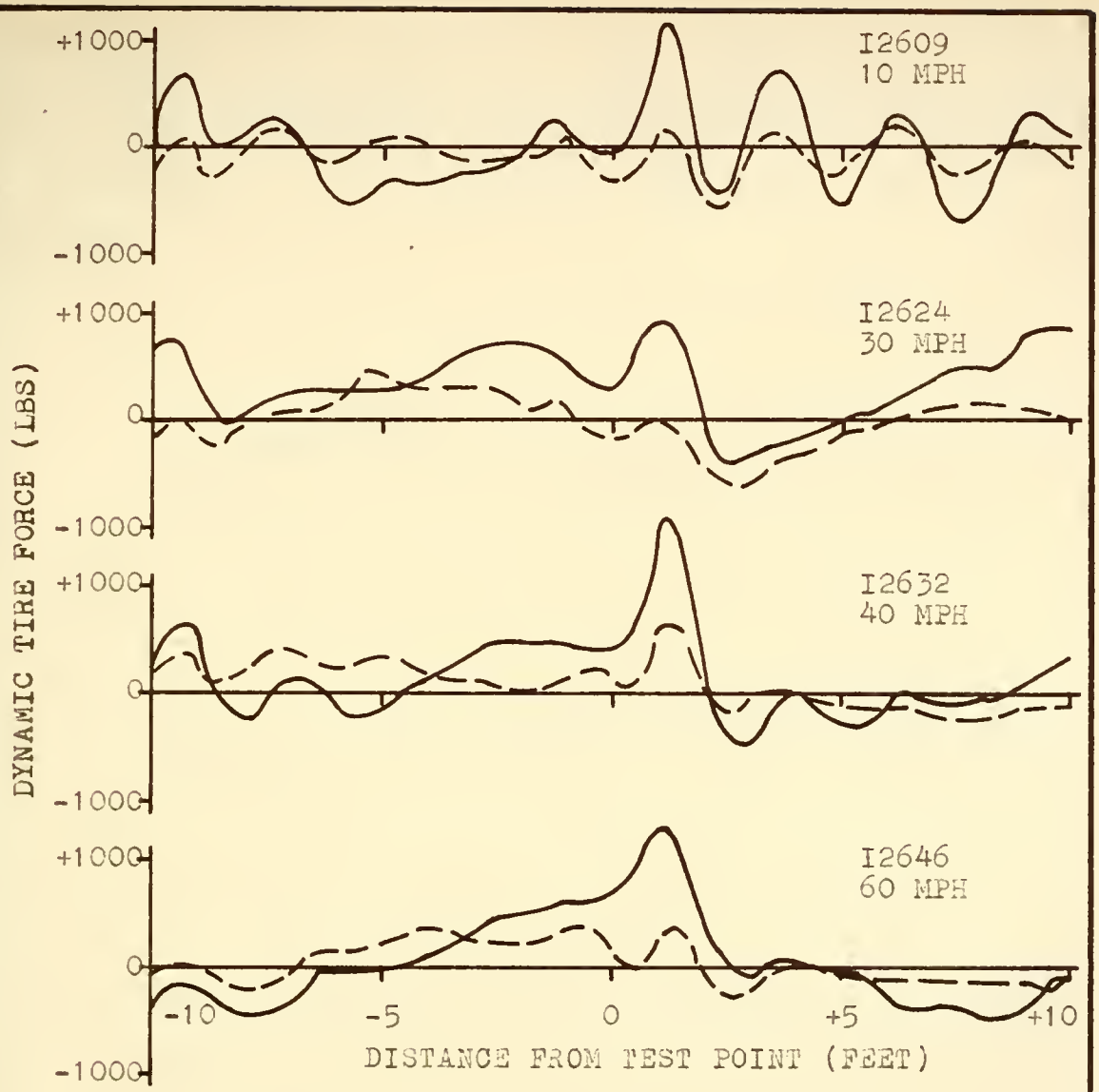

FIGURE 45 FORCE RECORDS OF LEFT REAR TIRES ON WHEEL PATHS CENTERED ABOUT TEST POINT

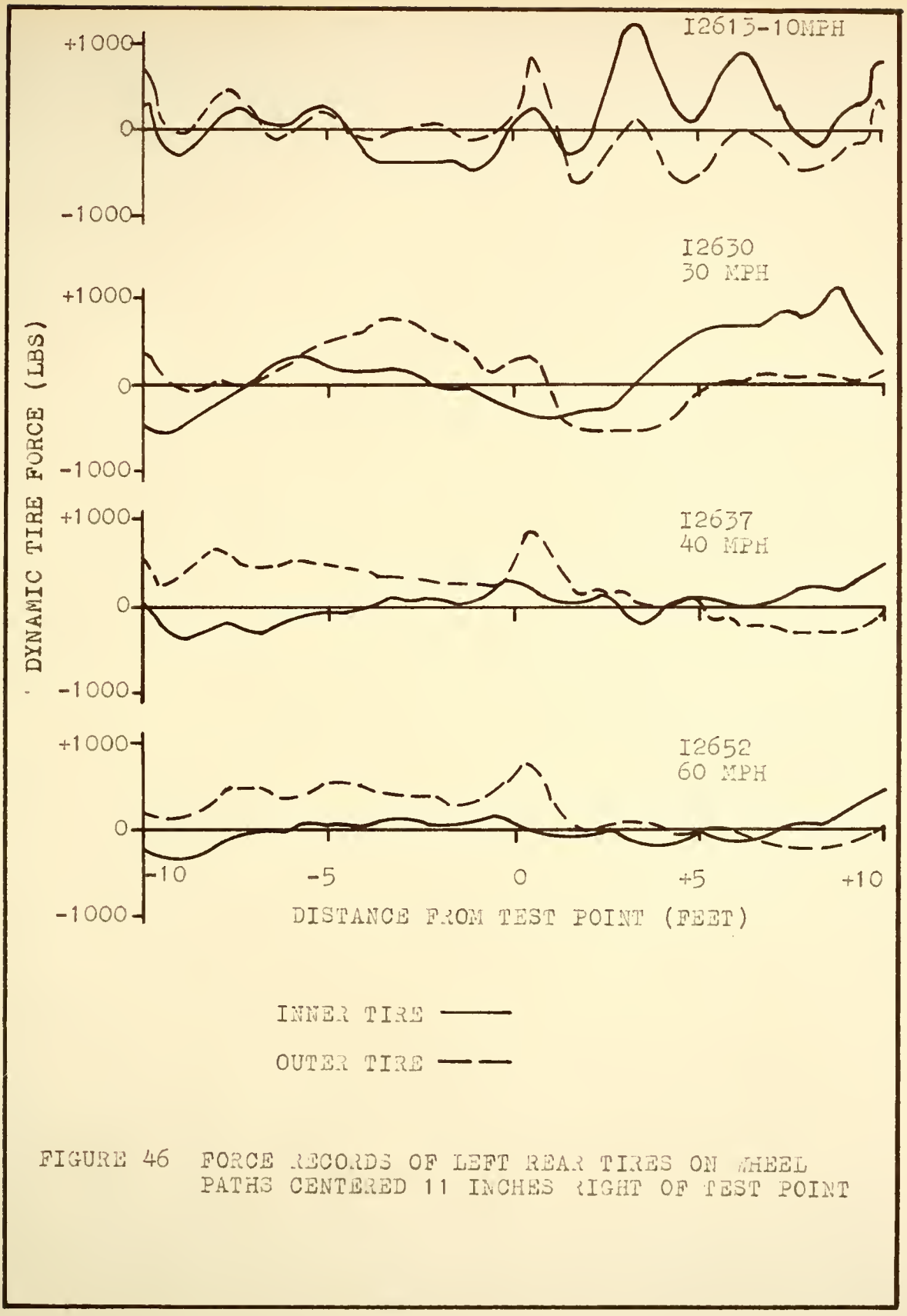

FIGURE 46 FORCE RECORDS OF LEFT REAR TIRES ON WHEEL PATHS CENTERED 11 INCHES RIGHT OF TEST POINT

on either side of the crown. It is interesting to note that the road profile near the test point appears to excite larger dynamic forces at the lowest speed rather than at a high speed.

Some typical combined results of the highway tests are given in Figure 47. The vehicle speed was 20 mph and the left rear wheel paths centered about the test point. In the upper portion of the figure, the total force of the inner and outer tire are shown as a function of the distance of the rear axle from the test point. In the lower portion, the results obtained by the Stresses and Deflections Group are illustrated. The curve shows the displacement of the pavement surface at the test point also as a function of distance of the rear axle from the test point.

The dynamic force records that are shown are typical of the highway test results. The records have been converted from the dynamic pressure records. The force records that were obtained during these tests were plotted, printed and punched on IBM cards. There were 131 sets of these records and, are now on file with the Stresses and Deflections Group.

The Vehicle Dynamic Group was primarily concerned with the problems involved in making these records and developing data processing procedures to convert the pressure records to force records.

Several procedures may be employed for the conversion

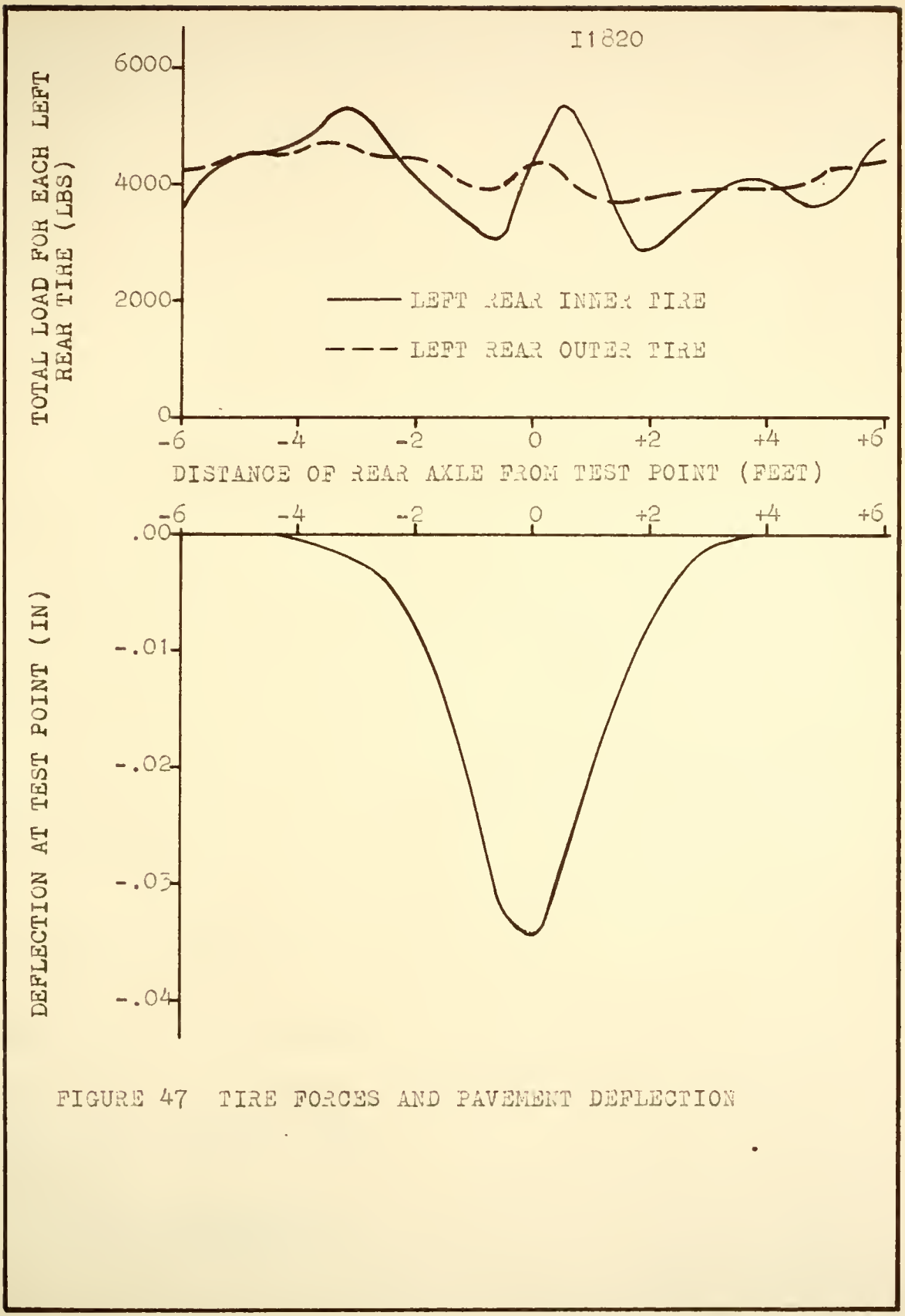

FIGURE 47 TIRE FORCES AND PAVEMENT DEFLECTION

of the tire pressure records to tire force records. One method involves the use of the impulse response of the pressure system and the convolution integral. If it were possible to subject the tire to a force impulse, the resultant pressure transient w(t) would be called the impulse response. If the system were linear, the pressure response p(t) to any general force excitation f(t) would be given by

$$p(t) = \int_0^\infty w(\tau) f(t - \tau) d\tau \tag{25}$$

The application of this technique to the present problem would require the solution of Equation 25 for f(t). This would not be an easy task.

However, by assuming f(t) and p(t) have the Fourier transforms F(f) and P(f) respectively, Equation 25 may be transformed to

$$P(f) = Y(f)F(f) \tag{26}$$

where Y(f) is the frequency response of the pressure system, or in terms of the F/P frequency response obtained from the calibration tests

$$F(f) = \left[(F/P)(f)\right] P(f) \tag{27}$$

Thus an expression for the Fourier transform for the force

record F(f) has a relatively simple character. In order to take a Fourier transform of p(t), the integral

$$\int_{-\infty}^{\infty} |p(t)|\, dt$$

must exist. The pressure records obtained from the road tests do meet this criterion since the truck started from rest and stopped after it passed through the test region. However, the runs were each several minutes long, and since there were 131 runs, this technique was judged not feasible because of the staggering amount of data required and data processing errors associated with such long records.

In order to bring the data processing procedure into reasonable bounds, an alternate procedure was used for the work with the Stresses and Deflections Group. A Fourier sine series was made of a portion of the pressure records that included the section near the test point. The components of this series were multiplied by the proper value of the magnitude of the F/P frequency response and the individual sine waves were shifted by a phase determined from the phase angle of the F/P frequency response.

In general, as more terms of the Fourier series are used, the series will more closely approximate the true function. However, finding the Fourier coefficients requires numerical evaluation of the following integrals:

$$b_n = \frac{2}{T_0}\int^{T} p(t)\sin\frac{n\pi t}{T}\,dt \qquad (28)$$

$n = 1,2,3,\ldots\ldots\ldots\ldots$

T = length of record containing the test section

These integrals are subject to the same data processing errors as were discussed in Chapter II. Only a finite number of these terms in the Fourier series will most accurately represent the pressure wave because of the various processing errors.

Since there are many records to be processed, the pressure values were read at a relatively large time spacing when compared to the calibration record reading discussed in Chapter III. The Nyquist frequency, the maximum resolvable frequency, is fixed by the time spacing selected to represent the record. The time spacing selection was based on (a) accuracy required to resolve the experimental record, and (b) the economy of reading the records. Thus the Nyquist frequency was limited to a relatively lower value for these tests. There was then some frequency content above the Nyquist frequency and hence a small amount of aliasing was to be expected.

Simpson's rule was used to perform the numerical integration, so the associated distortion was also expected. For an illustration of these effects, a typical pressure

record is illustrated in Figure 43a. It is desirable that the Fourier sine series representation should be identical to this original pressure record. Shown in Figure 43b is the Fourier sine series approximation of the pressure record that was made up of each sine component up to one-half of the Nyquist frequency. It is apparent that the sharp peaks in the original record have been filtered out by truncating the series, but the overall reproduction is good. The effect of increasing the number of components is illustrated in Figure 43c, where frequencies up to the Nyquist frequency are used. The data processing errors introduce an erroneous oscillation into the record. These results are typical of the records that were processed in this fashion. The optimum number of terms to use in the series representation of the pressure record has not been resolved.

Another condition must be considered when selecting the maximum frequency. That is, the F/P calibration results tend to become inaccurate as frequency increases (Figure 20).

Based on these considerations, in all calculations for the Stresses and Deflections Group, the limiting frequency of the Fourier sine series representation of the pressure record was taken as one-half of the Nyquist frequency.

Because of the relatively flat F/P frequency response, an estimate of the dynamic force can also be obtained from the pressure-time records by simply multiplying

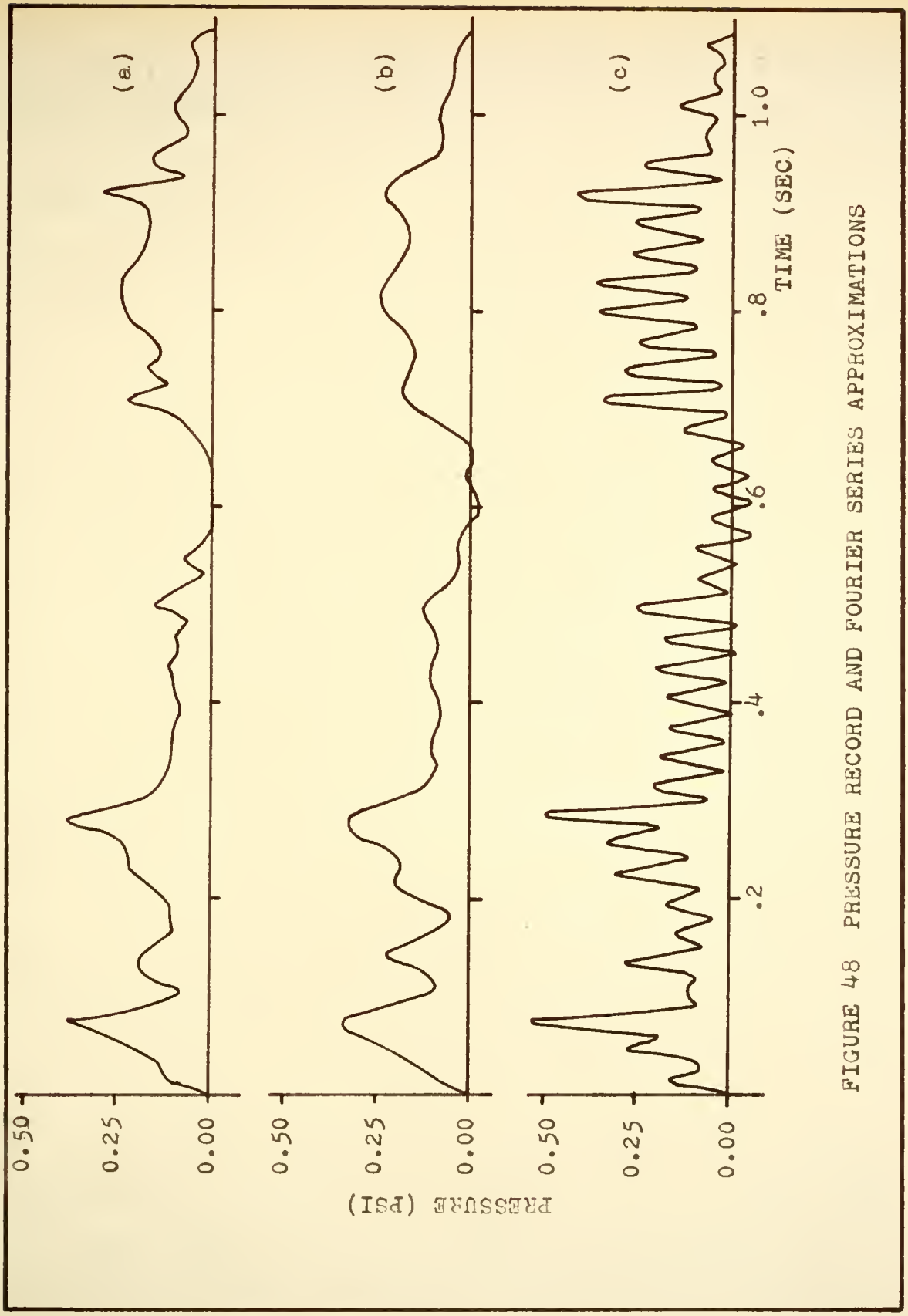

FIGURE 48 PRESSURE RECORD AND FOURIER SERIES APPROXIMATIONS

the pressure record by a suitably selected constant as previously discussed in Chapter III. Figure 49 is a comparison of the tire force obtained by using this method with the tire force obtained when the tire pressure record is resolved into frequency components. The vehicle speed is 40 mph. The force record obtained by simply multiplying the pressure record by a constant appears to lag the other record because of the lead characteristic of the F/P frequency response. The reason that the outer dynamic tire force is less than the inner tire force is because the inner tire was riding on the crown. The time lag may be easily accounted for by choice of the time origin.

There is no large difference in the magnitudes obtained by either of these two methods. Since the technique of converting to force records by Fourier methods allows the possibility of a varying frequency response, it should give the better results.

The impulses caused by the one inch pipes are apparent in the original pressure record in Figure 48a. Lack of pressure transients is a further indication that the frequency response is flat and that multiplication by a constant will give valid results.

Illustrated in Figure 50 are some comparative results of the total tire force of an automobile and the test truck. The truck results are for the right rear inner dual tire and the car results are for the right front tire. Both

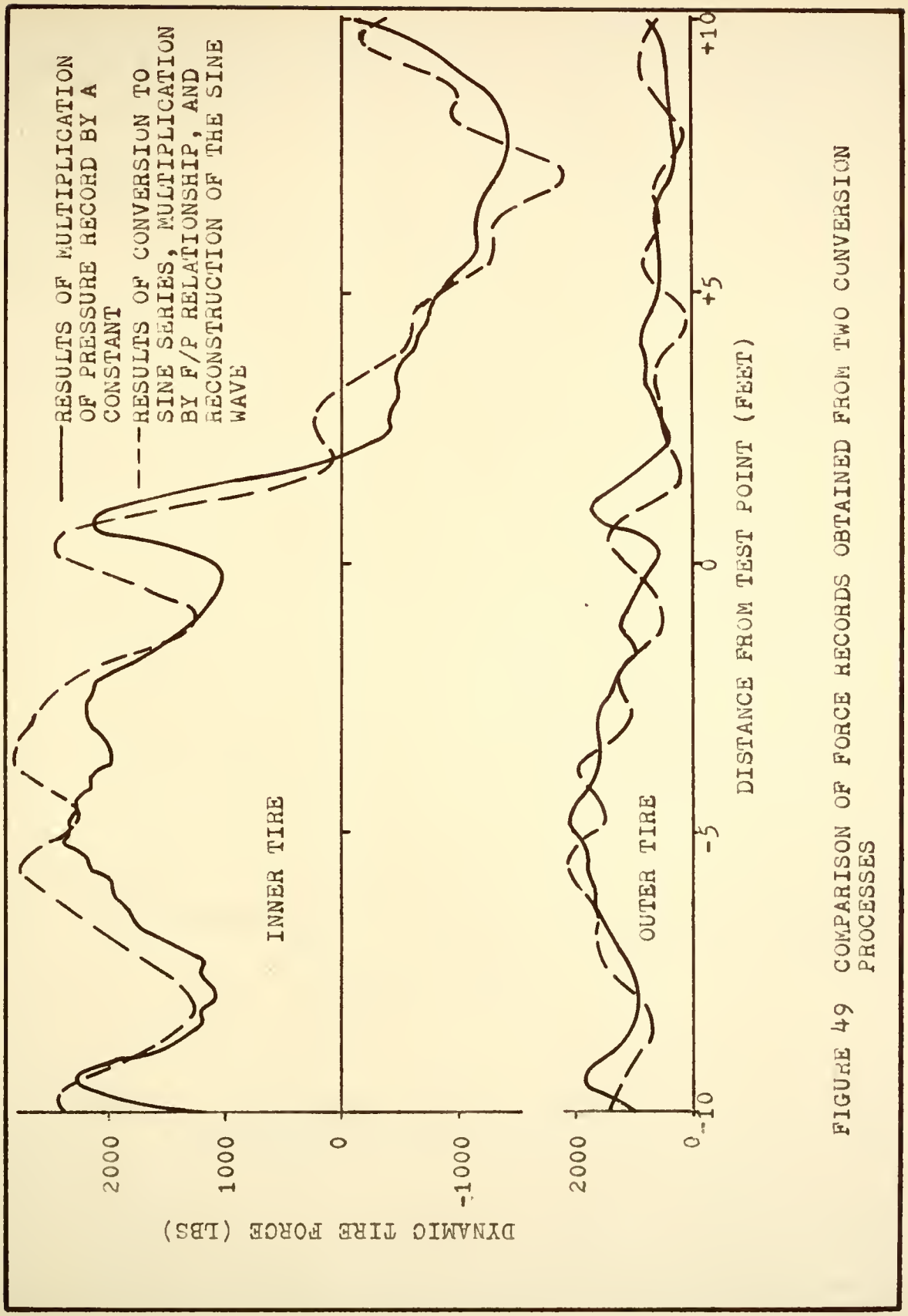

FIGURE 49 COMPARISON OF FORCE RECORDS OBTAINED FROM TWO CONVERSION PROCESSES

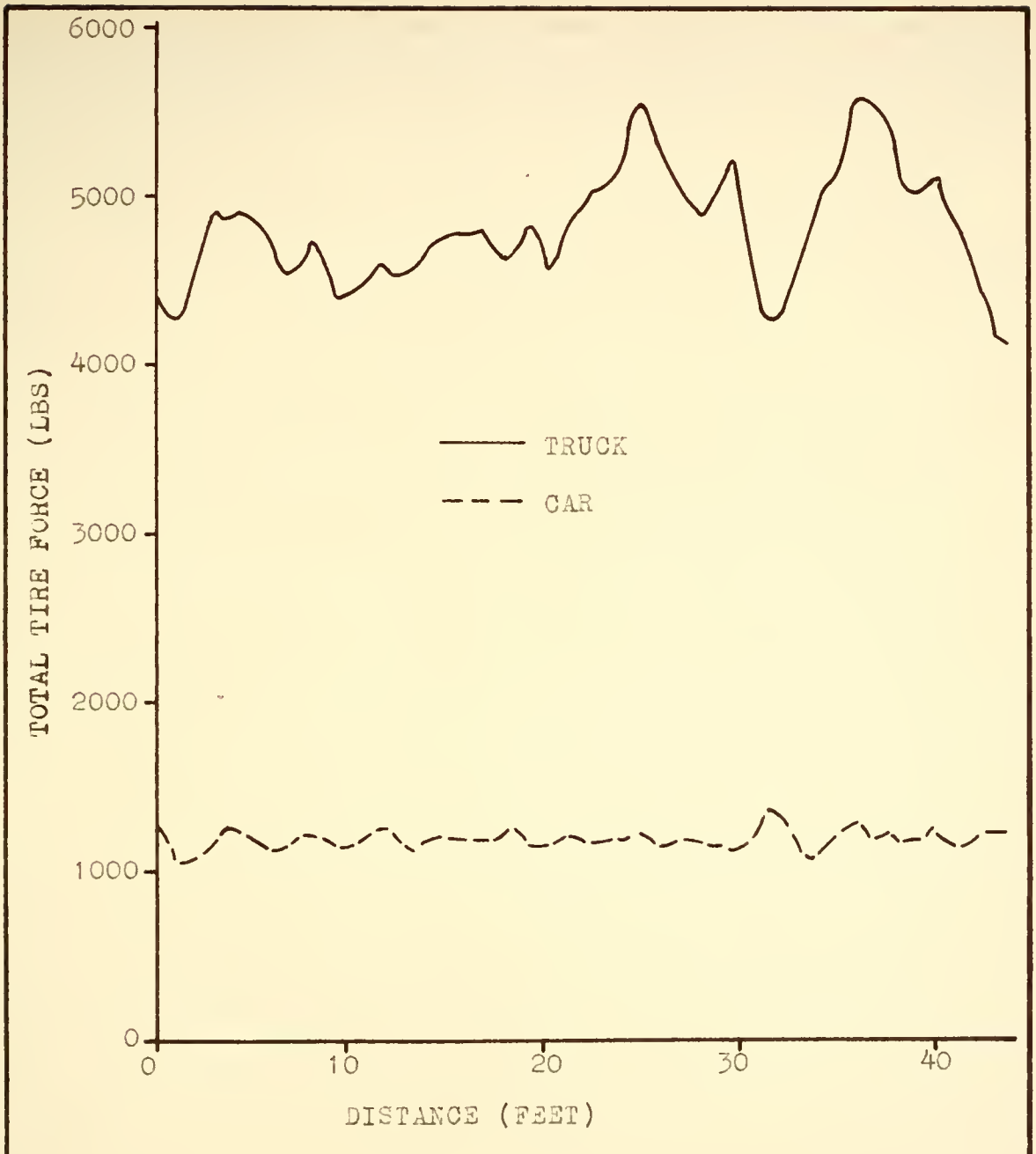

FIGURE 50 COMPARISON OF THE TOTAL FORCE OF AN AUTOMOBILE AND THE TEST TRUCK

vehicles were operated over the same section of pavement at 40 mph, but the record for the truck was made about one year after the record was made for the car.

Another interesting comparison is shown in Figure 51 where the dynamic force is expressed as a percentage of the static load for an automobile and the test truck. This plot was made from the same data used to make Figure 50. This comparison appears to indicate that the dynamic forces of an automobile and a truck are about the same percentage of the static tire forces.

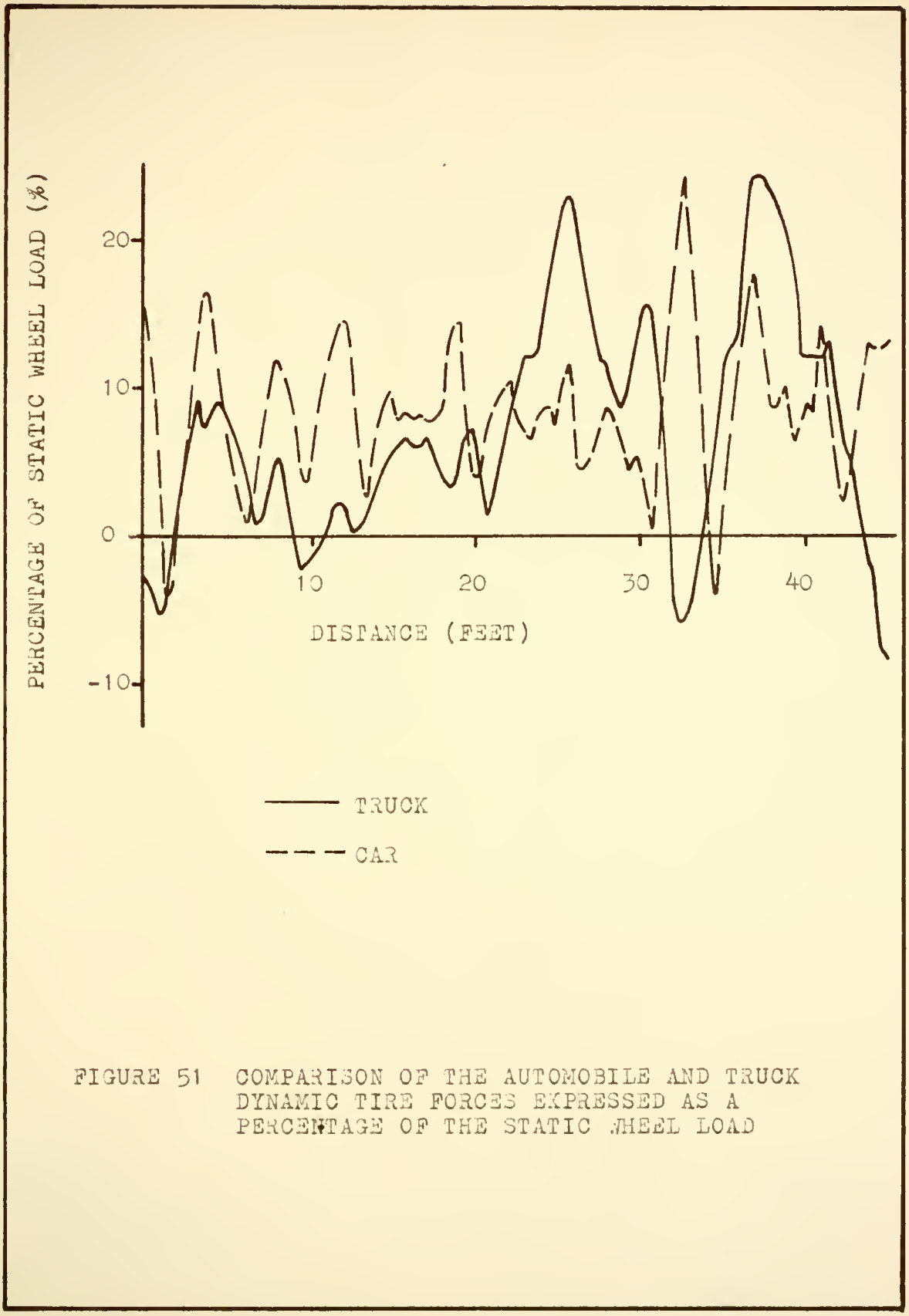

FIGURE 51 COMPARISON OF THE AUTOMOBILE AND TRUCK DYNAMIC TIRE FORCES EXPRESSED AS A PERCENTAGE OF THE STATIC WHEEL LOAD

CHAPTER V

MEASUREMENT AND PREDICTION OF FORCE POWER SPECTRA

A statistical method will now be considered for describing the highway profile and the dynamic tire forces. The statistical characteristic of interest is the power spectrum of the quantity in question.

The method of Blackman and Tukey[9] was used to calculate the required spectra for this investigation. For the complete details of this method, the reader is referred to the original reference. One attractive feature of this method is that an approximate confidence interval may be associated with the spectral estimates. The principle steps of the method as used in this investigation are as follows:

The first step is to preprocess the data in order to remove a nonzero mean value and undesirable low frequency components. If the data have a nonzero mean and large amounts of power concentrated at the low frequencies, the autocovariance function will not approach zero rapidly, a primary requisite when using spectral techniques. The next step is to calculate the autocovariance function from the preprocessed data. This function is calculated for lags

of lengths that are increment multiples of the data spacing.

The third step is to calculate the Fourier transform of the autocovariance function to form a first estimate of the power spectrum. These estimates may be further refined by convolution with an appropriate function. The expected value of each of these refined estimates is the average-over-frequency value of the true power spectrum of the process. The area under this curve is an estimate of the mean square value of the process.

Since equi-spaced discrete data are used, the spectral estimates are vulnerable to aliasing. Trapezoidal rule integration is used for the numerical calculation of the Fourier transform. This procedure is subject to the distortion as illustrated in Figure 9.

If the true spectrum is approximately flat or "white", a confidence interval may be assigned to these refined spectral estimates by treating them as if they followed a Chi-square distribution (χ^2_k) with k degrees of freedom[9]. A Chi-square random variable will become less variable as the number of degrees of freedom k increases. The equivalent number of degrees of freedom, which is a convenient indication of the statistical stability of the spectral estimates, is given by

$$k = 2\left(\frac{N}{m} - \frac{p}{3}\right) \qquad (29)$$

where

N = number of data values

m = number of lag values

p = number of independent records that are combined for the total data length.

The k for the zero frequency estimate and the highest frequency estimate, which is the Nyquist frequency, is one-half of the value given by Equation 29.

The confidence interval assigned to the ratio of the value of a χ^2_k random variable to the expected value of the random variable is illustrated in Figure 52. These curves may be plotted from a cumulative Chi-square distribution table or from the tabulations in reference (9). Use of the curves is exemplified as follows. If a power spectrum calculation was made from 1017 data values from a single record using 50 lag values, the equivalent degrees of freedom would be k = 2(1017/50-1/3) = 40. By entering Figure 52 at k = 40, it is found that there is 50 percent confidence that the ratio of each estimate to the expected value of the estimate will be between .73 and 1.3.

Since most real spectra are not white, the relation given by Equation 29 should serve only as an upper limit. If the spectrum consists of a single narrow peak, the equivalent number of degrees of freedom are approximately two (reference 9, page 24).

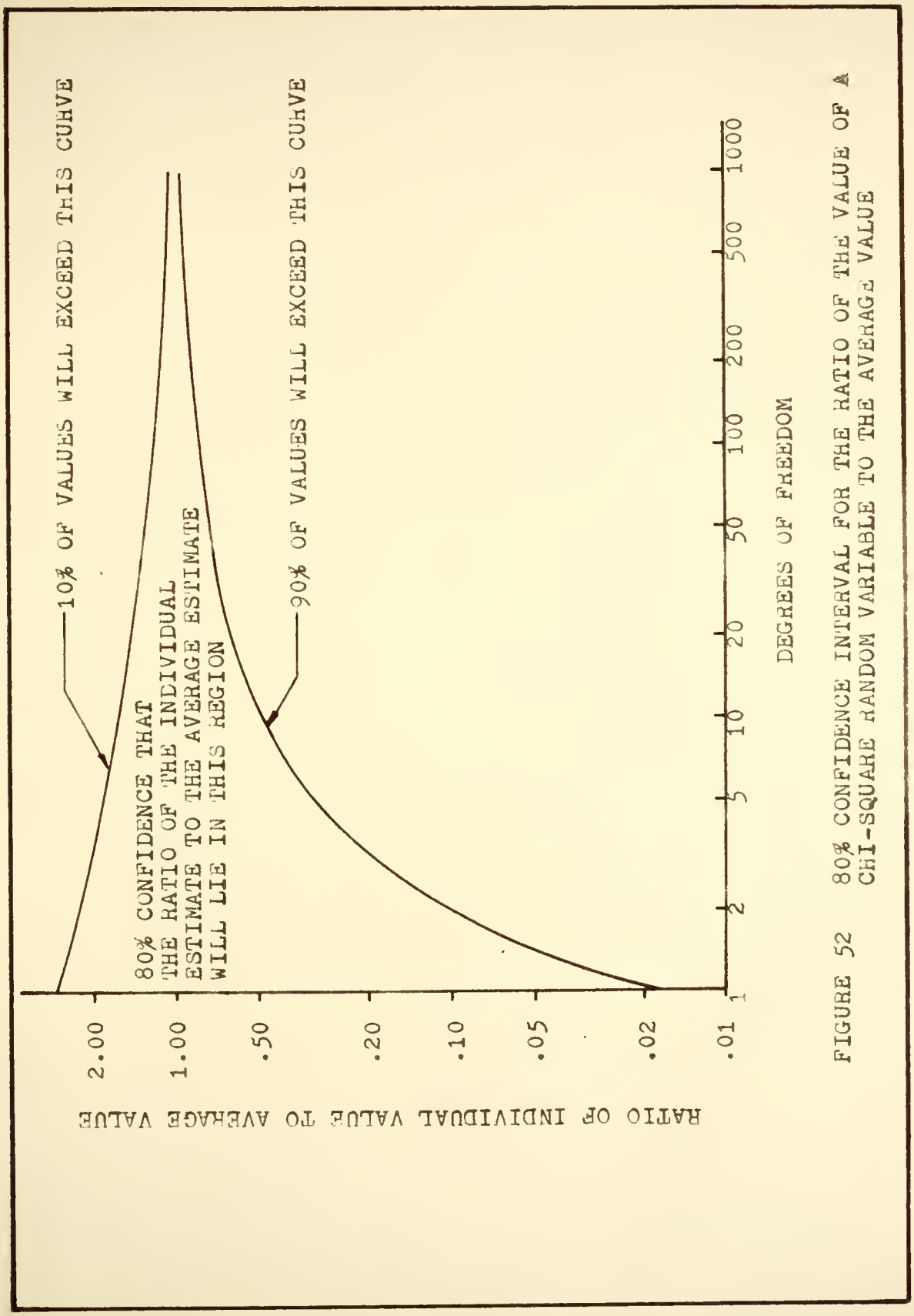

FIGURE 52 80% CONFIDENCE INTERVAL FOR THE RATIO OF THE VALUE OF A CHI-SQUARE RANDOM VARIABLE TO THE AVERAGE VALUE

As shown in Equation 29, the statistical quality of the spectral estimates increases when fewer lags m are taken. However, as m decreases, the frequency resolution of the spectrum decreases since there will be m+1 spectral estimates equally spaced between 0 and the Nyquist frequency. Thus the choice of m will be a compromise between frequency resolution and statistical quality.

For two degrees of freedom associated with a single narrow peak, Figure 52 indicates that poor results will be obtained. The best results are obtained when the power spectrum is white. This situation can sometimes be realized by subjecting the data to several preprocessing operations that remove every spectral peak before the power spectrum is calculated. This is called "prewhitening" the data. After the power spectrum is calculated, the filtering effect of the preprocessing may be divided out of the power spectrum. This is called "recoloring". Reference (10) gives examples of this process. However, in this investigation prewhitening greatly increases the computation effort and affects the results only slightly.

A power spectrum furnishes statistical information in the frequency domain. Spectral theory and linear system analysis can be combined to form very convenient relationships. An important result that is derived in reference (24) deals with the response of a linear time-invariant single input system having a stationary random

process as input. If the power spectrum of the input is $P_x(f)$ and the frequency response of the system is $Y(f)$, the spectrum of the output is

$$P_y(f) = |Y(f)|^2 P_x(f) \qquad (30)$$

Equation 30 can be used to predict a power spectrum of the dynamic forces exerted by the vehicle on the pavement. As was discussed in Chapter III, the conditions accompanying the equation are only approximately true for the truck used for this investigation and thus the predicted results must be viewed as estimates.

In addition, there are problems associated with the calculation of elevation power spectra. There are numerous articles that give the results of calculations of elevation power spectra for pavements, but the relationship between these calculations and other commonly used criteria of pavement condition has not yet been completely established. Until it has been shown that the elevation power spectrum correlates highly with other criteria of pavement condition, there exists the possibility of error when using the elevation power spectrum as a pavement characteristic. Further research in this area is described in reference (25).

An elevation power spectrum is a geometric statistical characteristic of the pavement that indicates the distribution of the mean square value of deviations of the elevation

measurements over a distance based frequency. The dimensions of frequency are cycles per foot (CPF) and the magnitude of the spectrum has the units of feet squared per cycle per foot (FT^2/CPF). This spectrum may be converted to a time based spectrum for any vehicle velocity.

The reason that reliable results are difficult to obtain when calculating an elevation power spectrum is that the amplitudes associated with hills and valleys are very large when compared to the shorter wave length components which are of more consequence to the vehicle suspension system performance. Consequently, there is an extremely large peak in the elevation power spectrum near zero frequency that will distort many of the other spectral estimates. An equivalent indication of this distortion for a narrow spike is given by the reduction to approximately two, of the equivalent Chi-square number of degrees of freedom of the spectral estimates.

A common procedure that is used for dealing with this situation is to prewhiten the data. De Vries[10] discusses in detail several variations of this procedure. A technique suggested in this reference was chosen for use in this investigation. The technique is to preprocess the data by dividing the record of the elevation profile into several subsections, find a least squares best fit second order curve for the data in each separate subsection, and then use the deviations of the data values from the curve

to calculate the elevation power spectrum. These deviations are illustrated in the upper part of Figure 53. This technique will filter out the longer wave lengths in the elevation profile data as indicated by the power filtering character associated with this procedure in the lower part of Figure 53. The power filtering characteristic is the square of the magnitude of the associated frequency response for this data preprocessing technique.[10] The 100 foot base line was used for the calculation of the elevation power spectra.

Normally, this characteristic would be divided out of the spectrum after the elevation power spectrum was calculated (recolored), but since a similar filtering procedure will automatically occur with the measured force data due to the equalization restriction of the pressure measuring system, this additional step was not taken for this investigation. Furthermore, the pavement must be divided into relatively short sections, so that the assumption that the vehicle derives the input from only one wheel may be used.

When interpreting these resulting elevation power spectra, it is necessary to recognize several points. The first is that the low frequencies (long wave lengths) will be removed and the spectra will only represent the higher frequencies. A second point is that a pseudo-peak will occur in the spectra near the break point of the data preprocessing filter. This peak is the result of combining

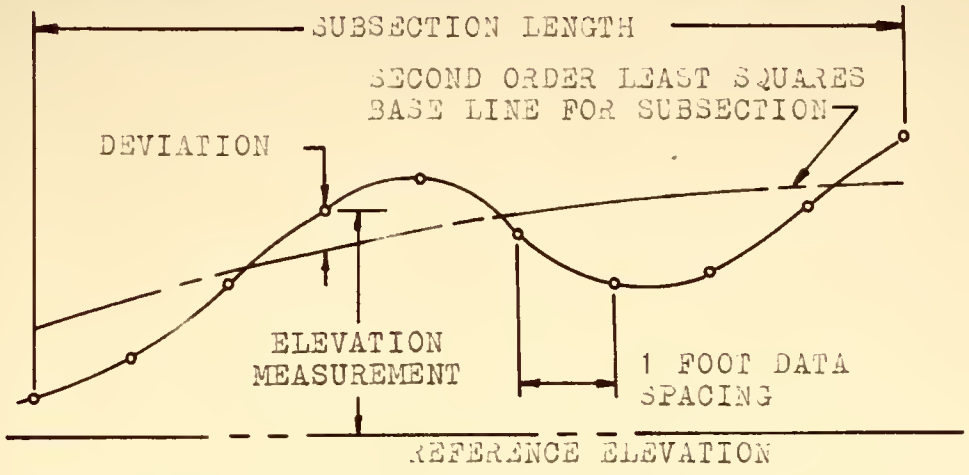

ILLUSTRATION OF DATA PREPROCESSING

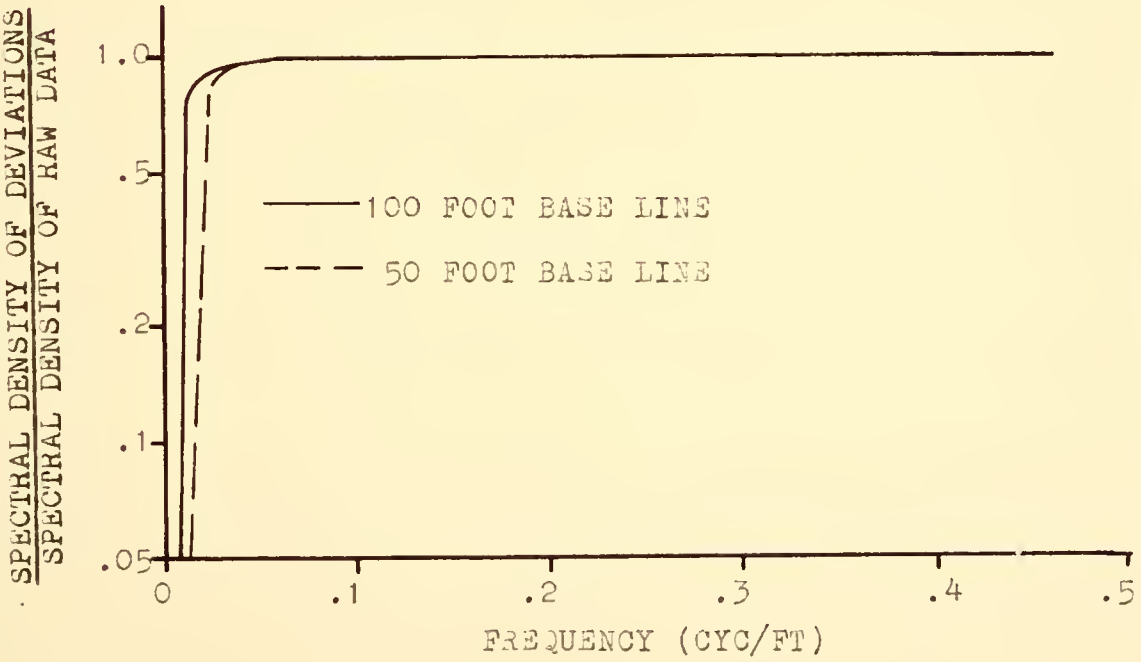

POWER FILTERING CHARACTERISTIC

FIGURE 53 DATA PREPROCESSING AND POWER FILTERING CHARACTERISTIC FOR DATA PREPROCESSING

the sharp low frequency cut-off of the data preprocessing filter (Figure 53) and the rapidly decreasing elevation power spectrum. The true elevation spectrum magnitude should be very large at zero frequency because of the hills and valleys and then decrease as frequency increases. The third point is that the statistical quality of the estimates of the calculated power spectra will be better than if no preprocessing were used. To illustrate these points, an elevation power spectrum was made for a 400 foot length of pavement using the deviations from the mean of all the data values to calculate the spectra. A spectrum was then made with the same data using the deviations from four second order least squares base lines 100 feet long. The results are shown in Figure 55. There are two degrees of freedom associated with the estimates of the first technique and $2<k<15.3$ associated with the second order base lines technique.

The section of pavement used to predict and measure the force power spectrum was on Indiana State Road 26 approximately three miles west of West Lafayette, Indiana. The pavement was of bituminous construction 21 feet wide. The elevation profile was measured with a rod and level at stations one foot apart, 30 inches in from the south edge of the southeast bound lane. This section was surveyed in 1962 and again in 1964.

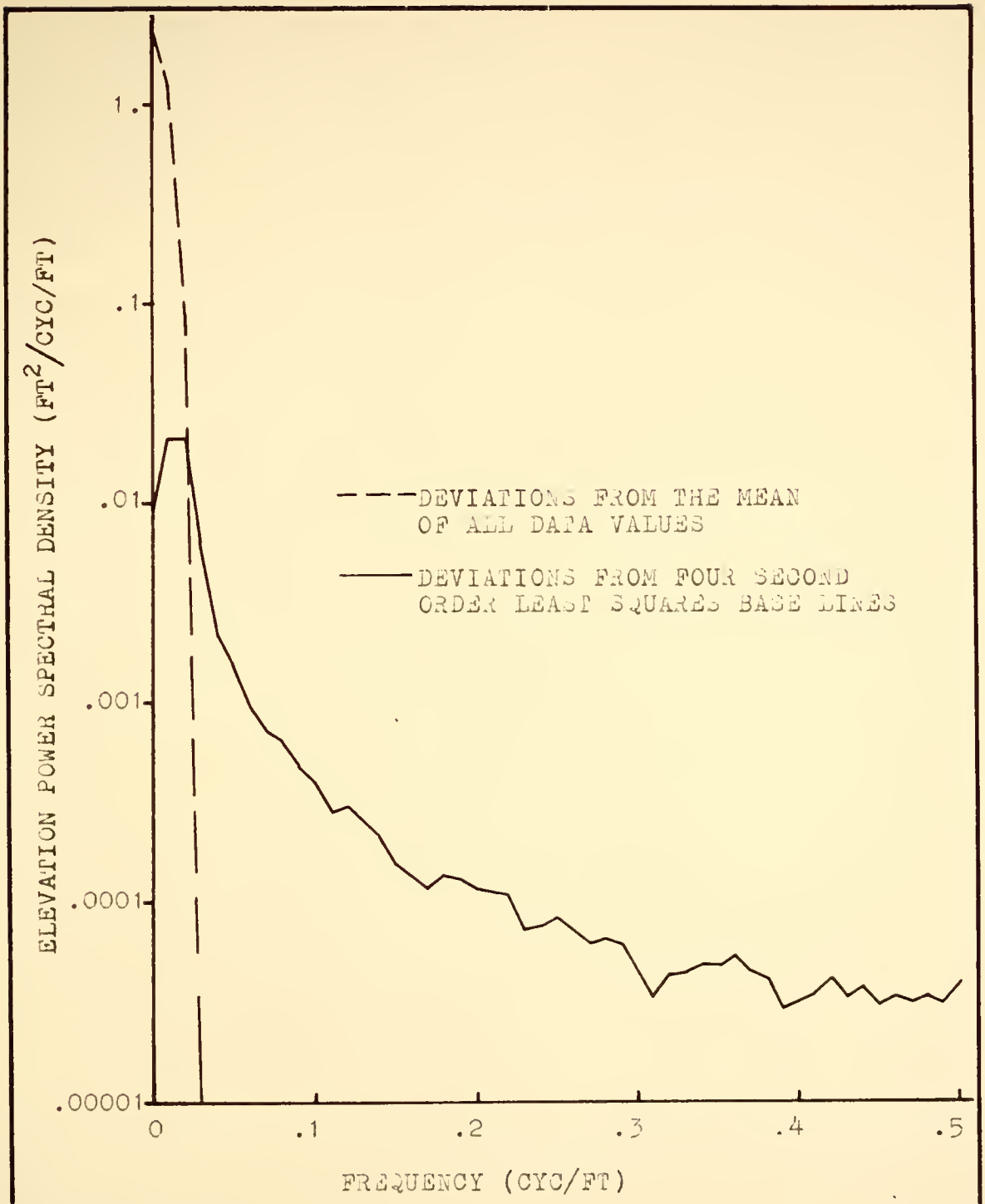

FIGURE 54 COMPARISON OF RESULTS USING TWO DIFFERENT DATA PREPROCESSING TECHNIQUES

The elevation power spectra for the 1962 and 1964 survey are shown in Figure 55. The small difference between the two curves indicates that the characteristics for this section were essentially unchanged after two years of usage. The mean square deviation of the 1962 survey was .5 percent larger than that of the 1964 survey. This small difference could possibly be due to the fact that the measurements in the 1962 survey were made with a .005 foot minimum elevation resolution while the 1964 survey was made with a .001 foot minimum elevation resolution.

It is interesting to note the comparison of the minimum resolution of the 1962 survey (.005 foot) to the magnitude of the minimum drop height used for calibration (.086 inch or .0072 foot). Another interesting comparison is that this resolution is about twice the pavement surface deflection indicated in Figure 47.

A predicted force spectrum was calculated for the right rear inner tire at the speed of 27.0 fps (approximately 20 mph). The experimental F/X characteristic from the .086 inch drop tests was used. For comparison, a predicted force power spectrum for the model described in Chapter III, assuming that left and right wheel paths were identical, was also calculated. The predicted force power spectrum for these two calculations are shown in Figure 56.

To illustrate the effect of speed upon the predicted force power spectrum, results that were available for

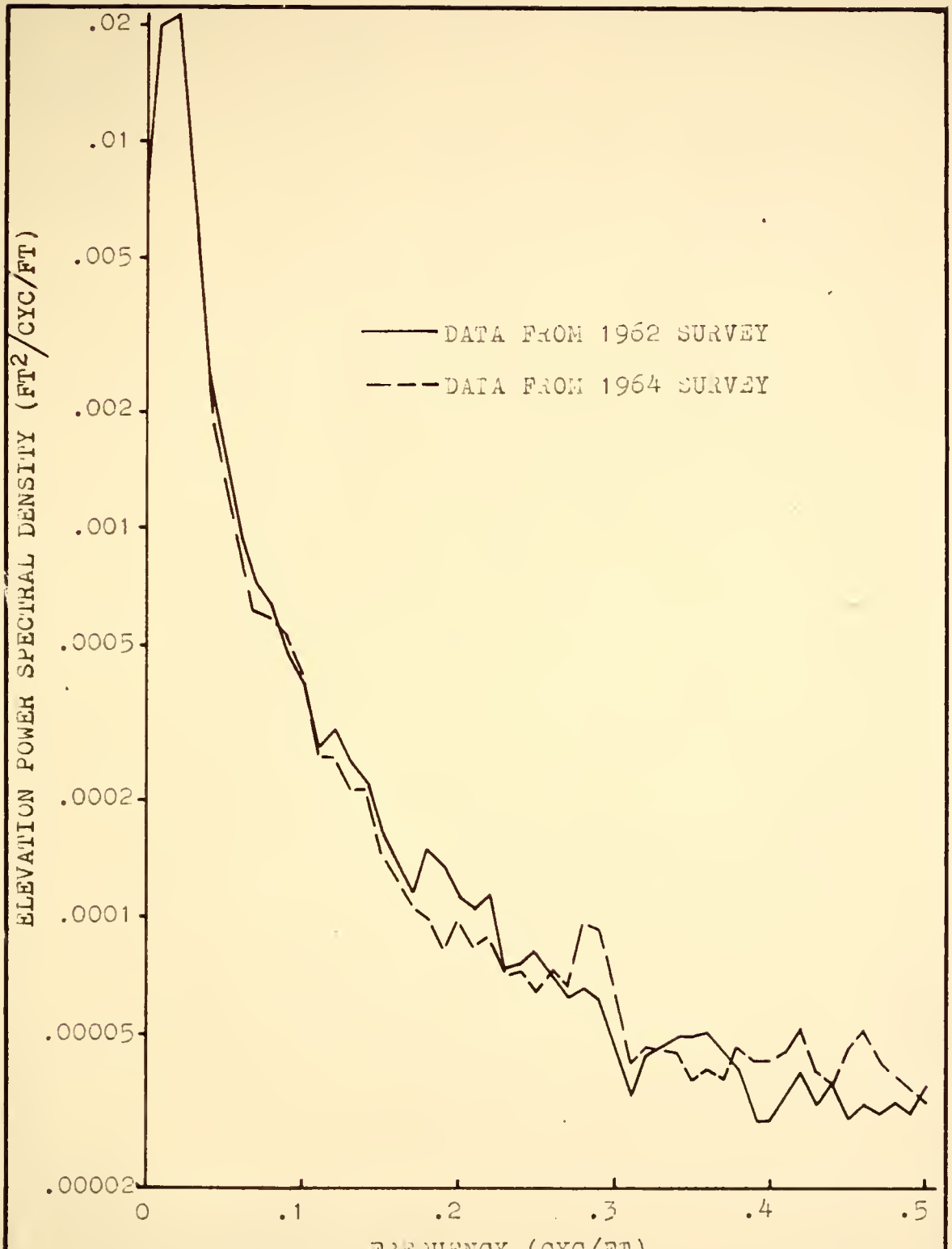

FIGURE 55 COMPARISON OF ELEVATION POWER SPECTRA OF THE SAME PAVEMENT SECTION FOR THE 1962 AND 1964 SURVEYS

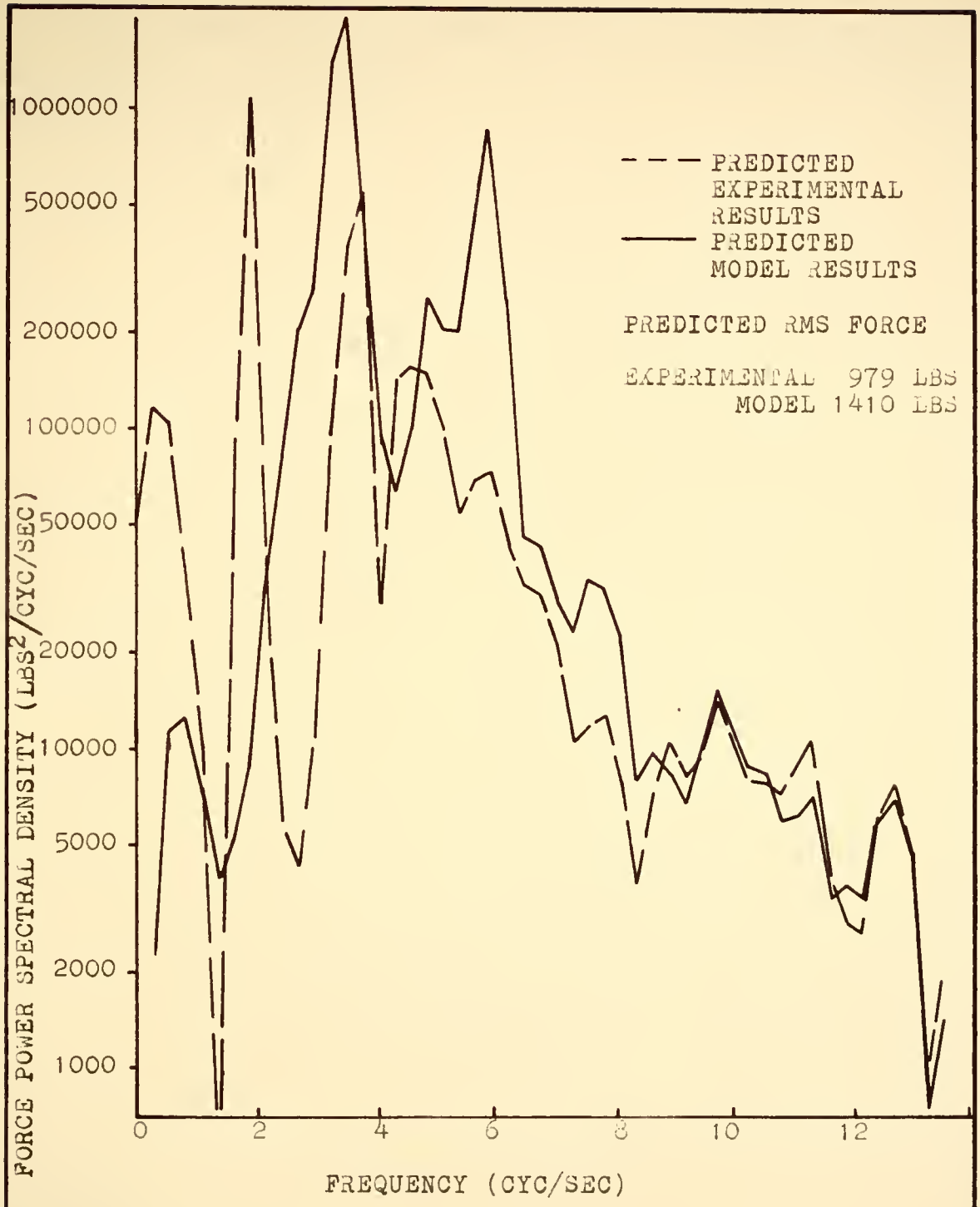

FIGURE 56 PREDICTED FORCE POWER SPECTRA FOR TRUCK AND MODEL OF TRUCK

spectra at five different speeds calculated from the elevation power spectrum using the .671 inch drop F/X frequency response characteristics for the right rear inner tire are shown in Figure 57 and 58. It should be noted that the one foot spacing of the elevation measurements limits the Nyquist frequency to only 13.5 cps for the 27.0 fps (20 mph) calculation. The Nyquist frequency will increase with speed. Because of a larger frequency increment associated with the higher speeds, some of the peaks in the frequency response characteristic will fall between adjacent spactral estimates and the associated curve between the spectral estimates will appear to be attenuated. This effect is especially apparent for the 78.7 fps (60 mph) curve at 3.5 cps.

Experimental tests were then conducted at the site previously described to check the results of these calculations. The Stresses and Deflections Group did not participate in this series of tests. The tests were conducted in a similar manner as described in Chapter IV. The truck used the normal wheel paths for these tests and the inner and outer right rear dual tires experienced forces of nearly equal magnitude.

Tests were conducted at vehicle speeds of approximately 20, 30, 40, 50, and 60 mph. The truck was in the standard condition as when calibrated. A series of tests were also conducted at 40 mph with tire inflation pressures of 55, 65, 75, 85, and 95 psi, but this data was not reduced.

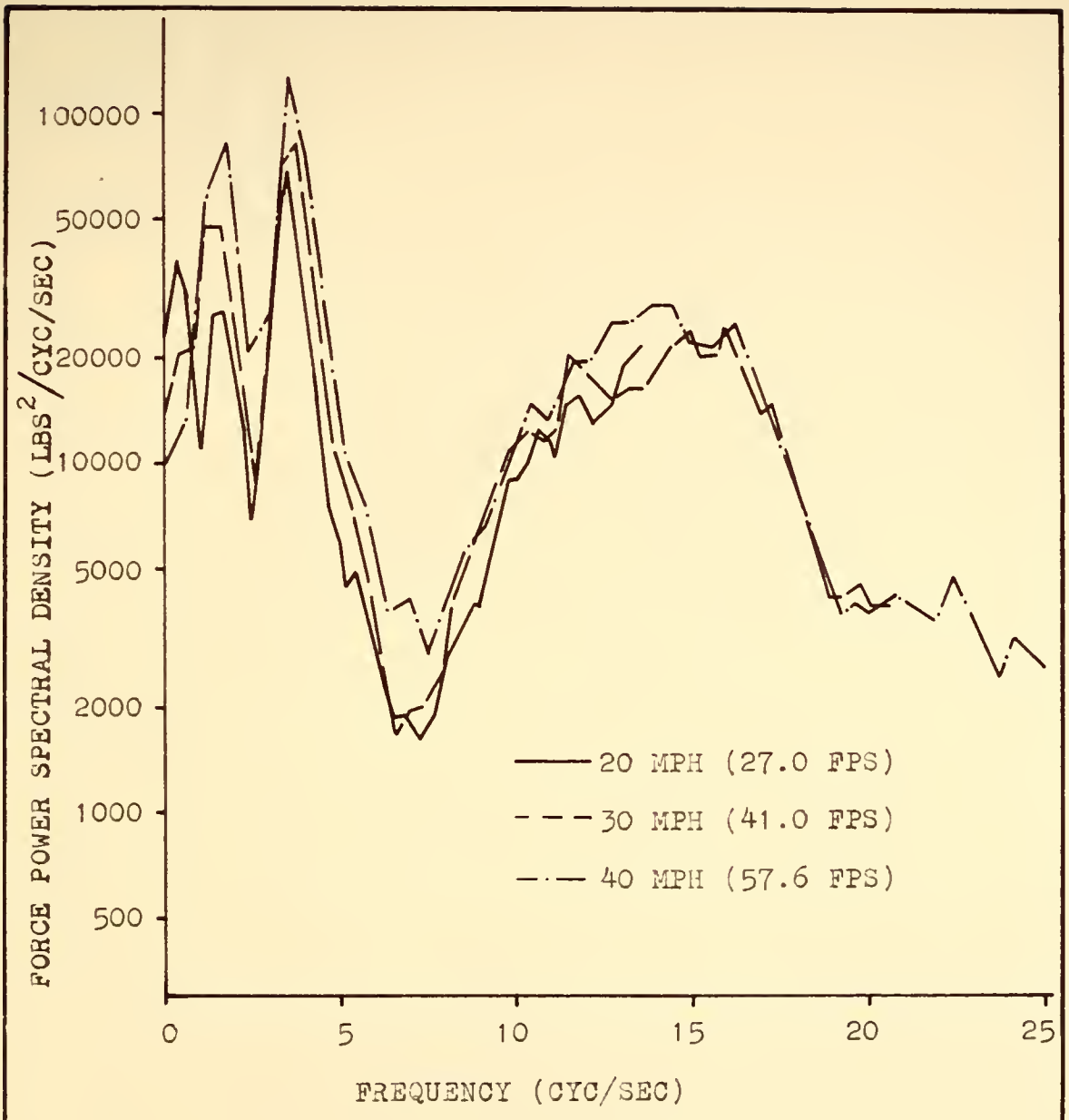

FIGURE 57 PREDICTED FORCE POWER SPECTRA FOR NOMINAL SPEEDS OF 20, 30, AND 40 MPH

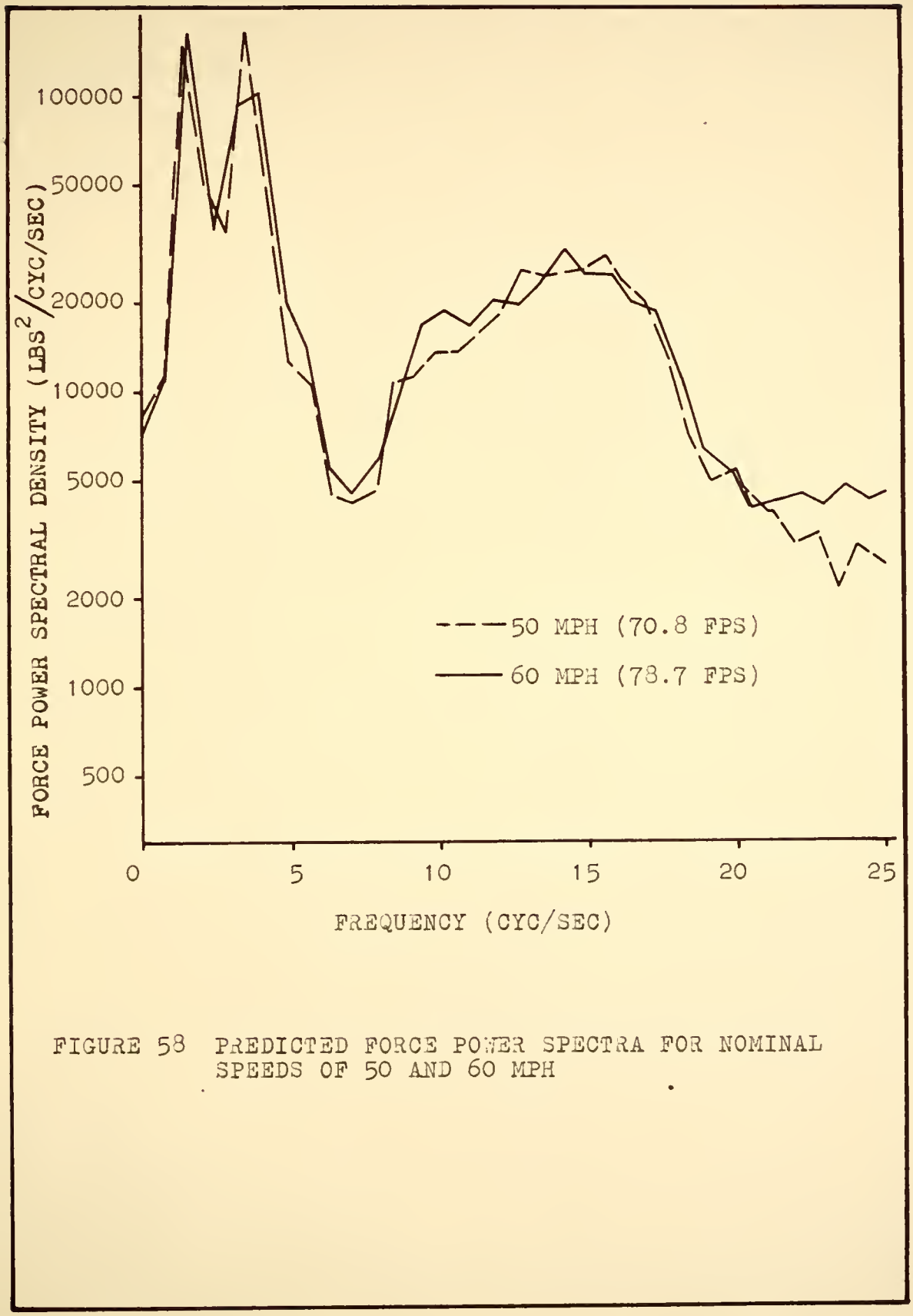

FIGURE 58 PREDICTED FORCE POWER SPECTRA FOR NOMINAL SPEEDS OF 50 AND 60 MPH

The experienced force power spectra that were calculated from force records of the right rear inner tire at various speeds are shown in Figures 59 and 60. These spectra were each calculated from 801 data values that covered 6.06 seconds for a Nyquist frequency of 66 cps. A second order base lines technique with a base line corresponding to 100 feet of pavement was used for preprocessing. Because the equalization restriction in the pressure system acted as a high pass filter, this preprocessing had little effect on the force spectra beyond the zero frequency estimates. There are approximately 23.8 degrees of freedom associated with each power spectrum curve except for the zero frequency values.

Note that the power is concentrated in one broad peak between 0 and 5 cps. This could be due to insufficient frequency resolution since each of the three peaks in the F/X frequency response had a width between half power points of only .2 cps (see Figure 32). Another explanation would be the possibility that only one mode was excited. It is apparent from these experimental spectra that above 8 cps, the curves are similar in that there is no definite trend associated with a speed change. Absent from the records is any indication that the wheel hop mode was excited. More noteworthy, perhaps, is the fact that as the speed is changed from 40 mph, the RMS force (the square root of the area under the curve from 0 to the Nyquist frequency)

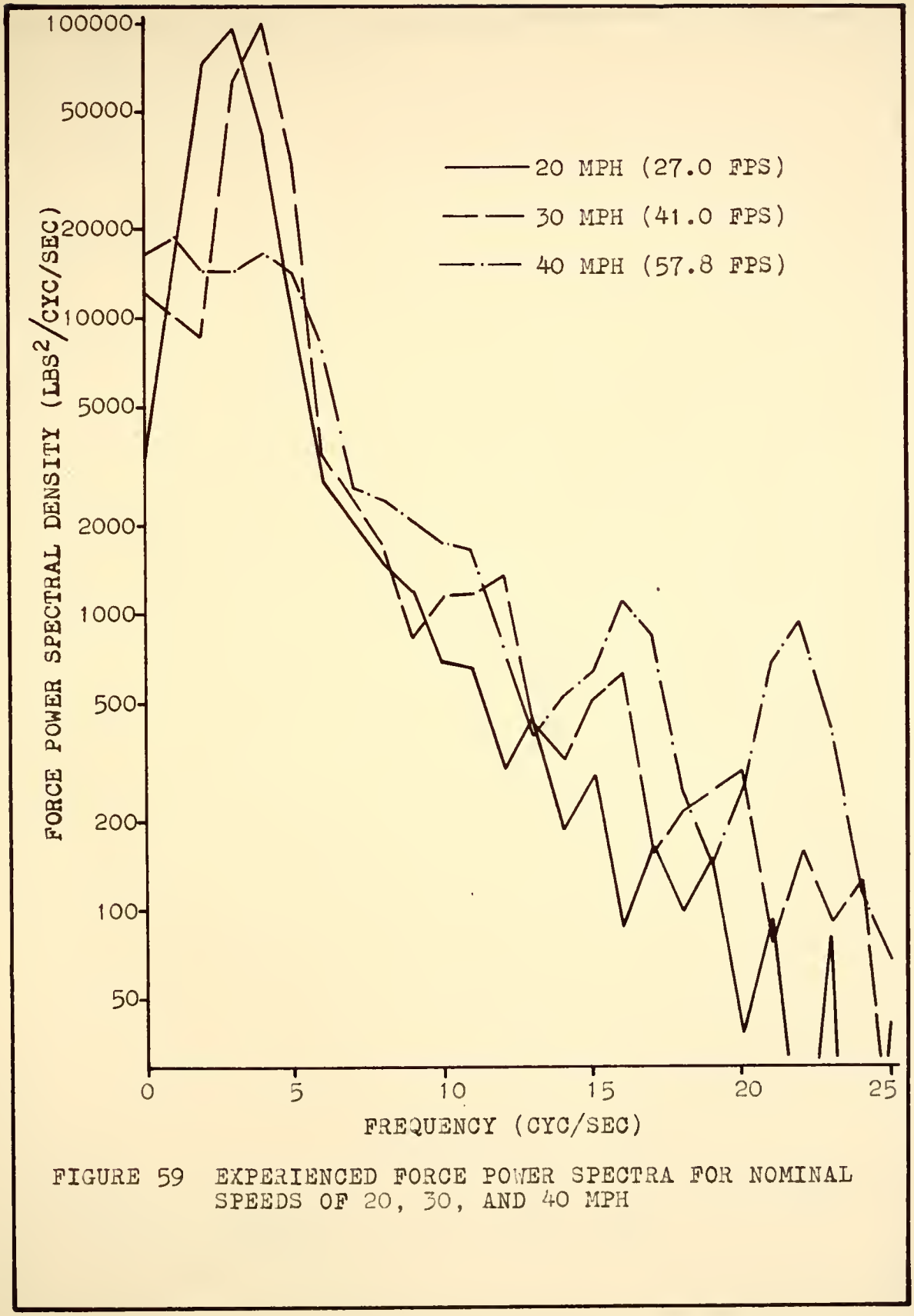

FIGURE 59 EXPERIENCED FORCE POWER SPECTRA FOR NOMINAL SPEEDS OF 20, 30, AND 40 MPH

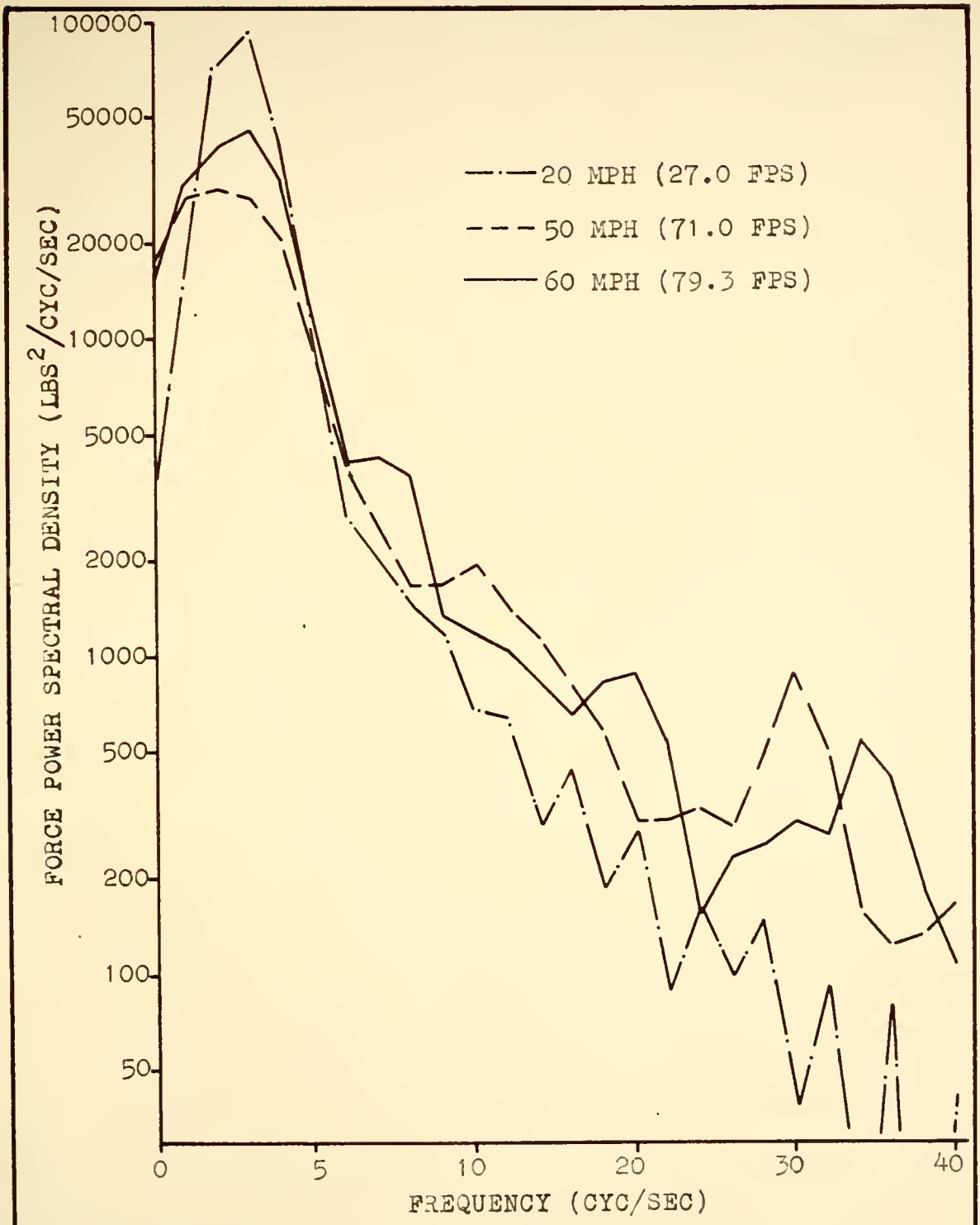

FIGURE 60 EXPERIENCED FORCE POWER SPECTRA FOR NOMINAL SPEEDS OF 20, 50, AND 60 MPH

increased. Thus 40 mph is the vehicle speed (for speeds ranging from 20 mph to 60 mph) for this particular section of pavement for which minimum dynamic tire force exists.

For each of these tests, the truck passed over at least two one inch pipe event markers. The corresponding pressure pulses were faired out of the record when the data was read.

Figure 61 was included to show the comparison of the performance of an automobile and the truck. These spectra were calculated from the same data that were used for Figures 50 and 51. At the automobile wheel hop frequency (15 cps), the automobile spectral magnitude is only slightly less than the value for the truck.

When calculating power spectra for the specific purpose of comparing the measured force spectra with the predicted force spectra for the same section of pavement, more importance was attached to the frequency resolution than to the statistical stability of these two spectral estimates. Thus these special purpose estimates were calculated using a larger maximum lag value than for usual calculations. This results in lower quality estimates for both of the true power spectra. However, the statistical fluctuation in the measured force power spectrum is not independent of the statistical fluctuations in the elevation power spectrum.

Figure 62 illustrates the comparison of the predicted spectrum with the measured spectrum for 20 mph. The maximum

FIGURE 61 COMPARISON OF EXPERIMENTAL RESULTS FOR AN AUTOMOBILE AND THE TEST TRUCK

FIGURE 62 PREDICTED AND MEASURED FORCE POWER SPECTRA

la; was 30 percent of the total data length. The predicted spectrum was calculated from an elevation spectrum using the .036 drop F/K frequency response results. The peaks of the predicted force power spectrum do not fall at the same frequencies as the experienced force spectrum. Further, the predicted spectrum shows much larger ordinates than the experienced force spectrum. The RMS force of the experienced spectrum (the square root of the total area under the power spectrum curve from zero to the Nyquist frequency) is 494 lbs and the RMS force of the predicted spectrum is 979 lbs.

Figure 63 facilitates the comparison between the experimental results and the predicted results that were shown in Figures 58, 59, 61 and 62. This figure illustrates the relationship between the vehicle speed and the RMS dynamic tire force. The predicted point at approximately 20 mph is expected to be in error because of the low Nyquist frequency of 13.5 cps as illustrated in Figure 57. The true value should be greater than that illustrated.

The RMS forces compare well for 20 and 30 mph, but differ by a factor of two at 40, 50, and 60 mph. The predicted spectra do not show the minimum RMS force at 40 mph as exhibited by the experimental results. However, as the speed increases above 40 mph, both curves increase at approximately the same rate.

Power spectrum techniques may be applied in order to

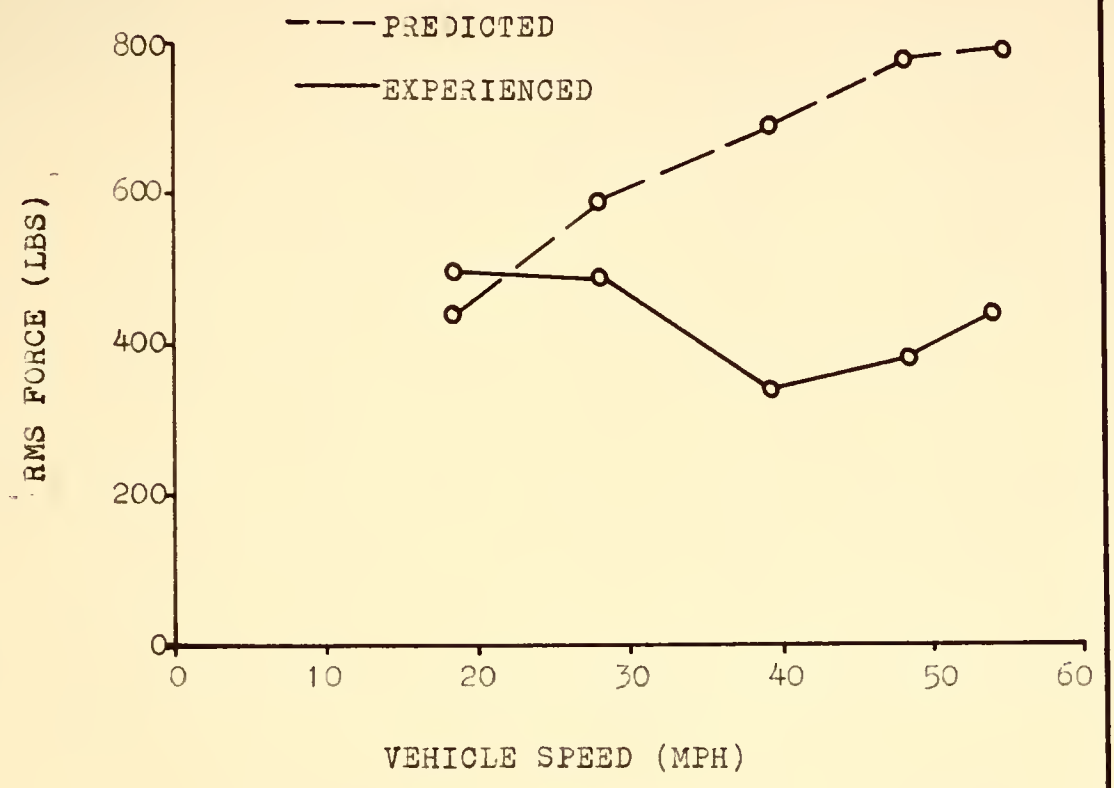

FIGURE 63 COMPARISON OF PREDICTED AND EXPERIENCED RMS FORCE

study related variables. The effect of speed upon the pressure measuring system could not be determined during the calibration tests. Power spectra of the pressure records for the right rear outer tire revealed an unexpected peak located away from the main single peak. This peak was not in the spectra of the right rear inner tire records for 40, 50, and 60 mph. The results of these tests are shown in Figures 64 and 65. The extra peak occurs at a frequency that coincides with the wheel rotation speed which indicates either an unbalanced or eccentric tire or a malfunction in the pressure system. The effect of any of these situations could not be duplicated with the calibration equipment. If the tire were out of balance, then the record would be correct; but if there were a pressure system malfunction, the results would not be correct.

To check the results for the left tires, a measured force power spectrum was made for two typical high speed runs. The results are shown in Figures 66 and 67.

Relatively speaking, only a negligible amount of additional power is observed at the wheel rotation frequency for these tires. It is therefore evident that virtually no extraneous effects are introduced by tire balance or wheel eccentricity for these tires.

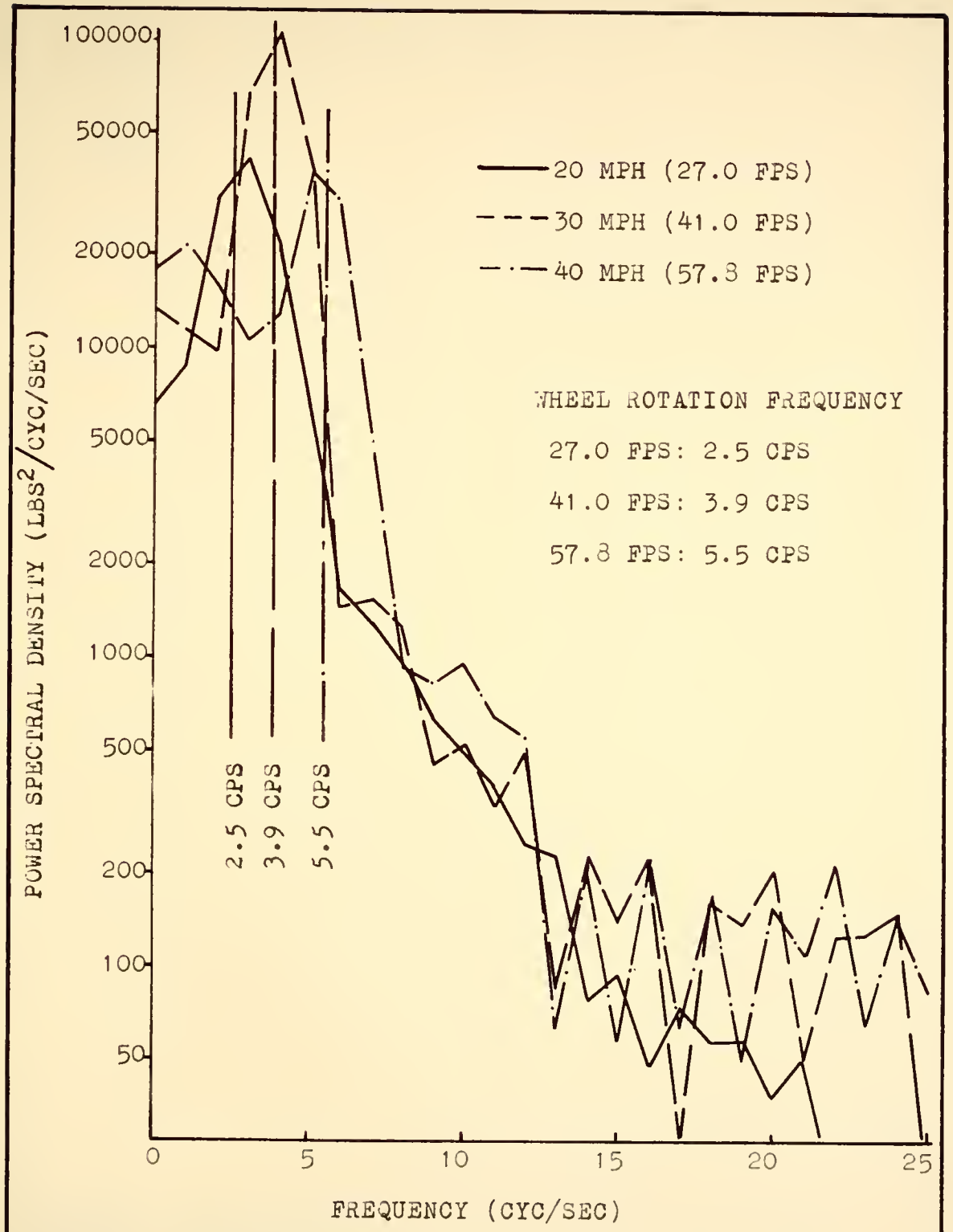

FIGURE 64 EXPERIENCED FORCE POWER SPECTRA FOR RIGHT REAR OUTER TIRE

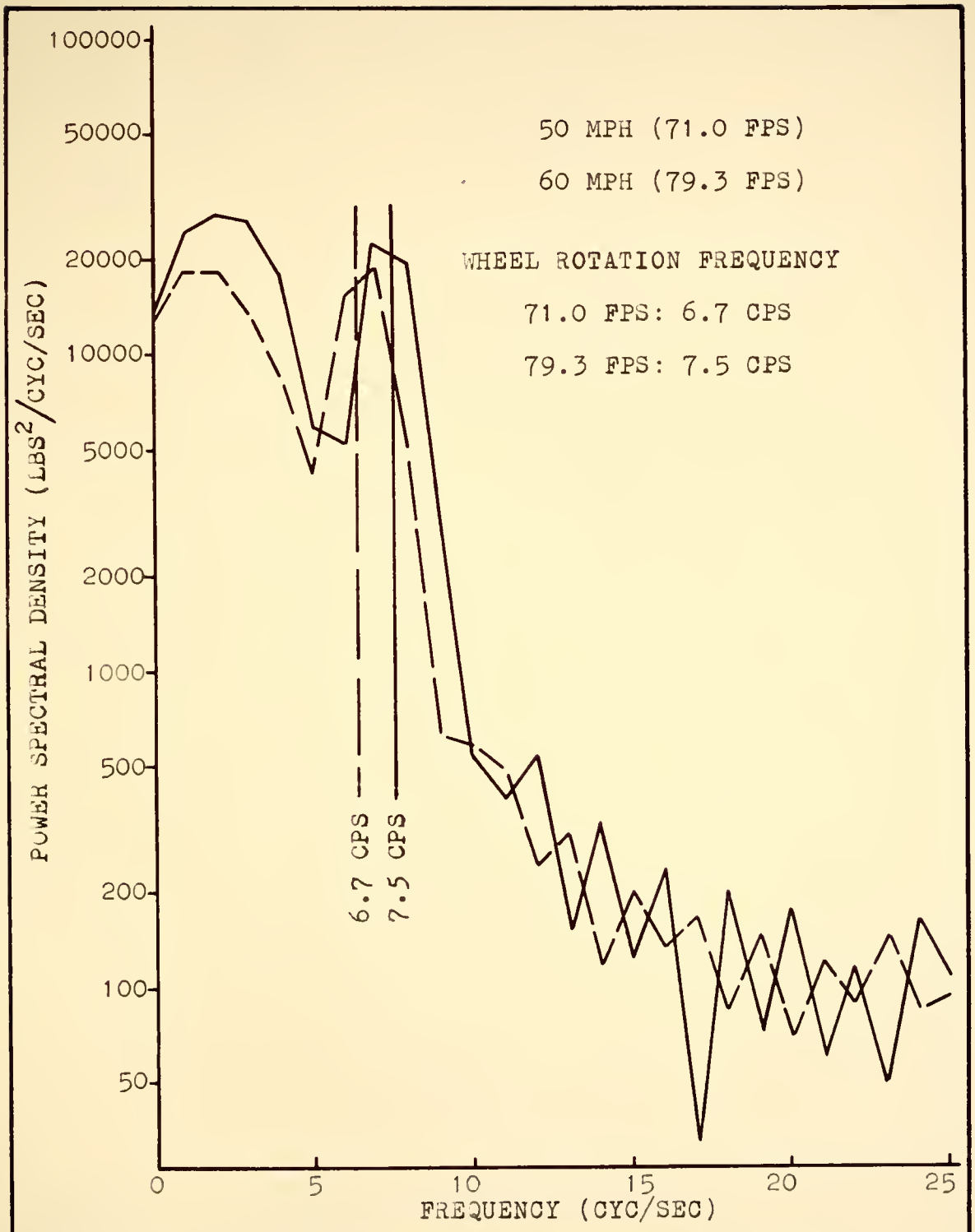

FIGURE 65 EXPERIENCED FORCE POWER SPECTRA FOR RIGHT REAR OUTER TIRE

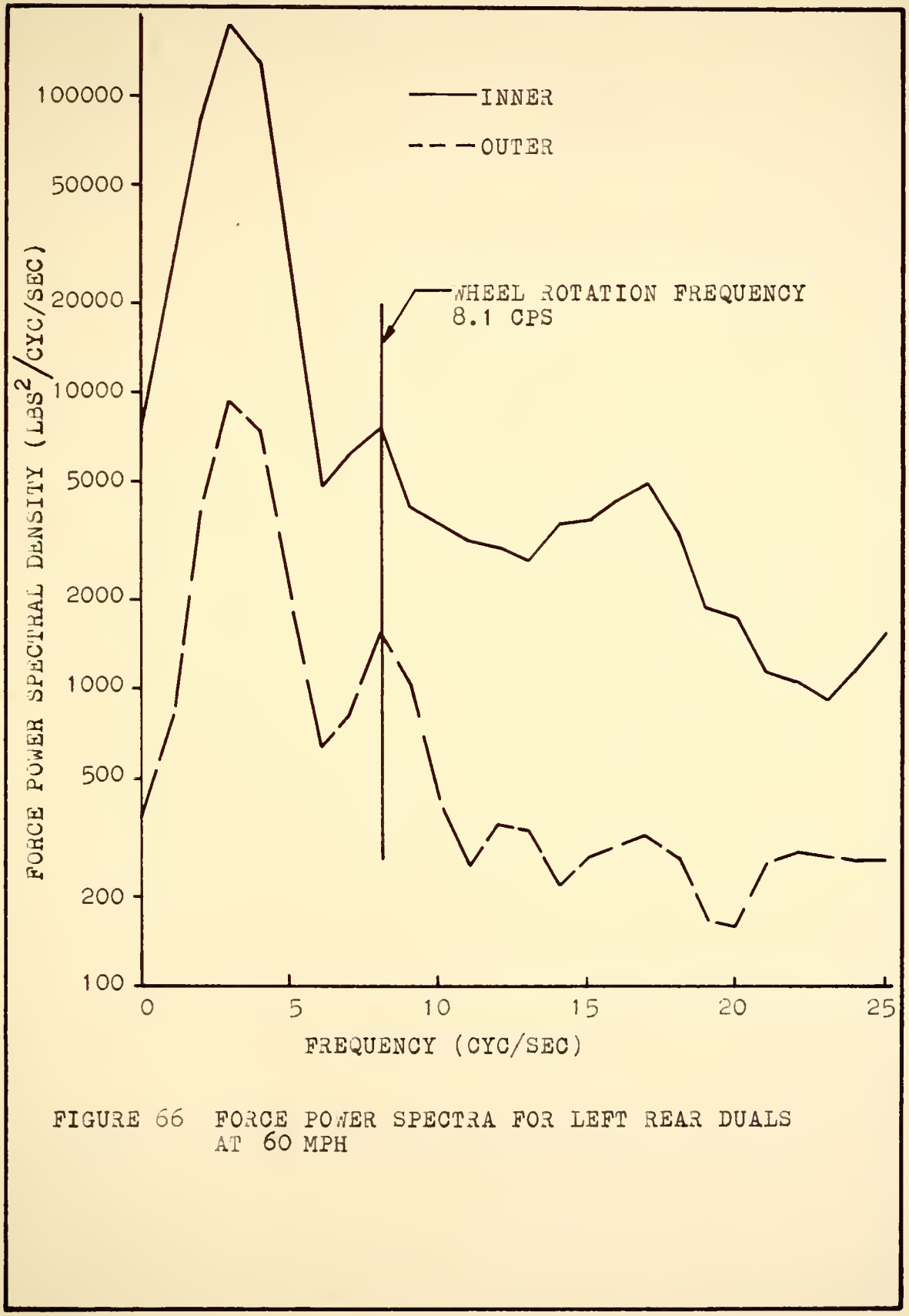

FIGURE 66 FORCE POWER SPECTRA FOR LEFT REAR DUALS AT 60 MPH

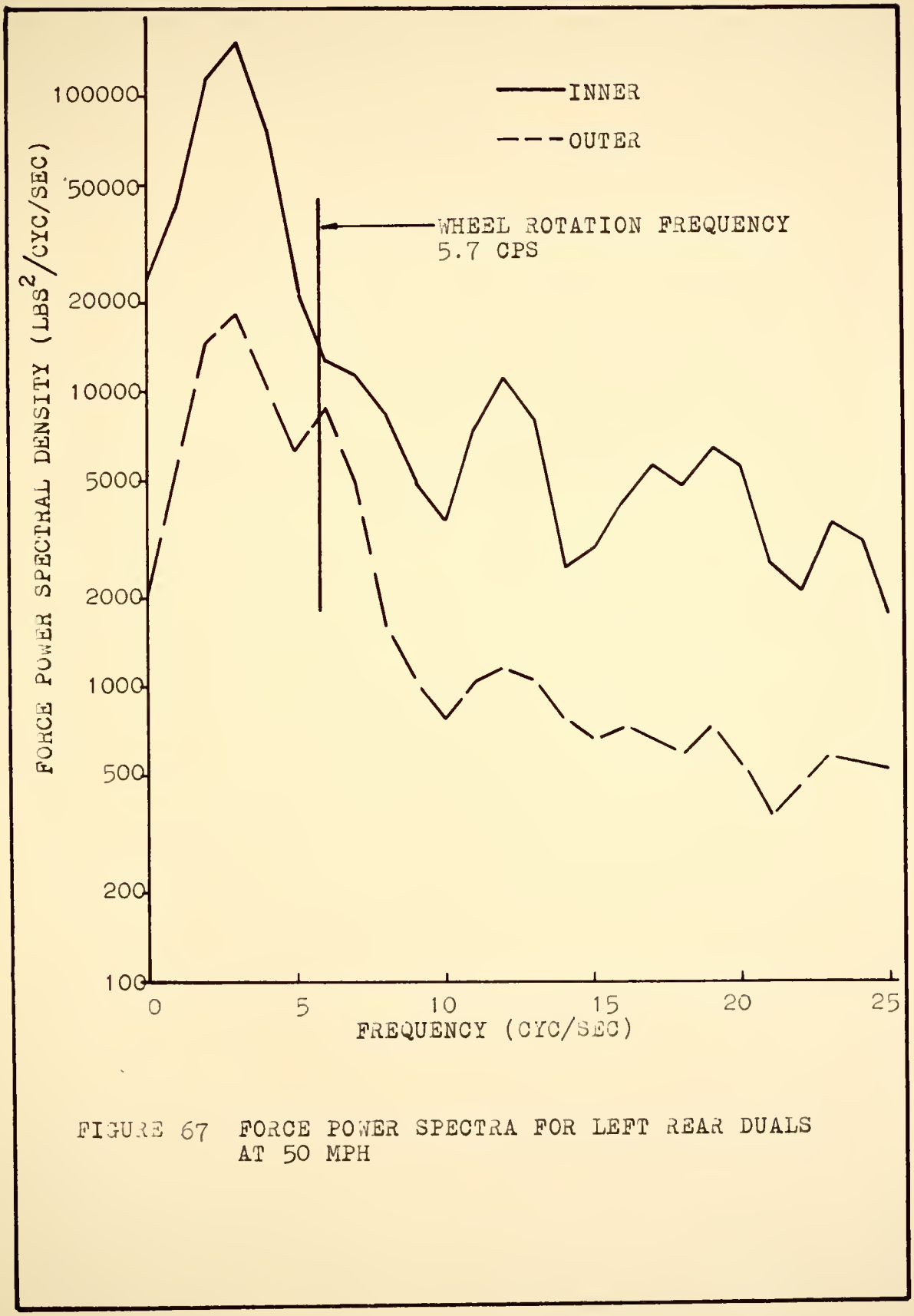

FIGURE 67 FORCE POWER SPECTRA FOR LEFT REAR DUALS AT 50 MPH

CHAPTER VI

CONCLUSIONS AND RECOMMENDATIONS

This investigation dealt with both the measurement and the prediction of dynamic tire forces. The conclusions and recommendations for each topic will be discussed separately.

Measurement of Dynamic Tire Forces

Equipment

1. The measurement of tire inflation pressure to indicate the dynamic tire force is a satisfactory procedure for large vehicles. For vehicles with dual tires, it offers the distinct advantage of indicating the inner and outer dual tire dynamic tire forces independently.

2. The pressure measuring system did not show any strong resonances for the frequencies of interest.

3. A magnetic tape recorder for data recording would be a major improvement over an oscillograph. The reduction of oscillograph records by hand is extremely costly in money, time, and patience.

4. The possibility of converting the pressure record to a force record on an analog computer should be investigated, particularly if the data is recorded on magnetic tape.

5. When the method of calibration by transient excitation is used in the future, the data recording instrumentation should have a larger full scale recording range in order to improve the accuracy with which the data can be read.

6. Because of the trouble experienced with the right rear outer tire, facilities for centering and balancing rear truck tires should be available.

Experimental Results

1. The major inaccuracy in the determination of the total tire force was the initial value of the static force. It was assumed, after measurements were carefully made, that the static force on each rear tire was 4500 lbs for all tests.

2. The force values obtained by multiplying the pressure records by a properly determined constant offers a substantial reduction in the calculations with only a small reduction in accuracy.

3. The dynamic tire forces for the truck are as great as the total force of one wheel of an automobile. However, when the dynamic tire forces are expressed as a percentage of the static load, the car and the truck indicate results of a similar magnitude.

4. The F/X characteristic for an automobile at approximately 18 cps has about the same magnitude as the

truck characteristic at the same frequency. This is also indicated by the fact that the magnitude of both force power spectra are approximately equal at this frequency.

5. The test results did not indicate that a wheel hop mode was excited for the truck.

Prediction of Dynamic Tire Forces

The predicted forces were generally much larger than the experimental forces. There are several possible reasons for this.

1. The procedure for calculating the elevation power spectrum should be improved. The spectrum is distorted by the large peak at zero frequency.

2. A better method for describing the highway profile is needed. This method should reject the long wave lengths that are not significant as far as vehicle excitation is concerned.

3. The assumption that the vehicle derives the input from only one wheel should receive further study.

4. The multiple peaks in the predicted force power spectra are not indicated in the experimental results for the truck. This is probably the result of the fact that there was insufficient frequency resolution in the experimental force power spectra.

5. Another procedure for the prediction of a force

power spectrum would be to subject a model of the vehicle to a record of an elevation profile. A force power spectrum could then be calculated from the force output of the model. This spectrum could then be compared with the experimental force power spectrum. In this way, the vehicle would act as a filter of the elevation profile.

BIBLIOGRAPHY

BIBLIOGRAPHY

1. Sanborn, J. L., "An Experimental Analysis of Transient Vehicle Loads and Response of Flexible Pavements," Ph.D. Thesis, Purdue University, August 1965.

2. Hopkins, R. C., and Boswell, H. H., "A Comparison of Methods Used for Measuring Variations in Loads Transferred Through Vehicle Tires to the Road Surface," Public Roads, Vol. 29, No. 10, October, 1957.

3. Fisher, J. W., and Huckins, H. C., "Measuring Dynamic Vehicle Loads," Highway Research Board Special Report 73, 1962.

4. The AASHO Road Test, Report 4, Bridge Research, Highway Research Board Special Report 61D, 1962.

5. Wilson, C. C., "A Dynamic Tire Force Measuring System," Ph.D. Thesis, Purdue University, June, 1964.

6. Hamilton, J. F., "Determination of Vehicle Characteristics Influencing Dynamic Reactions on Highways," Ph.D. Thesis, Purdue University, August, 1963.

7. McLemore, J. W., "Design of Equipment for Determining Suspension Characteristics of Heavy Vehicles," MSME Thesis, Purdue University, August 1963.

8. Morris, G. J., and Stickle, J. W., "Response of a Light Airplane to Roughness of Unpaved Runways," NASA Technical Note D-510.

9. Blackman, R. B., and Tukey, J. W., The Measurement of Power Spectra, Dover Publications, New York, 1959.

10. De Vries, T. W., "A Statistical Method for Estimating Dynamic Vehicle Loads on Highways," Ph.D. Thesis, January 1961.

11. Zable, J., "Problems Associated with Power Spectral Density Characterizations of Highways," MSME Thesis, Purdue University, January 1965

12. Morris, G. J., "Response of a Jet Trainer Aircraft to Roughness of Three Runways," NASA Technical Note D-2203, May 1964.

13. Wylie, C. R. Jr., Advanced Engineering Mathematics, McGraw-Hill Book Company, New York, 1951.

14. Karman, T. V., and Biot, M. A., Mathematical Methods in Engineering, McGraw-Hill Book Company, New York, 1940.

15. Hamming, R. W., Numerical Methods for Scientists and Engineers, McGraw-Hill Book Company, New York 1962.

16. Hildebrand, F. B., Advanced Calculus for Engineers, Prentice-Hall, Englewood Cliffs, 1949.

17. Shinbrot, Marvin, "On the Analysis of Linear and Nonlinear Dynamical Systems from Transient Response Data," NACA Technical Note 3288, December 1954.

18. Filon, L. N. G., "On a Quadrature," Proceedings of the Royal Society of Edinburg, Vol. 49, 1928-29.

19. Dreifke, G. E., "Effects of Input Pulse Shape and Width on Accuracy of Dynamic System Analysis from Experimental Pulse Data," Sc.D. Thesis, Washington University, 1961.

20. Janeway, R. N., "A Better Truck Ride for Driver and Cargo, Problems and Practical Solutions," SP-154, Society of Automotive Engineers, New York.

21. Carlson, J. A., "Analytical and Experimental Studies of Vehicle Dynamic Behavior," Industrial Mathematics, Vol 7, 1956.

22. Younger, J. E., Advanced Dynamics, The Ronald Press Company, New York, 1958.

23. Tung, C. C., Penzien, J., and Horonjeff, R., "The Effect of Runway Uneveness on the Dynamic Response of Supersonic Transports," NASA Contractor Report 119, October 1964.

24. Laning, J. H. Jr., and Battin, R. H., Random Processes in Automatic Control, McGraw-Hill Book Company, New York, 1956.

25. Quinn, B. E., "Problems Encountered in Using Elevation Power Spectra as a Criteria of Pavement Condition," A Supplement to the Final Report of NCHRP Project 1-2, March 1, 1965.

APPENDIX

APPENDIX 1

Theoretical Frequency Response Relationships for Model in Figure 39

Equations 17, 18, and 19 describe the motions of the three degrees of freedom model shown in Figure 39. The following derivations of the three frequency response relationships corresponding to Cases I, II, and III are simplified when operator notation is used. Using the operator $p \doteq d/dt$, these equations are

$$(Mp^2+6Cp+6K)Z+2(2B-A)(Cp+K)\theta_2=(Cp+K)(X_1+X_2+2X_3+2X_4) \qquad (A.1)$$

$$\left[I_1p^2+\left(\frac{T_F^2}{2}+T_R^2+T_T^2\right)(Cp+K)\right]\theta_1=(Cp+K)\left(-\frac{T_F}{2}X_1+\frac{T_F}{2}X_2-T_RX_3+T_RX_4\right) \qquad (A.2)$$

$$\left[I_2p^2+2(A^2+2B^2)(Cp+K)\right]\theta_2+2(2B-A)(Cp+K)Z = (Cp+K)(-AX_1-AX_2+2BX_3+2BX_4) \qquad (A.3)$$

For Case I (only one input X_4), these equations are solved for the ratios

$$\frac{\theta_1}{X_4}(p) = \frac{T_R(Cp+K)}{\left[I_1p^2+\left(\frac{T_F^2}{2}+T_R^2+T_T^2\right)(Cp+K)\right]} \qquad (A.4)$$

$$\frac{Z}{X_4}(p) = \frac{2\left[I_2p^2+2(A^2+2B^2)(Cp+K)\right](Cp+K)-4B(2B-A)(Cp+K)^2}{D(p)} \qquad (A.5)$$

$$\frac{\theta_2}{X_4}(p) = \frac{2B(Mp^2+6Cp+6K)(Cp+K)-4(2B-A)(Cp+K)^2}{D(p)} \qquad (A.6)$$

where

$$D(p)=(Mp^2+6Cp+6K)\left[I_2p^2+2(A^2+2B^2)(Cp+K)\right]-4(2B-A)^2(Cp+K)^2 \qquad (A.7)$$

Equation 20 in operator form is

$$F_I=(Cp+K)\left[X_4-Z-\left(\frac{T_R-T_T}{2}\right)\theta_1-B\theta_2\right] \qquad (A.8)$$

or

$$\frac{F_I}{X_4}(p)=(Cp+K)\left[1-\frac{Z}{X_4}(p)-\left(\frac{T_R-T_T}{2}\right)\frac{\theta_1}{X_4}(p)-B\frac{\theta_2}{X_4}(p)\right] \qquad (A.9)$$

The ratios A.4, A.5, and A.6 may then be substituted into A.9. The Case I frequency response may then be obtained by replacing p by $j2\pi f$. A computer was used to calculate the numerical values plotted in Figures 41 and 42.

The Case II frequency response (X_2 and X_4 inputs) may be obtained in a similar fashion except that X_2 is no longer zero. X_2 is expressed in terms of X_4 as

$$X_2(t) = X_4(t+\tau) \qquad (A.10)$$

where

$$\tau = \frac{A + B}{V} \tag{A.11}$$

For sinusoidal inputs ($X_4 = e^{j2\pi ft}$)

$$X_2(t) = e^{j2\pi f(t+\tau)} = e^{j2\pi f\tau} e^{j2\pi ft} = e^{j2\pi f\tau} X_4 \tag{A.12}$$

Thus for Case II

$$\frac{\theta_1}{X_4}(p) = \frac{(Cp+K)(T_R + \frac{T_F}{2} e^{j2\pi f\tau})}{\left[I_1 p^2 + (\frac{T_F^2}{2} + T_R^2 + T_T^2)(Cp+K)\right]} \tag{A.13}$$

$$\frac{Z}{X_4}(p) = \frac{(Cp+K)(e^{j2\pi f\tau}+2)\left[I_2 p^2 + 2(A^2+2B^2)(Cp+K)\right]}{D(p)}$$

$$- \frac{2(2B-A)(2B-Ae^{j2\pi f\tau})(Cp+K)^2}{D(p)} \tag{A.14}$$

$$\frac{\theta_2}{X_4}(p) = \frac{(Mp^2+6Cp+6K)(2B-Ae^{j2\pi f\tau})(Cp+K)}{D(p)}$$

$$- \frac{2(2B-A)(e^{j2\pi f\tau}+2)(Cp+K)^2}{D(p)} \tag{A.15}$$

Substituting A.13, A.14, and A.15 into A.9 and replacement of p by $j2\pi f$ will produce the Case II frequency response.

The Case III frequency response (X_1, X_2, X_3, and X_4 inputs) is also obtained in this manner. For this case, however,

$$X_1(t) = X_2(t) = X_3(t+\tau) = X_4(t+\tau) \tag{A.16}$$

Thus for Case III

$$\frac{\theta}{X_4}1(p) = 0 \tag{A.17}$$

$$\frac{Z}{X_4}(p) = \frac{2(e^{j2\pi f\tau}+2)\left[2p^2+2(A^2+2B^2)(Cp+K)\right](Cp+K)}{D(p)}$$

$$- \frac{4(2B-A)(2B-Ae^{j2\pi f\tau})(Cp+K)^2}{D(p)} \tag{A.18}$$

$$\frac{\theta}{X_4}2(p) = \frac{2(Mp^2+6Cp+6K)(2B-Ae^{j2\pi f\tau})(Cp+K)}{D(p)}$$

$$- \frac{4(2B-A)(e^{j2\pi f\tau}+2)(Cp+K)^2}{D(p)} \tag{A.19}$$

Substitution of Equations A.17, A.18, and A.19 into A.9 and replacement of p by $j2\pi f$ will produce the Case III frequency response.

VITA

VITA

The author, Gary Millard Kibbee, was born on December 9, 1938, in Kansas City, Kansas. He was graduated from Turner High School, Turner, Kansas in June 1956. He entered the University of Kansas in September 1956. During his senior year, he received the Vendo Scholarship for achievement. In June 1960, he received his B.S.M.E. degree (with distinction).

He was then employed as a Research Engineer at Smith & Loveless, Division of Union Tank Car Company in Lenexa, Kansas. For development work conducted at this time, he was named as inventor for United States Patents 3,168,595 and 3,195,727.

When he returned to the University of Kansas in September 1961 for graduate study, he also conducted research for Smith & Loveless. He did this research for his Master of Science thesis. This work was in the area of developing a new cooling device for squirrel cage induction motors. He was granted his M.S.M.E. degree in June 1962.

The author accepted a graduate research assistantship at Purdue University to complete his work toward a Ph.D. degree beginning in September 1962. He designed and developed laboratory experiments and their associated special equipment. He later received a dual appointment as one-half time teaching assistantship and one-half time research assistantship.

He is a member of Tau Beta Pi, Pi Tau Sigma and Sigma Tau professional fraternities.